

# **The Design of Novel Benzoin Acetate Photolabile Protecting Groups**

**by**  
**Laura J. McKay**

BSc, University of Victoria, 2018

Thesis Submitted in Partial Fulfillment of the  
Requirements for the Degree of  
Master of Science

in the  
Department of Chemistry  
Faculty of Science

© Laura McKay 2021  
SIMON FRASER UNIVERSITY  
Spring 2021

## **Declaration of Committee**

**Name:** **Laura McKay**

**Degree:** **Master of Science (Chemistry)**

**Thesis title:** **The Design of Novel Benzoin Acetate Photolabile  
Protecting Groups**

**Committee:** **Chair: Robert Britton**  
Professor, Chemistry

**Neil Branda**  
Supervisor  
Professor, Chemistry

**Peter Wilson**  
Committee Member  
Associate Professor, Chemistry

**Andrew Bennet**  
Committee Member  
Professor, Chemistry

**Vance Williams**  
Examiner  
Professor, Chemistry

## Abstract

Photoremovable protecting groups are powerful tools for the release or deprotection of a wide range of molecules. Benzoin type photoremovable protecting groups are renowned for their exceptional properties but have been significantly underdeveloped. This thesis concerns the design, synthesis, and evaluation of four molecules in the benzoin class. A review of the benzoin photolabile protecting group is presented in **Chapter 2**.

The first study, featured in **Chapter 3**, revisits the fundamental photochemistry of the 3',5'-dimethoxybenzoin acetate photolabile protecting group and explores that of two polyaromatic derivatives.

In a second study, **Chapter 4**, the unique photochemistry of a donor acceptor 4-dimethylamino-3',5'-dimethoxybenzoin photocage is examined. The implications of the deviation of this photorelease from all known mechanistic pathways are discussed. A second donor-acceptor derivative 4-methoxy-3',5'-dimethoxybenzoin was designed to combine the traditional photochemistry of dimethoxybenzoin acetate with the advantageous properties of the previous donor acceptor species.

**Keywords:** Photorelease; Benzoin; Caged compound; Structure-photoreactivity; Photo-deprotection; Photochemistry

## **Acknowledgements**

My senior supervisor Dr. Branda for his insight and the unique freedom to pursue my individual interests. I would also like to acknowledge members of my supervisory committee, Dr. Peter Wilson, Dr. Andrew Bennet, and internal examiner Dr. Vance Williams for their support and participation in the examining committee.

Dr. Colin Zhang and Dr. Hongwen Chen for the exceptional NMR and mass spectrometry services.

Members of the Branda group, past and present. A special thanks to CJ Carling.

Dr. Dev Sharma, for his mentorship and constant trust in me. He exudes pure wonder and excitement for teaching and discovery and is an inspiration to many.

My parents and extended family, who believe in me far more than I believe in myself.

For the tiny light of my life, Dove, as well as Linus and Jin, forever loved and missed.

## Table of Contents

Declaration of Committee.....	ii
Abstract.....	iii
Acknowledgements.....	iv
Table of Contents.....	v
List of Tables.....	vii
List of Figures.....	vii
Glossary.....	x
<b>Chapter 1. Introduction.....</b>	<b>1</b>
1.1. Light Triggered Release.....	1
1.1.1. Photoremovable Protecting Groups.....	1
1.1.2. Light as a Stimulus.....	1
1.2. The Model PPG.....	2
1.3. Significant Classes of Organic UV-Light Triggered Photocages.....	3
1.3.1. o-Nitrobenzyl.....	3
1.3.2. Coumarinylmethyl and Aryl Methyl.....	5
1.3.3. p-Phenacyl.....	7
1.3.4. Benzoin.....	7
<b>Chapter 2. A Comprehensive Review of the Discovery, Development, and Applications of the 3',5'-Dimethoxybenzoin Photoremovable Protecting Group.....</b>	<b>10</b>
2.1. Pioneering Work by Sheehan <i>et al.</i> ....	10
2.1.1. A New Photolytic Cyclization.....	10
2.1.2. The Photolysis of Methoxy Substituted Benzoin Esters.....	11
2.2. A Focus on Mechanistic Insight and Biological Application: 1984-1997.....	13
2.2.1. Mechanistic and Photochemical Studies of Phosphate Esters of Substituted Benzoin 13	
2.2.2. Photolabile Linkers Based on 3'-Methoxybenzoin.....	17
2.3. Modern Tools and Novel Applications: 1997-Present.....	18
2.3.1. Mechanistic Studies of Benzoin Esters and Phosphates.....	18
2.3.2. Unconventional Applications.....	24
2.3.3. Outlook.....	27
<b>Chapter 3. Preparation and Photochemistry of Polyaromatic Benzoin Acetate Photoremovable Protecting Groups.....</b>	<b>29</b>
3.1. Abstract.....	29
3.2. Introduction.....	29
3.3. Results and Discussion.....	31
3.3.1. Photochemical Properties of the Parent Benzoin Acetate: A Reinvestigation	31
3.3.2. Polyaromatic Derivatives.....	37

3.4.2.1 Naphthalene (1-(3,5-dimethoxyphenyl)-2-(naphthalen-2-yl)-2-oxoethyl acetate)	37
3.4.2.2 Phenanthrene (1-(3,5-dimethoxyphenyl)-2-oxo-2-(phenanthrene-9-yl)ethyl acetate)	40
3.3.3. Presence of Minor Photoproducts	44
3.4. Conclusions	46
3.5. Experimental	48
3.5.1. General Methods	48
3.5.2. Photochemical Studies	48
3.5.3. Synthetic Procedures and Characterization	49
3.5.4. Mercury-Free Dethioacetalization Alternative	54
<b>Chapter 4. Preparation and Photochemistry of Novel Donor-Acceptor Benzoin Photoremovable Protecting Groups</b>	<b>56</b>
4.1. Abstract	56
4.2. Introduction	56
4.3. Results and Discussion	58
4.3.1. 1-DMA [1-(3,5-dimethoxyphenyl)-2-(4-(dimethylamino)phenyl)-2-oxoethyl acetate]	58
4.3.2. 1-OMe [1-(3,5-dimethoxyphenyl)-2-(4-methoxyphenyl)-2-oxoethyl acetate]	67
4.4. Conclusions	72
4.5. Experimental	74
4.5.1. General Methods	74
4.5.2. Photolysis	74
4.5.3. Synthetic Procedures and Characterization	75
<b>References</b>	<b>80</b>
<b>Appendix A. NMR Characterization</b>	<b>85</b>
<b>Appendix B. Kinetics</b>	<b>99</b>

## List of Tables

Table 1-1 Comparison of the properties of significant PPGs. ....	8
Table 3-1 Summarized properties of <b>1P</b> , <b>1a</b> , and <b>1b</b> . ....	46
Table 3-2 First order rate constants of uncaging.....	47
Table 4-1 Summarized properties of <b>1P</b> , <b>1-DMA</b> , and <b>1-OMe</b> .....	72
Table 4-2 First order rate constants for photorelease of acetic acid.....	73

## List of Figures

Figure 1-1 Release of caged species from photolabile protecting groups.....	1
Figure 1-2 Photorelease of glycine. ....	3
Figure 1-3 Nitroso-benzaldehyde.....	3
Figure 1-4 Photorelease of benzoic acid from first generation ONB and a simple substituted analogue. .....	4
Figure 1-5 Photorelease of a phosphate ester from a coumarinyl diethyl phosphate.....	5
Figure 1-6 The effect of meta substitution on the photolysis of arylmethyl esters.....	6
Figure 1-7 Photorelease of carboxylic acids from a phenacyl PPG.....	7
Figure 1-8 The Favorskii intermediate.....	7
Figure 1-9 Photorelease of carboxylic acids from a benzoin acetate PPG.....	7
Figure 1-10 The synthetic extension of conjugation.....	9
Figure 1-11 The Donor- $\pi$ -Acceptor framework. ....	9
Figure 2-1 General I. desyl and II. benzoin structures. ....	10
Figure 2-2 The effect of meta methoxy substitution on cyclization yield. ....	11
Figure 2-3 Mechanism of benzofuran formation proposed by Sheehan et al. in 1971. ....	12
Figure 2-4 Carbene Mechanism ruled out by Givens et al. in 1993.....	14
Figure 2-5 Ion Pair Mechanism proposed by Givens et al. in 1993.....	15
Figure 2-6 Photosolvolysis Mechanism proposed by Shuey and Pirrung in 1994.....	16
Figure 2-7 Synthesis of 3',5'- dimethoxybenzoin based alcohol protecting group for solid phase synthesis. .....	16
Figure 2-8 Use of protecting groups in solid phase DNA synthesis. ....	17
Figure 2-9 A benzoin acetate based photolabile linker. ....	17
Figure 2-10 Exciplex mechanism proposed by Shi et al. in 1997.....	19
Figure 2-11 Mechanistic pathways proposed by Rock and Chan in 1998. ....	20
Figure 2-12 Pathways for release of diethyl phosphoric acid proposed by Rajesh et al. in 2000..	21
Figure 2-13 Mechanism proposed by Pirrung et al. in 2006.....	23
Figure 2-14 Mechanism for reaction in acetonitrile proposed by Boudebous et al. in 2007. ....	24
Figure 2-15 Hydrolytic and photochemical release of salicylic acid. ....	25

Figure 2-16 Photorelease of ibuprofen from a polymeric scaffold for application as a light controlled drug dosing device. ....	26
Figure 2-17 Release of acetic acid from benzoin acetate decorated upconverting nanoparticles with NIR light. ....	26
Figure 3-1 Photochemical release of acetic acid from compounds <b>1P</b> , <b>1a</b> , and <b>1b</b> with conversion to corresponding benzofuran cyclization products <b>1P-r</b> , <b>1a-r</b> , and <b>1b-r</b> .....	30
Figure 3-2 Synthesis of PPGs <b>1a</b> , <b>1b</b> from commercially available polyaromatic benzaldehydes and synthesis of parent <b>1P</b> from commercially available phenyl dithiane. ....	31
Figure 3-3 UV-Vis absorption spectra of photolysis of <b>1P</b> ( $3.82 \times 10^{-5} \text{M}$ in $\text{CH}_2\text{Cl}_2$ ) with I. 254, II. 312, and III. 365 nm light. IV. Molar extinction coefficient plot of <b>1P</b> (Inset: Appearance of product at 302 nm and loss of <b>1P</b> at 246 nm with 254 nm irradiation).....	32
Figure 3-4 Evolution of selected regions of $^1\text{H}$ NMR spectra throughout duration of irradiation of <b>1P</b> with 312 nm light. ....	34
Figure 3-5 $^1\text{H}$ NMR comparison of (I) Isolated benzofuran, (II) Photolysis mixture-75 m, and (III) Photocage 0 m.....	36
Figure 3-6 Normalized UV-Vis absorbance spectra of isolated benzofuran ( $30 \mu\text{M}$ in DCM) and photolyzed solution of <b>1P</b> . ....	36
Figure 3-7 UV-Vis absorption spectra of photolysis of <b>1a</b> ( $9.88 \times 10^{-6} \text{M}$ in $\text{CH}_2\text{Cl}_2$ ) with I. 254, II. 312, and III. 365 nm light. IV. Molar extinction coefficient plot of <b>1a</b> (Inset: Appearance of product at 323 nm and loss of <b>1a</b> at 255 nm with 254 nm irradiation).....	37
Figure 3-8 $^1\text{H}$ NMR comparison of (I) Isolated benzofuran (II) Photolysis mixture- 240 m, and (III) Photocage <b>1a</b> .....	39
Figure 3-9 Evolution of selected regions of $^1\text{H}$ NMR spectra throughout duration of irradiation of <b>1a</b> with 312 nm light. ....	39
Figure 3-10 UV-Vis absorption spectra of photolysis of <b>1b</b> ( $11.0 \times 10^{-6} \text{M}$ in $\text{CH}_2\text{Cl}_2$ ) with I. 254 II. 312 nm and III. 365 nm light. IV. Molar extinction coefficient plot of <b>1b</b> .....	40
Figure 3-11 Comparative molar extinction coefficient plots of <b>1P</b> , <b>1a</b> , <b>1b</b> and their corresponding benzofurans.....	41
Figure 3-12 Evolution of selected regions of $^1\text{H}$ NMR spectra throughout duration of irradiation of <b>1b</b> with 312 nm light. ....	42
Figure 3-13 $^1\text{H}$ NMR comparison of (I) Isolated benzofuran (II) Photolysis mixture- 240 m, and (III) Photocage <b>1b</b> .....	43
Figure 3-14 Progression of fluorescence emission spectra of a $1 \mu\text{M}$ solution of <b>1b</b> . Inset: A photolyzed $10 \mu\text{M}$ solution of <b>1a</b> is illuminated by a 312 nm handheld UV lamp.....	44
Figure 3-15 Minor photoproduct 3,5-dimethoxybenzaldehyde is observed in photolyzed solutions of I. <b>1P</b> , II. <b>1a</b> , and III. <b>1b</b> . ....	45
Figure 3-16 Molar Extinction Coefficient comparison of photocages <b>1a</b> , <b>1b</b> , and <b>1P</b> (left) and corresponding benzofurans (right). ....	46
Figure 3-17 Copper mediated dethioacetalization of <b>2a</b> . ....	54
Figure 4-1 Photochemical release of acetic acid from <b>1-OMe</b> with conversion to cyclization product <b>OMe-r</b> .....	57
Figure 4-2 Photochemical release of acetic acid from <b>1-DMA</b> . ....	57
Figure 4-3 Synthesis of PPGs <b>1-DMA</b> and <b>1-OMe</b> from commercially available benzaldehydes.....	58



Figure 4-4 UV-Vis absorption spectra of photolysis of <b>1-DMA</b> ( $1.97 \times 10^{-5} \text{M}$ in $\text{CH}_2\text{Cl}_2$ ) with I. 254, II. 312, and III. 365 nm light. IV. Molar extinction coefficient plot of <b>1-DMA</b> . (Inset: Appearance of product at 300 nm and loss of <b>1-DMA</b> at 348 nm with 356 nm irradiation). .....	59
Figure 4-5 Evolution of selected regions of $^1\text{H}$ NMR spectra throughout duration of irradiation of <b>1-DMA</b> with 312 nm light. ....	60
Figure 4-6 Progression of selected region of $^1\text{H}$ NMR spectra throughout duration of irradiation with 312 nm light with removal of NMR cap between cycles.....	61
Figure 4-7 . $^1\text{H}$ NMR (500 MHz, $\text{CD}_2\text{Cl}_2$ ) spectrum of isolated 3,5-dimethoxybenzaldehyde. ....	62
Figure 4-8 4-(dimethylamino) benzaldehyde.....	62
Figure 4-9 $^1\text{H}$ NMR (500 MHz, $\text{CD}_2\text{Cl}_2$ ) of isolated 4-(5,7-dimethoxybenzofuran-2-yl)-N,N-dimethylaniline. ....	63
Figure 4-10 $^1\text{H}$ NMR (500 MHz, $\text{CD}_2\text{Cl}_2$ ) of isolated 2-(3,5-dimethoxyphenyl)-1-(4-(dimethylamino)phenyl)ethan-1-one. ....	64
Figure 4-11 Pathways for formation of cyclized and deacetylated products in the presence of triethylamine proposed by Bisht et al in 2018. ....	65
Figure 4-12 Mechanism I proposed for formation of deacetylated photoproduct. ....	66
Figure 4-13 Mechanism II proposed for formation of deacetylated photoproduct. ....	67
Figure 4-14 UV-Vis absorption spectra of photolysis of <b>1-OMe</b> ( $1.12 \times 10^{-5} \text{M}$ in $\text{CH}_2\text{Cl}_2$ ) with I. 254, II. 312, and III. 365 nm light. IV. Molar extinction coefficient plot of <b>1-OMe</b> . (Inset: Appearance of product at 312 nm with 312 nm irradiation).....	68
Figure 4-15 Molar extinction coefficient comparison of <b>1-OMe</b> and corresponding benzofuran <b>OMe-r</b> . ....	69
Figure 4-16 Evolution of selected regions of $^1\text{H}$ NMR spectra throughout duration of irradiation of <b>1-OMe</b> with 312 nm light .....	70
Figure 4-17 $^1\text{H}$ NMR comparison of (I) Isolated benzofuran, (II) Photolysis mixture-120 m, and (III) Photocage <b>1-OMe</b> .....	71
Figure 4-18 Normalized UV-Vis absorbance spectra of isolated benzofuran <b>OMe-r</b> and photolyzed solution of <b>1-OMe</b> . ....	71
Figure 4-19 Molar Extinction coefficient comparison of photocages <b>1P</b> , <b>1-OMe</b> , and <b>1-DMA</b> ...	72

## Glossary

%	Percent
~	Approximately
$\phi$	Quantum yield
$\delta$	Chemical shift
$\lambda$	Wavelength
$\lambda_{\max}$	Wavelength as which maximum absorption occurs
$\mu\text{M}$	Micromolar
2NB	2-Nitrobenzyl photocage
Ar	Aryl
ATP	Adenosine triphosphate
$^{\circ}\text{C}$	Degrees Celsius
Calc.	Calculated
cAMP	Cyclic adenosine monophosphate
$\text{CDCl}_3$	Deuterated chloroform
$\text{CD}_2\text{Cl}_2$	Deuterated dichloromethane
$\text{CD}_3\text{CN}$	Deuterated acetonitrile
d	Doublet
dd	Doublet of doublets
DNA	Deoxyribonucleic acid
DMA	Dimethylamino
DMB	Dimethoxybenzoin
ESI+	Electrospray ionization
Et	Ethyl
EtOAc	Ethyl acetate
Eq.	Equivalents
$\text{Et}_3\text{N}$	Triethylamine
$\epsilon\phi$	Cross section of uncaging
$\epsilon$	Molar extinction coefficient
g	Grams
g/mol	Grams per mole
GC-MS	Gas chromatography-mass spectrometry

H <sup>+</sup>	Proton
Hex.	Hexanes
HRMS	High resolution mass spectrometry
hν	Photon energy
Hz	Hertz
ISC	Intersystem crossing
J	Coupling constant
k	Rate constant
K <sub>b</sub>	Base dissociation constant
LC-MS	Liquid chromatography-mass spectrometry
M	Molar
m	Multiplet
Me	Methyl
mmol	Millimoles
m/z	Mass to charge ratio
mL	Millilitre
mg	Milligrams
n-BuLi	n-Butyllithium
NIR	Near infrared
NMR	Nuclear magnetic resonance
nm	Nanometres
ns	Nanoseconds
Ph	Phenyl
PPG	Photolabile protecting group
ppm	Parts per million
pH	Potential of hydrogen
RT	Room temperature
s	Singlet
t	Triplet
THF	Tetrahydrofuran
TLC	Thin layer chromatography

TMS	Tetramethylsilane
UCNP	Upconverting nanoparticle
UV	Ultraviolet
UVA	Ultraviolet light 315-400 nm
UV-Vis	Ultraviolet-visible

# Chapter 1. Introduction

## 1.1. Light Triggered Release

### 1.1.1. Photoremovable Protecting Groups

A remarkable number of terms exist in order to describe molecules from which light liberates a previously inactive ‘trapped’ species. These include but are not limited to the following: Phototrigger, Caged Compound, Photocage, Photoremovable Protecting Group, Photolabile Protecting Group. The moniker “caged”, introduced by Kaplan *et al* in their study of release of ATP, conjures an image of a physically trapped species.<sup>1</sup> While this is not the case, as the photosensitive group is linked to the precursor to the active species via a covalent bond, the term caged captures interest and presents a simple view of a more complex concept.

Herein, the term Photolabile protecting group (PPG) will be primarily used to refer to these molecules.

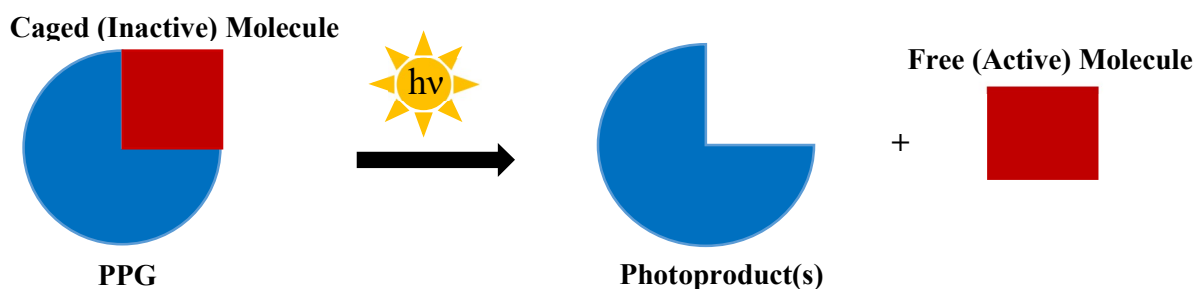


Figure 1-1 Release of caged species from photolabile protecting groups.

### 1.1.2. Light as a Stimulus

The most noteworthy property of photoremovable protecting groups is the ability to release a substrate with the exceptional spatial and temporal control that light provides. Light, regarded as a ‘traceless’ reagent, presents an attractive alternative to traditional reaction methods.<sup>2</sup> Photochemical reactions, requiring only the absorption of photons, bypass the need for activating reagents, catalysts, and thermal energy. As a stimulus, light affords control to the user, who may tune and focus the light. Halting photochemical reactions does not require quenching and workup, but rather simply switching off the light source. These properties are particularly attractive in

biological systems, where the use of most reagents is not suitable and reaction sites are not easily accessible. While the primary use of PPGs is the targeted release of molecules to probe biological processes, the full range of documented applications is exceptionally diverse. This includes but is not limited to the fields of solid phase synthesis, chemical synthesis, surface chemistry, nanotechnology, drug delivery, and enzymology. A wide variety of functional groups may be protected, including carboxylic acids, phosphates, amines, alcohols, and sulfonic acids. The photorelease of inorganic species and cations is also possible.

## 1.2. The Model PPG

A set of requirements originally presented by Lester and Nerbonne is often used to describe the properties of an ideal PPG.<sup>3</sup> It is vital to understand no system will fulfill each requirement and that desired properties are highly specific to individual applications. This highlights the importance of having a large toolbox of available well studied molecules out of which a suitable candidate can be chosen for the specific needs of a study. The below list is tailored to biological studies, where the majority of PPGs find their use.

### 1. *Absorption*

Extinction coefficients above 300 nm should be high. Irradiation with higher energy UV light risks absorption and subsequent damage to a biological environment, such as thymine dimerization and associated DNA damage. Additionally, the photoproduct(s) resulting from release should not absorb strongly at the excitation wavelength.

### 2. *Efficiency*

The one-photon uncaging cross section, defined as the extinction coefficient multiplied by the quantum yield at the excitation wavelength ( $\epsilon\phi$ ), should be high. In the context of photorelease, the quantum yield of release is defined as the moles of the liberated species divided by the number of photons absorbed at the irradiation wavelength.

### 3. *Stability*

Both the chromophore and generated photoproduct should be nonreactive and biocompatible with the local environment. A 'clean' reaction generating a single photoproduct is preferred.

### 4. *Solubility*

Solubility in water and solutions of high ionic strength is advantageous.

## 5. Kinetics

In kinetic studies involving rapid response to the released compound, the rate constant of release must exceed that of the process of interest.

### 1.3. Significant Classes of Organic UV-Light Triggered Photocages

While previous work had focused on release of specific functional groups for use in chemical synthesis, Bartlop and Schofield were the first to successfully release a biologically important species.<sup>4</sup> Their 1962 report on the photorelease of the amino acid glycine sparked considerable interest and ultimately led to the development of numerous PPGs. These molecules are often grouped into classes based on their structural characteristics.

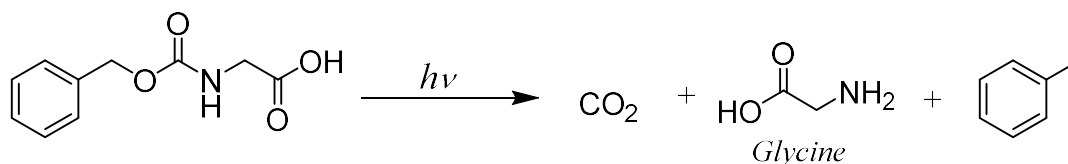


Figure 1-2 Photorelease of glycine.

#### 1.3.1. o-Nitrobenzyl

Bartlop *et al* were again the first in the case of the now ubiquitous o-nitrobenzyl (ONB) or 2-nitrobenzyl ester PPGs.<sup>5</sup> The incredible effects of simple structural variation were demonstrated by the first ONB derivatives, initially tested for the release of benzoic acid in this 1966 publication.

The first generation ONB released benzoic acid with a dismal 17% yield. This was found to be a result of the primary photoproduct, 2-nitrosobenzaldehyde. This aldehyde quickly converted to a secondary photoproduct which was seen to be highly absorbing, competing with the photoreaction for incident light. Substitution in the  $\alpha$  position yielded a less reactive nitroso benzophenone photoproduct, and as a result nearly quantitative release of benzoic acid. The successful release of ATP from an o-ONB into physiological media in 1978 attracted further widespread interest.<sup>1</sup> In the following decades further modifications, primarily with the goal of increased quantum yield and reaction rate, may be grouped into two categories.

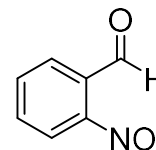


Figure 1-3  
Nitroso-  
benzaldehyde.

Substitution at the benzylic site primarily influences quantum yields while modification of the aromatic moiety tunes absorbance.<sup>6,7</sup>

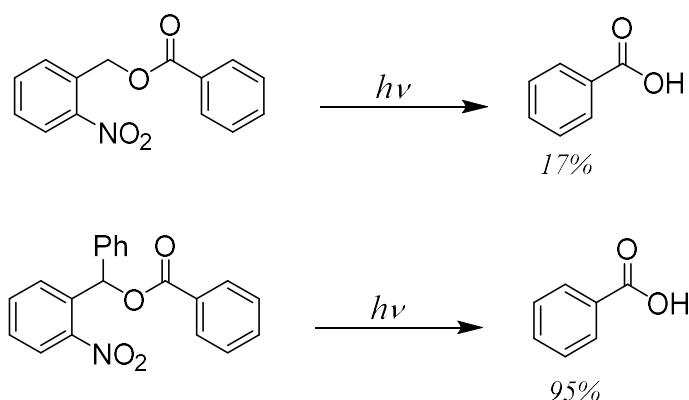


Figure 1-4 Photorelease of benzoic acid from first generation ONB and a simple substituted analogue.

ONB cages have since been widely studied and remain a fixture in the literature. A plethora of ONB caged molecules are commercially available, a sure sign of the success of this class of PPG. Despite their status and the number of derivatives available, there are persistent issues associated with these PPGs. The primary photoproduct in ONB molecules without alpha substitution, the nitroso benzaldehyde, presents a major problem. The aldehyde itself has been seen to be mildly toxic, forming an imine which interferes with biological systems.<sup>8</sup> For this reason, alpha substitution is preferable in systems where free amines are present to react with the nitroso benzaldehyde. The ketone byproduct is thought to be less reactive in the case of imine formation. The photochemistry of release is complicated by pH dependence, a result of hydrogen transfer to the nitro group from the alkyl ortho substituent. Time resolved techniques indicate that the rate determining step depends on solution pH.<sup>9</sup>

Additionally, GC-MS analysis of photolysis mixtures indicates that the photochemistry of release is not as clean as would be desired.<sup>10</sup> Multiple unidentified byproducts were observed in the reaction of both ONB and substituted analogues. These may be a result of secondary reaction of the nitroso photoproducts. Further work is necessary to evaluate the implications of these findings.



### 1.3.2. Coumarinylmethyl and Aryl Methyl

Coumarin cages began to increase in popularity in the late 1990s though their discovery dates back to 1984, when Givens *et al.* observed release of a phosphate ester from a coumarylmethyl group.<sup>11</sup> Irradiation of this moiety in the presence of nucleophiles including piperidine, cysteine, tyrosine, and chymotrypsin results in release of the phosphate ester and substitution with the nucleophile. The highly fluorescent nature of the coumarin structure results in a fluorescent tagging of these nucleophiles.

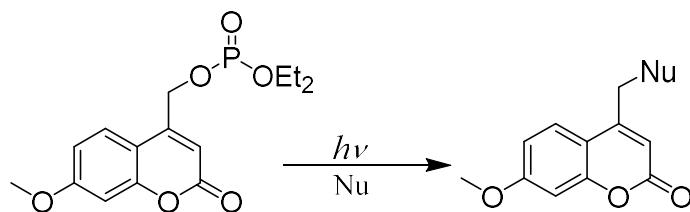


Figure 1-5 Photorelease of a phosphate ester from a coumarinyl diethyl phosphate.

The mechanism of this reaction has since been elucidated to proceed via a singlet excited state.<sup>12</sup> Heterolytic bond cleavage occurs subsequent to the excitation to yield a singlet ion pair. Fluorescence and non-radiative decay processes proceed in competition with bond heterolysis. The leaving group is then liberated and the resulting coumarinylmethyl cation reacts with the relevant nucleophile. In the case of the coumarinylmethyl class, a strong understanding of this mechanism is beneficial for further tuning of properties. The use of electron donating substituents in the aromatic system stabilizes the coumarylmethyl cation. The paired anion may similarly be stabilized by the selection of species large  $pK_b$  values. These two stabilizations were seen to have a significant effect on the photorelease reaction, both in increasing the rate of the first step and in overall efficiency of product formation.

While first generation coumarin-based PPGs already had exceptional promise due to their fluorescent properties, long-wavelength absorption, and reasonable release rates, recent modifications such as those described above have been successful. The remaining drawbacks with this class are primarily poor quantum yields, which have been only marginally increased with modified analogues, and the strong absorbance of photoproducts.

In the same time period arylmethyl ester PPGs, often considered a close relation or analogue of coumarinylmethyls, were being investigated. Studies of arylmethyl compounds are synonymous with Zimmerman, Pincock, and their observations on the excited state meta effect, which addresses the differing reactivity of excited state molecules and their ground state counterparts.<sup>13-15</sup>

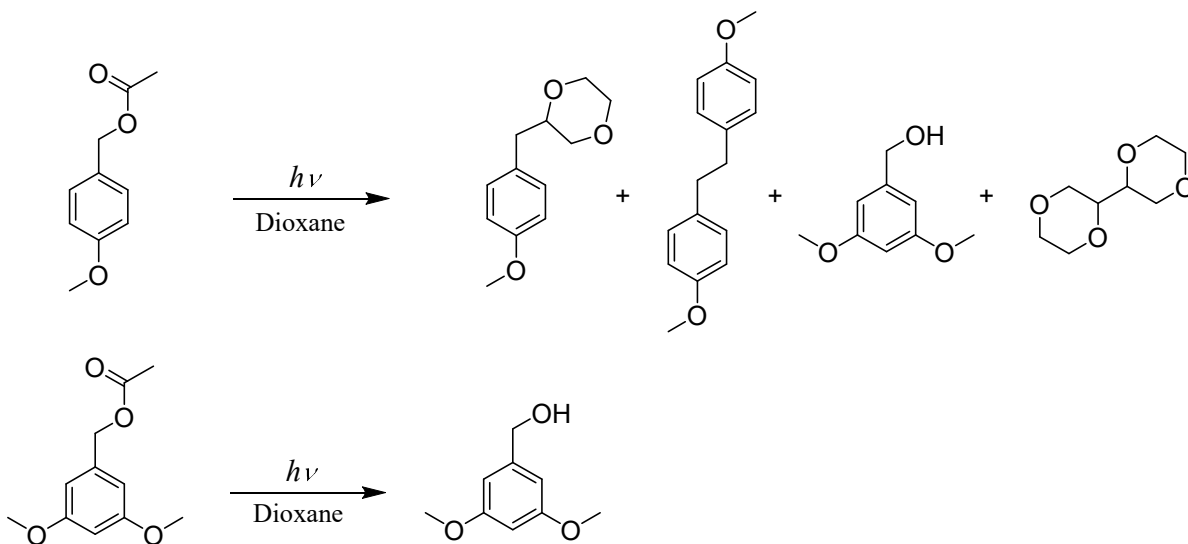


Figure 1-6 The effect of meta substitution on the photolysis of arylmethyl esters.

Simple non-substituted or para substituted arylmethyl PPGs yield photoproducts derived from both radical and ion pair intermediates alongside the released species. Zimmerman first proposed that meta substitution results in an approach of the singlet excited and ground state energy surfaces.<sup>15</sup> This is expected to lead to heterolysis of the benzyl ester bond. Conversely, para substitution results in homolytic bond cleavage and radical derived products. Pincock believed the mechanistic pathway to be bond homolysis followed by a competition between electron transfer, yielding an ion pair, and ground state radical reactions.<sup>14</sup> In meta substituted derivatives, radical processes proceed at a slower rate than electron transfer and as a result ion pair derived intermediates dominate. In these compounds meta substitution additionally increases quantum yield of photorelease by an order of magnitude.

Meta substituted arylmethyl PPGs release quickly and yield primarily products derived from heterolysis. Study of these compounds has been focused on mechanistic insight and as a result fewer derivatives with fine-tuned properties exist.

### 1.3.3. p-Phenacyl

The phenacyl type PPG, published first by Sheehan and Umezawa in 1973, has been proven an exceptional tool for monitoring fast biological processes despite its structural simplicity.<sup>16</sup>

Release rates in this class are high and quantum yields are reasonable.

Yields of the two primary photoproducts, a rearrangement product and acetophenone, are highly dependent on the solvent system.

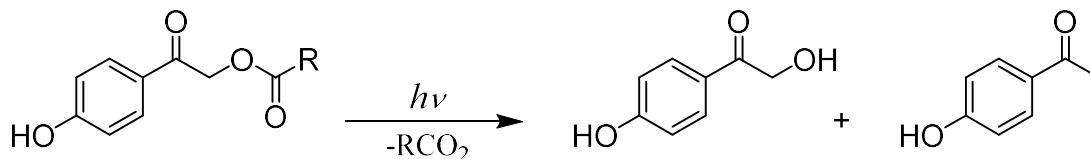


Figure 1-7 Photorelease of carboxylic acids from a phenacyl PPG.

Reactions of the p-phenacyl PPG are generally accepted to proceed through the triplet excited state and a highly strained spirodiketone known as the Favorskii intermediate.<sup>17-19</sup> This structural rearrangement pathway is reminiscent of the ground state Favorskii rearrangement.

The primary issue with the class of PPG is the low extinction coefficients above 300 nm. Attempts to remedy this by introducing meta methoxy substituents were successful in shifting absorption but yielded additional photoproducts and diminished quantum yields.<sup>20</sup>

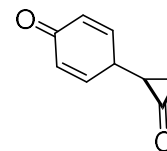


Figure 1-8 The Favorskii intermediate.

### 1.3.4. Benzoin

Benzoin type PPGs were discovered by Sheehan and Wilson in 1964, at the advent of work on photolabile protecting groups.<sup>21</sup>

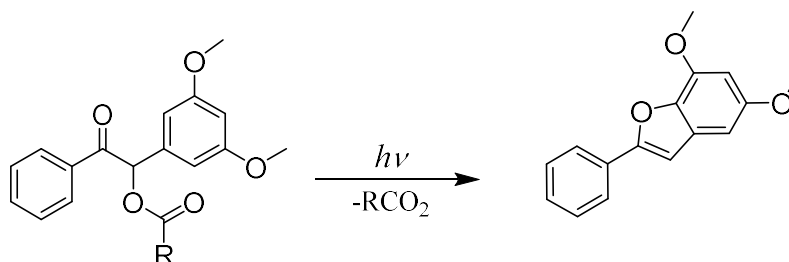


Figure 1-9 Photorelease of carboxylic acids from a benzoin acetate PPG.

The plethora of exceptional attributes exhibited by PPGs in this class includes a quantum yield approaching unity, clean photoreaction yielding a single benign and highly fluorescent photoproduct, and a rapid release rate for numerous functionalities. Drawbacks of this system are primarily the strongly absorbing benzofuran photoproduct, low extinction coefficients past 300 nm, and poor water solubility.

Interest in this class has primarily been focused on mechanistic aspects. As a result, the benzoin PPG has been remarkably underdeveloped in contrast to other prominent classes. A detailed review of the history and development of this class is presented in Chapter 2.

<i>Class</i>	✓	✗
2-Nitrobenzyl	<ul style="list-style-type: none"> <li>· Extensively studied</li> <li>· Commercially available</li> </ul>	<ul style="list-style-type: none"> <li>· Reactive photoproduct</li> <li>· Low-moderate <math>\phi</math></li> </ul>
Coumarinylmethyl	<ul style="list-style-type: none"> <li>· High <math>\epsilon_{\text{UVA}}</math></li> <li>· Fluorescent photoproduct</li> </ul>	<ul style="list-style-type: none"> <li>· Low <math>\phi</math></li> <li>· Strongly absorbing photoproduct</li> </ul>
p-Phenacyl	<ul style="list-style-type: none"> <li>· Release rate</li> <li>· Moderate <math>\phi</math></li> </ul>	<ul style="list-style-type: none"> <li>· Low <math>\epsilon_{\text{UVA}}</math></li> <li>· Multiple photoproducts</li> </ul>
Benzoin	<ul style="list-style-type: none"> <li>· Release rate</li> <li>· High <math>\phi</math></li> <li>· Fluorescent photoproduct</li> </ul>	<ul style="list-style-type: none"> <li>· Low <math>\epsilon_{\text{UVA}}</math></li> <li>· Strongly absorbing photoproduct</li> </ul>

*Table 1-1 Comparison of the properties of significant PPGs.*

As is summarized in Table 1-1, each class of PPG has properties which may be classified as drawbacks. However, certain undesirable properties are more difficult to remedy even with extensive structural modification, such as the reactive nitroso photoproduct of the 2-NB class. Similarly, the low quantum yield of coumarylmethyl compounds is seemingly inherent and has not been successfully increased. While the phenacyl group is promising, the number of photoproducts released is a detrimental property. The base characteristics the of benzoin PPG are exceptional. The negative properties, poor absorption above 300 nm and a strongly absorbing photoproduct, are more easily altered.

This work seeks to increase UVA absorption via structural modification of the benzoin PPG. Meta methoxy substituents on the non-conjugated ring are essential to the characteristic photochemistry of the benzoin class.<sup>27</sup> Consequently, this moiety remains untouched in the present work. Introduction of additional groups to these positions, discussed in Chapter 2, is acceptable to improve water solubility without altering the course of these photoreactions.<sup>41</sup> However, as a reasonable protocol has been established in literature, water solubility is not investigated or altered in these studies. While structure photoreactivity relationships are specific to each class and mechanisms of photorelease, there are a few general strategies which are commonly employed. Here extension of conjugation and donor-acceptor effects will be examined. In the absence of clear mechanistic information, a trial and error method is necessary to determine result of these structural modifications and begin to establish structure-reactivity relationships.

**Strategy I** (Chapter 3) involves the extension of conjugation.<sup>22-24</sup> As these photoreactions are most likely based on  $n\pi^*$  transitions, the  $\pi$ -system was extended here by the installation of additional rings on the benzoyl moiety.

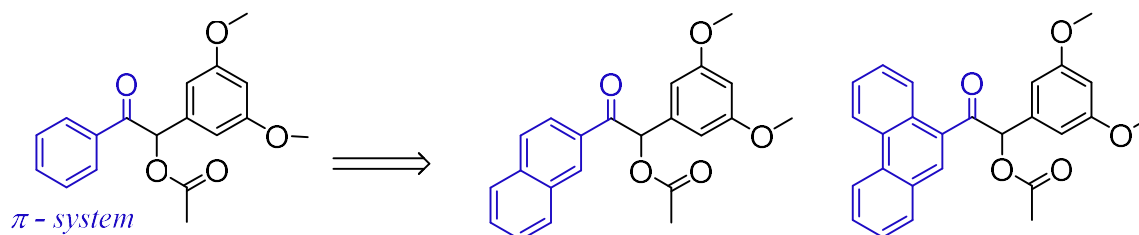


Figure 1-10 The synthetic extension of conjugation.

The basis of **Strategy II** (Chapter 4) is the introduction of electron donating substituents to induce a donor-acceptor effect.<sup>25,26</sup> In this small system, the carbonyl serves as the electron deficient (acceptor) moiety. An electron donor, linked by conjugation, is installed in the para position.

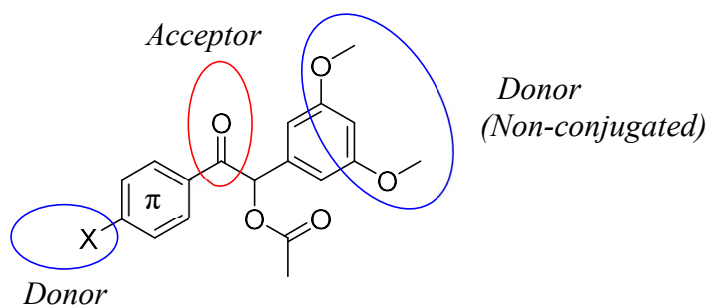


Figure 1-11 The Donor- $\pi$ -Acceptor framework.

## Chapter 2. A Comprehensive Review of the Discovery, Development, and Applications of the 3',5'-Dimethoxybenzoin Photoremovable Protecting Group

The lengthy history of the benzoin class is explored here in order to provide necessary context to the work described in this thesis. A complete review of the development of these molecules is essential in understanding the place of this class in current literature and to chart a course forward.

### 2.1. Pioneering Work by Sheehan *et al.*

#### 2.1.1. A New Photolytic Cyclization

Intrigued by the dependence of photoproduct distribution on solvent polarity and nature of the leaving group, Sheehan and Wilson sought to further work done on the photoactive desyl moiety in the 1950s and synthesized several new benzoin type derivatives.<sup>21</sup> While all previous desyl compounds yielded a number of photoproducts, photolysis of benzoin acetate yielded a novel cyclization product. This 2-phenylbenzofuran appeared with a yield ranging from 8-15%, depending on the solvent. A variety of leaving groups were then tested within the benzoin framework, including chloride, tosylate, and dimethylamine hydrochloride. Photolysis of desyl chloride and desyl tosylate resulted in only 1% and 3% cyclization yield, respectively. Conversely, photolysis of the desyldimethylamine hydrochloride yielded 54% of the respective benzofuran, representing the first known case of an  $\alpha$ -aminoketone hydrochloride undergoing a photochemical elimination

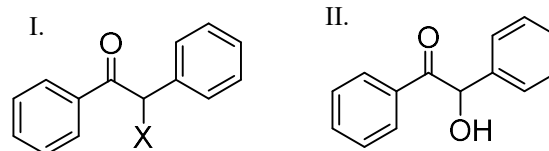


Figure 2-1 General I. desyl and II. benzoin structures.

reaction. Finally, addition of substituents onto the two rings of benzoin acetate was explored. Two compounds, 4,4'-dimethoxybenzoin acetate and 3,3'-dimethoxybenzoin acetate, were synthesized at this time to determine the effects of para and meta substitution. Photolysis of 4,4'-dimethoxybenzoin acetate yielded primarily anisil and 1% benzofuran. In sharp contrast, 3,3'-dimethoxybenzoin acetate yielded 48% cyclization product.

These results, coupled with investigation of the UV-Vis spectra of these compounds, allowed Sheehan and coworkers to propose that this reaction is a result of an  $n\pi^*$  excitation in which the nonbonding oxygen orbital and  $\pi$  electrons of the isolated ring interact strongly. Reduced cyclization yield of the 4,4'-dimethoxybenzoin acetate was rationalized by the effect of electronic delocalization on the carbonyl, resulting in decreased ability to release the acetate. A full mechanism was not presented at this time.

### 2.1.2. The Photolysis of Methoxy Substituted Benzoin Esters

Seven years after their first paper on the subject, Sheehan *et al.* published an in-depth study on the influence of methoxy substitution on benzoin esters.<sup>27</sup> The initial look at simple symmetrical substitution spurred Sheehan to synthesize unsymmetrical benzoin esters to further investigate meta methoxy substitution. The previously prepared symmetric compounds, with their highly variable yields, do not provide the necessary mechanistic insight in terms of substitution on the two separate rings (conjugated and isolated). Thus, 4'-dimethoxybenzoin acetate and 3'-dimethoxybenzoin acetate were synthesized, and photochemical studies were performed on both. The para substituted compound 4'-dimethoxybenzoin acetate yields only 10% of the cyclization product. In this reaction, radical dimerization products dominate, suggesting that the para compound dissociates homolytically into benzoyl and methoxyphenyl acetoxyethyl radical fragments, which may either recombine or form the observed dimers. In sharp contrast, irradiation of 3'-dimethoxybenzoin acetate afforded 88% of the benzofuran. These results further confirmed that benzofuran formation is highly reliant on the position of methoxy substitution. Placement of these substituents on the isolated phenyl enhanced cyclization yield, whereas substitution of the benzoyl group was seen to impede the reaction. With the intention of reinforcing this idea, 3,5-dimethoxybenzoin acetate was synthesized.

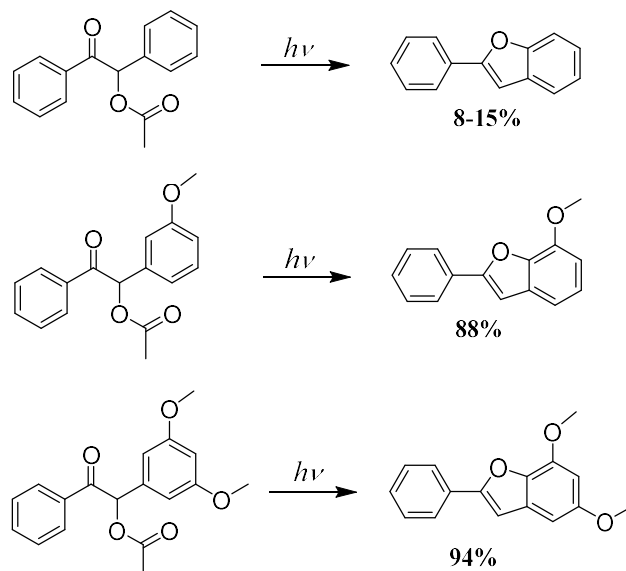


Figure 2-2 The effect of meta methoxy substitution on cyclization yield.

When a UV-Vis photolysis study was performed, Sheehan and coworkers immediately noticed the exceptionally smooth course of reaction, complete with two clear isosbestic points. Photolysis on this scale was found to afford an incredible 99.5% of the expected cyclization product 2-phenyl-5,7-dimethoxybenzofuran (determined spectroscopically). When isolated and purified, 94% of the benzofuran remained.

Quantum yield of release was determined to be  $0.644 \pm 0.029$ , at the time the highest quantum yield of all known photocages. Quantitative quenching studies demonstrated that formation of the cyclization product was not quenched by either naphthalene or neat piperylene, implying either a singlet or extremely short-lived triplet excited state. Interestingly, reactions of the synthesized p-methoxy substituted molecules were found to be completely quenchable, suggesting that they proceed through a long-lived triplet.

On the basis of recent evidence for highly strained oxetane intermediates in the rearrangement of  $\beta, \gamma$  unsaturated ketones, the following mechanism for benzofuran formation was proposed.<sup>28,29</sup>

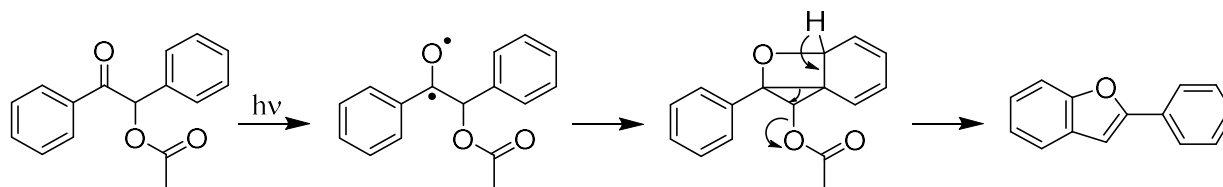


Figure 2-3 Mechanism of benzofuran formation proposed by Sheehan et al. in 1971.

This mechanism, involving bond homolysis followed by intramolecular Paterno-Buchi cycloaddition, attempts to rationalize the drastic differences in cyclization yield with varying methoxy substitution patterns. If the oxetane intermediate should form in a para substituted compound, the methoxy substituent encourages rearrangement to the original chromophore. Conversely, a meta methoxy substituent on the non-conjugated ring facilitates electrophilic attack of the carbonyl oxygen. Once the oxetane is formed, the methoxy encourages loss of the carboxylate and formation of the benzofuran. The authors conclude that the novel 3',5'-dimethoxybenzoin acetate has strong potential as a protecting group for carboxylic acids, particularly in the context of peptide synthesis. In the first test of this practical application, the phthaloyl glycinate ester was prepared and found to yield 87% released phthaloylglycine after a 45-minute photolysis.



## 2.2. A Focus on Mechanistic Insight and Biological Application: 1984-1997

### 2.2.1. Mechanistic and Photochemical Studies of Phosphate Esters of Substituted Benzoin

For a period of more than 10 years after Sheehan's 1971 publication, the 3',5'-dimethoxybenzoin was absent from literature. In 1984, Givens and Matuszewski demonstrated that this highly versatile PPG was also able to release phosphates.<sup>11</sup>

Their first report noted that benzoin diethylphosphate yielded the intramolecular rearrangement product 2-phenylbenzofuran regardless of solvent. For simplicity the parent symmetrical benzoin structure was used, despite the impressive properties of the methoxy substituted derivative. Quenching studies suggested that this reaction occurs via the triplet manifold. This publication demonstrated the benzoin to be an attractive protecting group for release of a phosphate moiety, and from this point onward, release of phosphates (and thus biologically important nucleotides) motivated the vast majority of work in the area, spurred onward by the increasing popularity of 'light flash physiology' studies.

In their 1992 publication Corrie and Trentham focused primarily on developing an efficient route for synthesis of phosphate monoesters of methoxy substituted benzoin.<sup>30</sup> Once a viable synthetic route was in place, these compounds were studied via flash photolysis to examine their suitability for applications in muscle physiology. When irradiated with a single 347 nm pulse, a remarkable 10% of the 3',5'-dimethoxybenzoin was converted into the benzofuran. The second of several publications by Givens *et al.* focuses on the release of cyclic adenosine monophosphate (cAMP) from the benzoin framework as well as the synthesis of water-soluble benzoin phosphate derivatives.<sup>31</sup> Cyclic adenosine monophosphate, a cyclic derivative made from adenosine triphosphate (ATP), is a messenger important in biological processes. The two soluble derivatives, benzoin isopropyl phosphate and benzoin phosphate were found to release the caged phosphate in nearly quantitative yields. Further quenching studies determined triplet lifetimes between 1-4 ns. With the synthesis of caged benzoin cAMP and successful release, it was confirmed that the benzoin could serve as a PPG for nucleotides. At this time no intermediates in the photochemical reaction were observed.

Next, Givens *et al.* turned their focus to mechanistic aspects of this reaction.<sup>32</sup> Two alternatives were presented, the first involving a carbene intermediate (Figure 2-4) and the second based on a charge transfer excited state which decays to an ion pair (Figure 2-5). In the more than 20 years since the mechanism proposed by Sheehan *et al.*<sup>27</sup>, these were the first alternative mechanisms published.

In order to test the carbene mechanism (Figure 2-4), an  $\alpha$ -deuterated desyl ester was synthesized. Irradiation yielded the cyclization product, 3-deuterio-2-phenylbenzofuran, which was found to possess the same degree of deuteration as the starting material. This result ruled out the proposed carbene mechanism as well as any route in which the methine hydrogen is removed.

Figure 2-5 illustrates the second possible mechanism, in which the triplet excited state undergoes homolysis. Rapid single electron transfer of the radical pair structure yields the ion pair. After ring closure, the released phosphate anion may then remove the bridgehead proton, yielding the observed benzofuran. One proposed variation of this ion pair route would involve formation of a charge-transfer excited state which would decay to the ion pair by homolysis of the carbon oxygen bond. At this time no evidence for any variation of the ion pair mechanism was obtained.

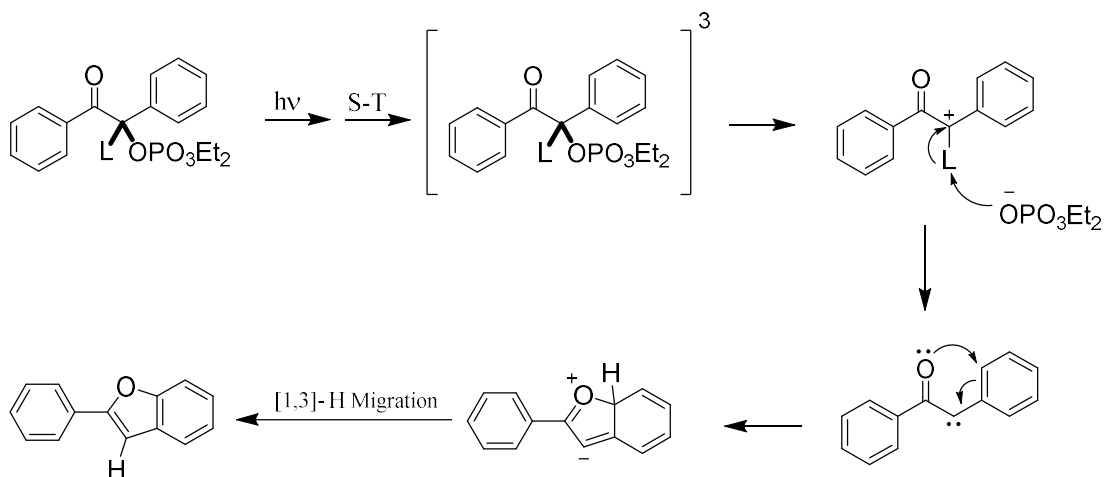


Figure 2-4 Carbene Mechanism ruled out by Givens *et al.* in 1993.

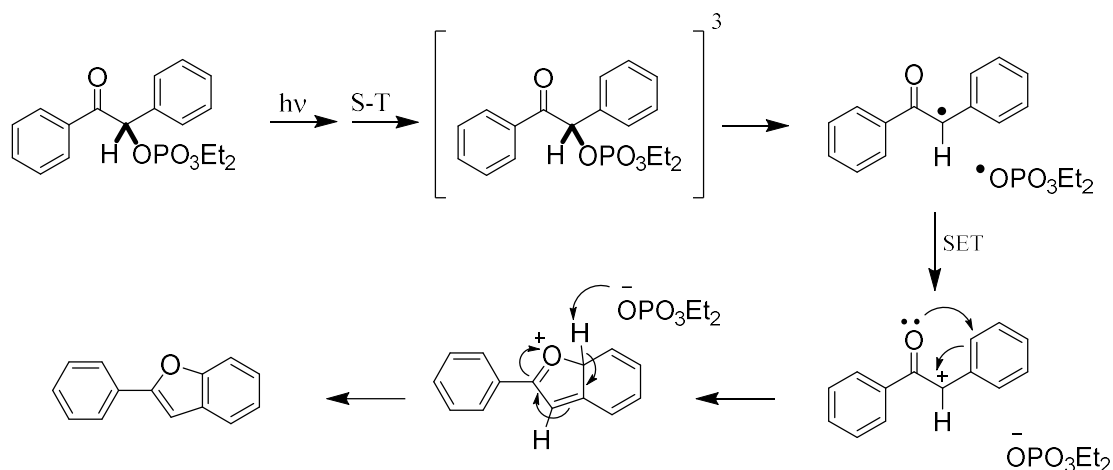


Figure 2-5 Ion Pair Mechanism proposed by Givens et al. in 1993.

Additionally, release of cAMP from the desyl ester was investigated in greater detail. The unsubstituted benzoin, known to possess a significantly lower quantum yield and release rate, was used due to ease of synthesis. The nucleotide was released nearly quantitatively, with a calculated quantum efficiency of 0.33. These investigations suggested that the even the unsubstituted desyl cage is kinetically preferable to *o*-nitrobenzyl esters, as the determined rates of release were seen to be three orders of magnitude greater than existing literature values. Quenching studies again supported the triplet excited state, calculated here to exist with a lifetime of 0.52 ns in a solution of aqueous buffer and dioxane.

In 1994 Pirrung and Shuey sought to further previous work on phosphotriesters of dimethoxybenzoin, in particular to develop derivatives with the highest efficiency of photochemical deprotection.<sup>33</sup> The authors identified the marked divergence in behaviour between benzoin acetates and phosphates, a topic which had not before been addressed. Previous work had found that reactions of benzoin phosphates are consistently quenched and thus likely to proceed via a triplet excited state, while deprotection of their acetate analogues is not, suggesting either a short-lived triplet or reaction from the singlet state. However, both the benzoin carboxylates and phosphates prepared in this study were found to not be quenched by even high concentrations of naphthalene. Additionally, optically pure (-)-3',5'-Dimethoxybenzoin was synthesized. In phosphotriesters of dimethoxybenzoin, stereogenic centers exist. In order to minimize possible complications in characterization, the optically pure molecule was synthesized.

This work confirmed the 3,'5' pattern of substitution as the most desirable in achieving high conversion rates, with the ortho 2',3' not far behind. The authors proposed a photosolvolysis mechanism and presence of a cationic intermediate (Figure 2-6) but believed both homolytic and heterolytic bond cleavage to be plausible.

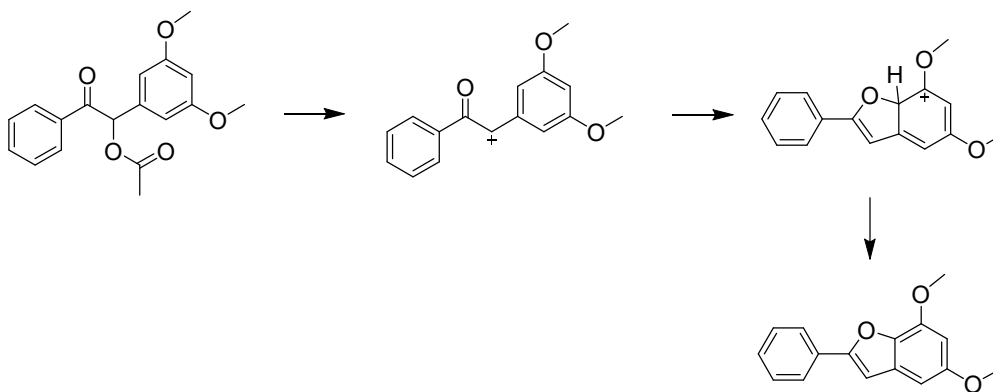


Figure 2-6 Photosolvolysis Mechanism proposed by Shuey and Pirrung in 1994.

### 2.2.2 Application to Solid Phase Synthesis

In 1995, Pirring and Bradley became the first to develop the dimethoxybenzoin cage for use in DNA synthesis.<sup>34</sup> While primarily used for protection of carboxylic acids, the authors reasoned that the dimethoxybenzoin could be converted to an alcohol protecting group via transformation to the carbonate ester. This development was expected to be applicable in light directed synthesis of DNA on a solid support. Rates of deprotection of these novel benzoin carbonates were found to be extremely similar to those of benzoin acetates, indicating a comparable quantum yield.

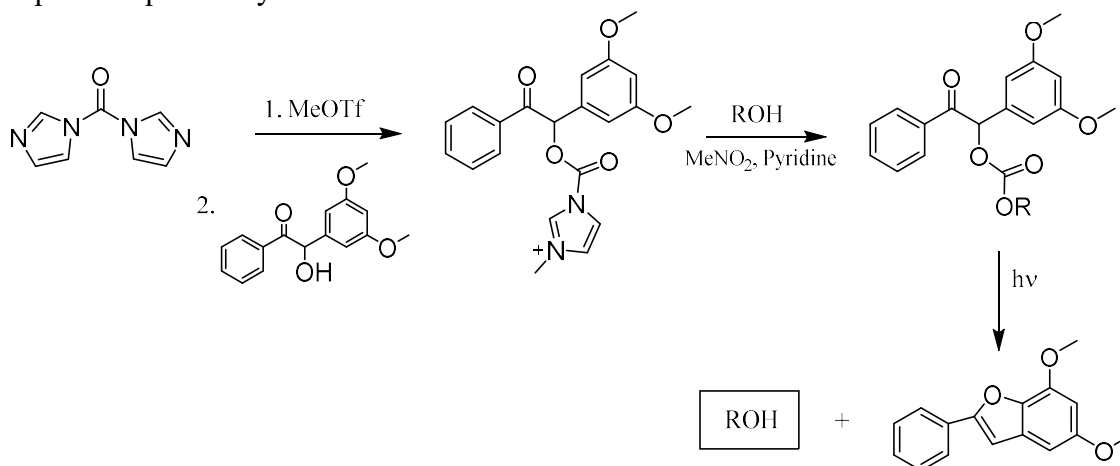


Figure 2-7 Synthesis of 3',5'- dimethoxybenzoin based alcohol protecting group for solid phase synthesis.

The authors noted the highly fluorescent photoproduct and suggested exploiting this feature for the measurement of deprotection by optical methods.

The subsequent publication by Pirrung *et al.* takes further steps towards the development of a novel solid-phase DNA synthesis methodology.<sup>35</sup> This method involved the use of light to deprotect a nucleoside 3'-phosphotriester protect by the dimethoxybenzoin PPG. This generates a phosphodiester which may then be coupled with a free 5'-OH nucleotide.

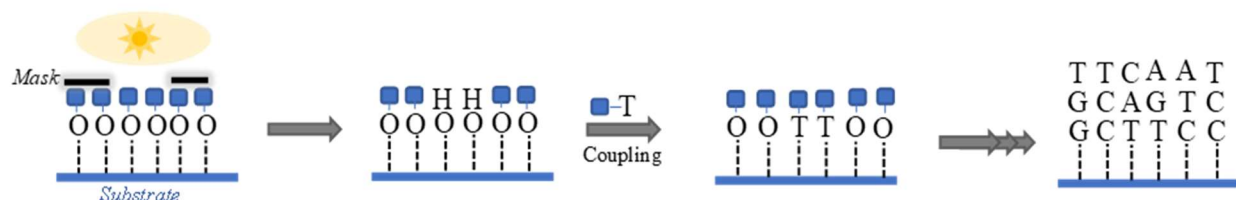


Figure 2-8 Use of protecting groups in solid phase DNA synthesis.

### 2.2.2. Photolabile Linkers Based on 3'-Methoxybenzoin

A lesser known application of photolabile compounds is as a linker, a moiety which bonds two components until light activated release. In 1993 Rock and Chan published their investigation of a benzoin class derivative, 3'-dimethoxybenzoin, for use as a linker in solid phase synthesis and protein folding studies.<sup>36</sup>

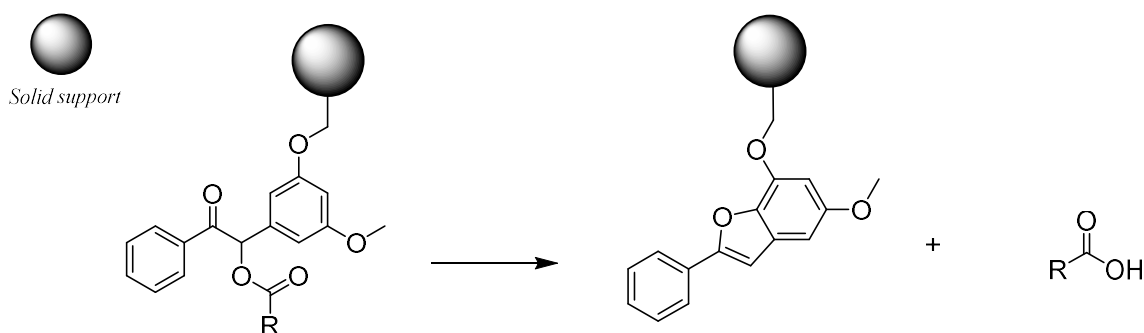


Figure 2-9 A benzoin acetate based photolabile linker.

In order to serve as a linker, the molecule must possess two functional groups suitable for linkage. A carboxylic acid moiety was added to the 3' position of the isolated ring to provide the second linkage location. Here, Rock and Chan tested a synthetic method involving a 1,3-dithiane 'safety catch' to prevent premature photolysis. This is particularly necessary in the seven-step route used to install the carboxyl moiety.

In order to demonstrate its functionality, the synthesized linker was then incorporated into the backbone of a decapeptide and successfully photolyzed to yield the expected products. In the following years the use of the benzoin PPG in photolabile linker technologies, with a specific focus on the dithiane protecting group, was further explored and perfected by Balasubramanian *et al.*<sup>37-39</sup> For use in solid phase synthesis, linkers should be tolerant of a wide range of reaction conditions. HPLC-MS analysis revealed that the dithiane protected linker was reactive towards oxidizing agents and alkylating agents (commonly used in removal of the dithiane moiety), as well as strong acids.

Three reagents, (bis[(trifluoroacetoxy)iodo]benzene, mercury (II) perchlorate, and periodic acid) were tested and each found to cleanly remove the dithiane group from the resin loaded compound. However, use of mercury perchlorate for deprotection is discouraged in biological settings due to the high toxicity of residual Hg(II).

### **2.3. Modern Tools and Novel Applications: 1997-Present**

The period from 1997 to the 2010s is characterized primarily by the use of advanced techniques and instrumentation to probe for mechanistic insight. The emergence of a water-soluble derivative brought new interest to the benzoin class of PPG and further investigation into the mechanism of photorelease. Remarkably, this interest has been sustained, continuing into present day.

#### **2.3.1. Mechanistic Studies of Benzoin Esters and Phosphates**

Driven by the increasing importance of benzoin PPGs in literature, Shi *et al.* began an in-depth study of the mechanism of photorelease, employing nanosecond laser flash photolysis for greater insight.<sup>40</sup> The authors believed that increased knowledge of this mechanism would be not only intrinsically important but would allow for targeted modifications to the molecule. Nanosecond laser flash photolysis in acetonitrile revealed a transient absorption at 485 nm forming within the first 10 ns laser pulse and decaying with first order kinetics. This band was assigned to a new proposed intermediate, a cyclohexadienyl cation (Figure 2-10).

The authors proposed a new mechanism in which the methoxy substituted ring and  $n,\pi^*$  benzoyl form a singlet intramolecular exciplex. This exciplex may then react and break the methine carbon-leaving group bond heterolytically to give the proposed cyclohexadienyl cation precursor to the benzofuran photoproduct.

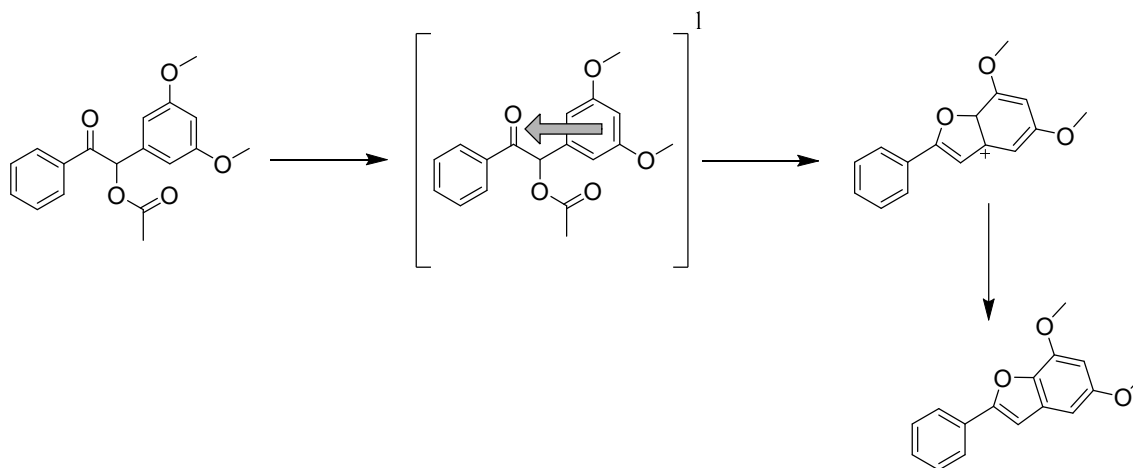


Figure 2-10 Exciplex mechanism proposed by Shi *et al.* in 1997.

The  $\alpha$ -keto cation generated by bond heterolysis proposed by Shuey and Pirrung<sup>33</sup> is not ruled out here, despite no observation of nucleophilic trapping products. In the case that it is formed, it would need to rearrange to the observed cyclohexadienyl cation within 10 ns, not unreasonable for a highly reactive cation such as this. Four leaving groups were tested, including a pivalate ester. The work of Pincock in the area of benzyl and naphthylmethyl ester photosolvolysis inspired this choice.<sup>14</sup> In the studies of these relatively structurally similar molecules, release of the pivalate ester gave high yields of radical derived products as a result of the rapid rate of decarboxylation of acyloxy radicals. Shi *et al.* expected that use of the pivalate leaving group would uncover bond homolysis if present. No radical derived photoproducts were detected, thus supporting a heterolytic mechanism.

The poor water solubility of benzoin-type PPGs is a significant roadblock for use in biological settings. In 1998 Rock and Chan set about modifying the existing 3',5'-dimethoxybenzoin for enhanced water solubility.<sup>41</sup> The introduction of charged functionalities produced a derivative which was found to be water soluble up to 6 mM. The benzofuran photoproduct, known to be even less soluble than the cage itself, was also soluble in this concentration range.

When the water soluble DMB ester was irradiated in methanol, the corresponding benzofuran was formed in the expected quantity. However, irradiation in aqueous buffer yielded only 30% of the benzofuran. GC-MS analysis of the aqueous solutions revealed the cause of reduced yield of the cyclization product, a second major photoproduct. Further characterization revealed this compound to be 3',5'-bis(carboxymethoxy)benzoin, never before observed (Figure 2-11). The authors reason that this is likely due to the low water solubility of the 3',5'-dimethoxybenzoin acetate. When photolysis proceeds in organic solvent the benzoin is not expected to be produced. Additionally, the extinction coefficients of this compound are low in the region of the UV spectrum which is commonly monitored (250-300 nm). These results opened up discussion of the mechanistic pathways and related intermediates. The formation of the benzoin product suggests that an intermediate is open to nucleophilic attack by water. The authors believed this to disfavour the proposed oxetane intermediate.<sup>27</sup> The  $\alpha$ -keto cation suggested by both Givens *et al.*<sup>32</sup> and Shuey and Pirrung<sup>33</sup> was not immediately ruled out. However, the formation of this intermediate by heterolytic cleavage was thought to be associated with  $\sigma,\sigma^*$  rather than  $n,\sigma^*$  excited states. Consequently, a new cyclized biradical intermediate was proposed (Figure 2-11). From this biradical, acetoxy migration may proceed. The resulting intermediate is open to one of two pathways. If water is present, nucleophilic attack at the benzylic carbon will yield the benzoin. In organic solvent the intermediate may rearomatize, yielding the benzofuran.

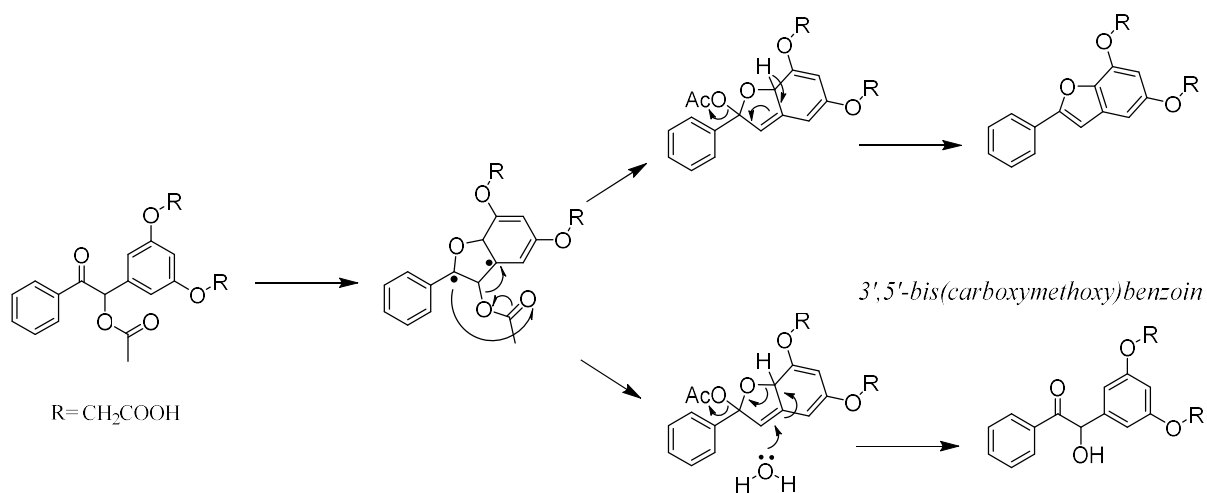


Figure 2-11 Mechanistic pathways proposed by Rock and Chan in 1998.



The development of this water-soluble derivative was not only successful in increasing the number of systems which benzoin type PPGs may be applied in, but also in gaining important insight into this complex photolysis.

The next significant advance in mechanistic understanding came in 2000.<sup>42</sup> This study by Rajesh *et al.* made use of nanosecond and picosecond laser flash photolysis and focused on reactivity of the triplet excited state of benzoin phosphates. The observation of the benzoin photoproduct in aqueous media<sup>41</sup> was also considered and incorporated into the proposed mechanism.

The lifetime of the lowest triplet state, with an absorption maximum at 340 nm, was found to have a lifetime of 10-24 seconds. Previous quenching studies also indicated reaction from a triplet excited state.<sup>11,32,33</sup> In excitation by sub picosecond pump probe spectroscopy experiments the initial singlet excited state underwent intersystem crossing to the observed triplet within a few picoseconds. Two pathways were proposed for the release of diethyl phosphate, both proceeding from the triplet excited state. These pathways are presented in Figure 2-12.

Pathway II, in which the 2-phenylbenzofuran is formed, was proposed to be dominant in most solvents, excluding water and fluorinated alcohols. In order to observe this exceptionally rapid transformation, photolysis was done in solutions of ethanol cooled to -100 °C. At room temperature this transformation occurs within 20 ns, but at -100 °C the transient was observed to decay with a rate constant of approximately  $2 \times 10^6 \text{ s}^{-1}$ . The authors proposed cyclization of the triplet to a biradical benzofuran as the rate determining step. The rapid nature of this reaction did not allow for observation of this intermediate, previously proposed by Rock and Chan.<sup>41</sup>

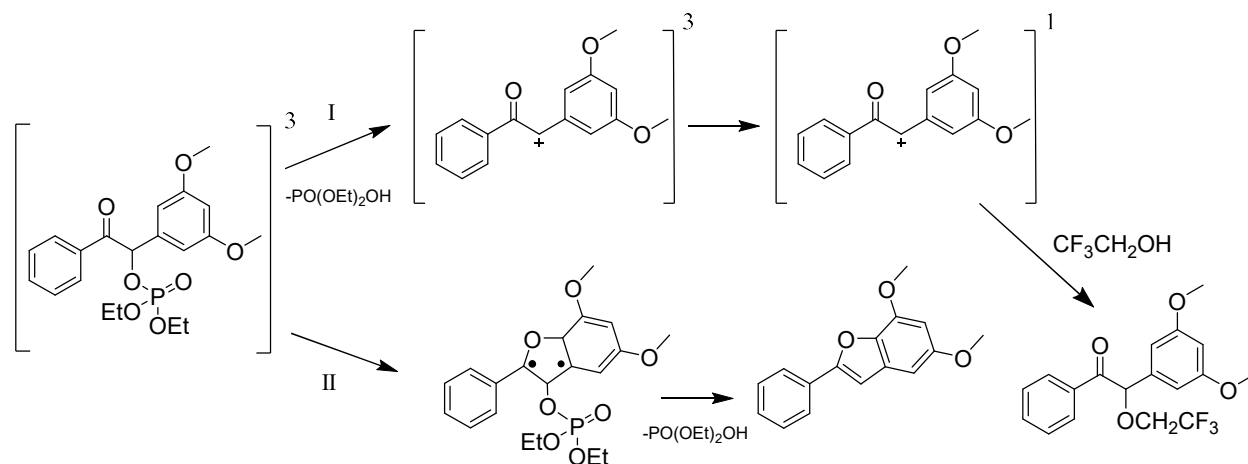


Figure 2-12 Pathways for release of diethyl phosphoric acid proposed by Rajesh *et al.* in 2000.

Pathway I, leading to the nucleophilic addition product, was seen to be dominant only in water and fluorinated alcohols. A new transient intermediate absorbing at 570 nm was observed. Computational work led the authors to identify this transient as the triplet  $\alpha$ -keto cation formed by heterolytic dissociation. ISC of the triplet  $\alpha$ -keto cation is thought to occur quickly thereafter, followed by nucleophilic addition of the solvent. The time scale of this process inhibits the rearrangement of this cation to the cyclization product.

An explanation for the prevalence of these pathways in differing solvents was presented by the lens of computational work. Two conformations of the triplet benzoin phosphate are possible, anti and gauche. The anti-conformation is favored in hydrogen-bonding solvents such as fluorinated alcohols and water. Cyclization of the triplet requires the carbonyl to be in close proximity to the non-conjugated ring, a requirement fulfilled by the gauche conformation. Conversely, the anti-conformation is expected to yield the cationic intermediate via heterolytic bond cleavage and thus the nucleophilic addition product.

Several years later in 2006, Pirrung *et al.* published their account of the photochemical deprotection of benzoin esters, in which several mechanistic alternatives were presented.<sup>43</sup> The authors identified the major unanswered question, whether the photoreaction proceeds via homolysis, heterolysis, or electron transfer. In order to determine whether heterolysis occurs, a Bronsted study on the rates of benzofuran formation with a variety of leaving groups was performed. In the case that the mechanism involves initial heterolysis, this study should uncover a relationship between the enthalpy of heterolysis and the  $K_b$  of the anion. Interestingly this Bronsted study did not reveal any relationship between the parameters, implying that reaction rate is not dependent on the basicity of leaving group. Rate constants for release from cages with a variety of leaving groups with varying  $K_b$  values, spanning 10 orders of magnitude, were essentially identical.

With the confirmation that the bond cleavage step is not rate limiting, femtosecond transient absorption spectroscopy was then employed with the intention of observing evidence of the nature of this bond cleavage. In order to confirm the identity of the expected  $\alpha$ -keto cation, calculations of the energy transitions were carried out. A transient intermediate with absorptions at 650, 620, and 490 nm was observed experimentally. The correlation of these experimental absorptions with the calculated values for the cation led the authors to confirm this intermediate as the expected  $\alpha$ -keto cation formed by initial bond heterolysis.

This species was generated in less than 100 fs and thus it was not possible to identify the relationship between the rate of heterolysis and the basicity of the leaving group.

With these experimental findings a revised mechanism for this photorelease was presented (Figure 2-13).

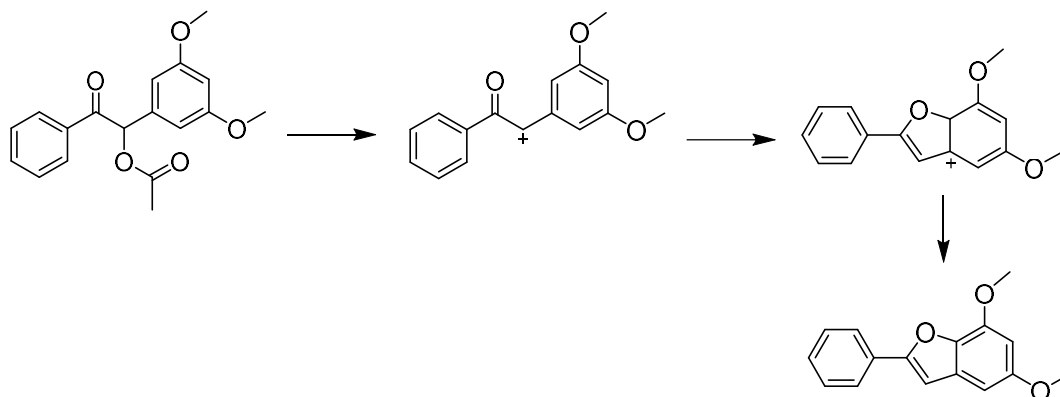


Figure 2-13 Mechanism proposed by Pirrung *et al.* in 2006.

In this proposed mechanism, heterolytic bond cleavage yields the  $\alpha$ -keto cation, which undergoes electrocyclization to a secondary intermediate. Deprotonation of this conjugated intermediate yields the benzofuran. The heterolytic nature of this bond cleavage suggests that generation of the first intermediate is reversible, as seen in ground state ion pair return. The authors suggest that this ion pair return is at least partially responsible for the  $>100\%$  quantum yield. While isotopic labelling studies did not find evidence of ion pair return, this does not mean the process does not occur. The notion that exciplex formation may occur<sup>40</sup> is addressed here. While the authors found this idea reasonable, the time scale on which the cationic intermediate was seen to form would likely discount this mechanism. Further, this time scale also suggested reaction from the singlet excited state.

In 2007 Boudebous *et al.* published their investigation of benzoin acetate and benzoin fluoride with subpicosecond laser flash photolysis and pump probe spectroscopy.<sup>44</sup> The biradical intermediate first proposed by Rock and Chan<sup>41</sup> and later Rajesh *et al.*<sup>42</sup> was evidently observed here.

Excitation of 3',5'-dimethoxybenzoin cages with acetate and fluoride leaving groups and subsequent investigation by pump-probe spectroscopy was the primary focus of this study. The lowest singlet excited state was observed within 1 ps of excitation as a strong 330 nm peak with additional broad absorption in the visible region.

As this band decays, a new 355 nm peak attributed to the biradical intermediate increases. This intermediate was observed to have a lifetime of approximately 2 ns. Two other transients were subsequently observed. The absorptions at 330 and 480 nm were assigned to the triplet excited state. This  $\pi\pi^*$  state, with a lifetime of  $>2$  ns, decays to the ground state without participation in the reaction course. As a result, cyclization to the biradical from the singlet excited state competes with ISC. Decay of the biradical in acetonitrile was accompanied by the increase of a 480 nm peak, attributed to a cyclic cation (Figure 2-14) with a 500 ns lifetime. This cation finally yields the observed benzofuran photoproduct.

For reaction in water or aqueous acetonitrile, the authors state their belief in addition through the keto cation rather than pathway suggested by Rock and Chan.<sup>41</sup> This classification of solvents into polar and nonpolar is in opposition to the previously noted differing behaviour of hydrogen-bonding solvents.<sup>42</sup>

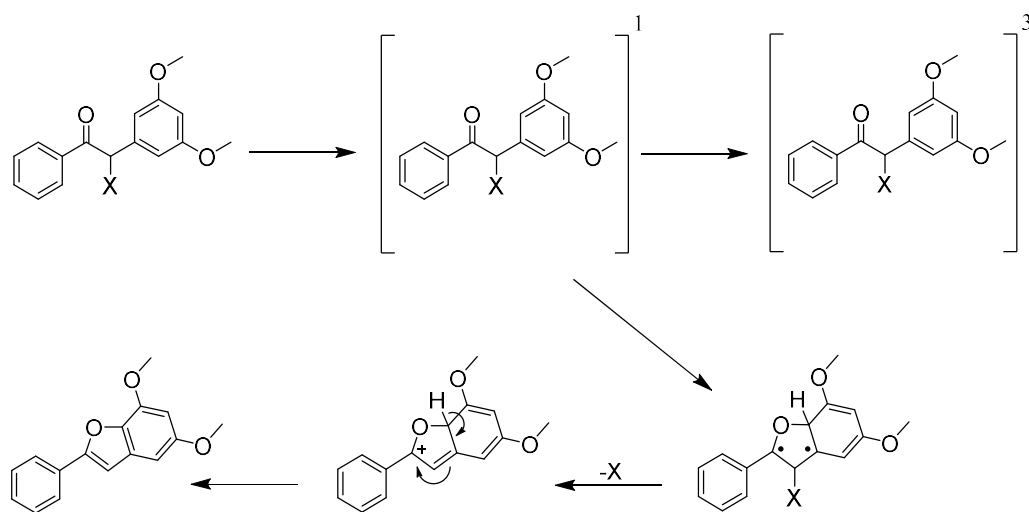


Figure 2-14 Mechanism for reaction in acetonitrile proposed by Boudebous et al. in 2007.

### 2.3.2. Unconventional Applications

The sheer number of publications focused on mechanistic insight have overshadowed those which concern clever applications of the benzoin cage. A refocus on practical applications, as well as targeted improvements to the class, is key to increasing the use of benzoin PPGs. Recent literature involving the innovative application of these PPGs is presented here, as a direct contrast to the plentiful computational and Raman studies on the mechanism of photorelease which have dominated the 2000s.<sup>45-48</sup>

With the increasing importance of drug delivery systems which are responsive to remote stimuli such as light, chromophores such as PPGs have found new application.<sup>49-53</sup>

The benzoin PPG has potential in such applications due to the exceptional properties of this photoreaction. The fluorescent nature of the benzofuran, which itself is inert and highly stable, makes for a convenient 'release and report' method for monitoring reaction progress in drug delivery systems.

Prodrugs are molecules in which an inactive form of a drug may be converted to the active compound by a stimulus. In 2006, McCoy *et al.* incorporated the benzoin PPG into a dual mode prodrug of acetyl salicylic acid.<sup>54</sup> This system is responsive to both the chemical environment and an external light stimulus. Release via hydrolysis is slow and sustained while liberation of the drug via photolysis is rapid and controllable. The success of this dual mode prodrug was important in the context of the development of innovative compounds for light triggered drug delivery.

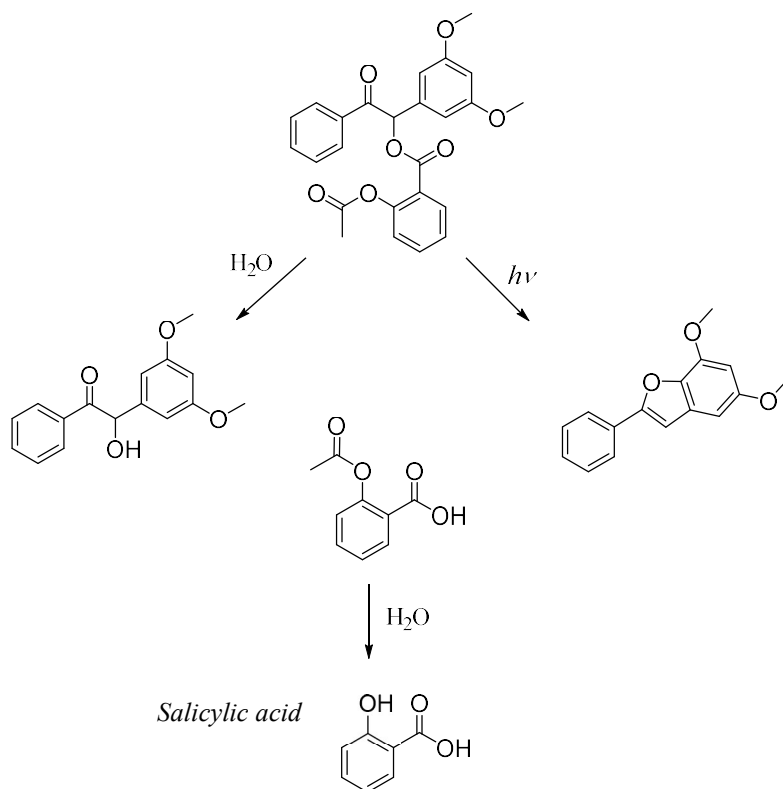


Figure 2-15 Hydrolytic and photochemical release of salicylic acid.

McCoy *et al.* then investigated the ability of dimethoxybenzoin conjugates to release a range of model drugs.<sup>55</sup>

After demonstrating the release of acetyl salicylic acid, ibuprofen, and ketoprofen from benzoin pro-drugs, this reaction was then translated into macroscale drug dosing via incorporation into a polymeric scaffold. A suitable scaffold retains the photoproduct(s) while simultaneously allowing the released drug to diffuse. Additionally, the material must not absorb at the wavelength of irradiation. A 365 nm light source was utilized in order to minimize tissue damage from UV light. The successful release of acetyl salicylic acid, ibuprofen, and ketoprofen from a polymeric scaffold was demonstrated. This was an important proof of concept for the ability of the benzoin PPG to deliver highly controlled doses of numerous medications.

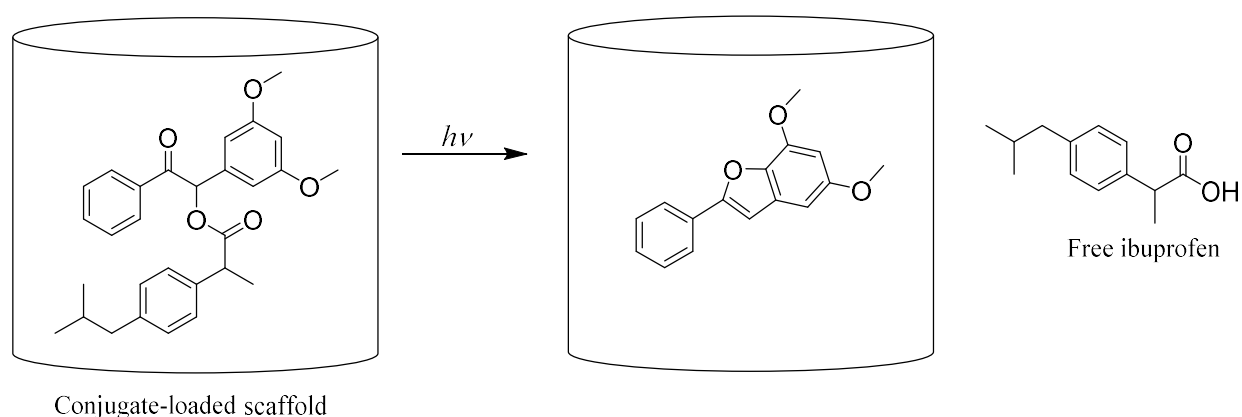


Figure 2-16 Photorelease of ibuprofen from a polymeric scaffold for application as a light controlled drug dosing device.

The union of upconverting nanoparticles and PPGs for release of caged compounds with low energy light was both unexpected and extraordinary. A hybrid system of this type was first published by Carling *et al.* in 2010.<sup>56</sup>

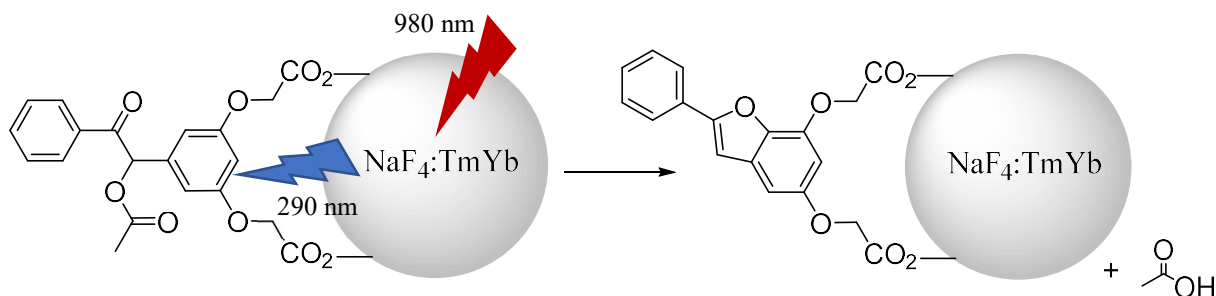


Figure 2-17 Release of acetic acid from benzoin acetate decorated upconverting nanoparticles with NIR light.

Direct multiphoton excitation with near infrared (NIR) light is an alternative to high energy UV light. However, many PPGs do not have sufficient two photon cross sections and thus are not suited for multiphoton excitation. This deficiency may be overcome by the use of upconverting nanoparticles (UCNP). Lanthanide doped NaYF<sub>4</sub> nanoparticles are capable of converting NIR light to UV light of various wavelengths. When chromophores such as benzoin acetate PPGs are anchored to the surface of these nanoparticles, the UV light resulting from the upconversion of NIR photons triggers the desired photorelease.

The success of this hybrid organic-nanoparticle system in overcoming the need for high energy UV light in photorelease was significant. The authors suggested modification of the PPG in order to better overlap with emission from the UCNPs and subsequently improve the overall efficiency of this remote-control release. The most intense emission bands from these specific UCNP are at 333-355 nm, and thus redshifted derivatives would be more suitable for application in this system.

### 2.3.3. Outlook

A complete picture of the lengthy history of the benzoin class of PPGs is necessary to chart a course forward. Practical use of the cage, primarily in biochemistry, peaked in the late 1990s. These studies made use of the molecule conceived by Sheehan *et al.* in 1971, 3',5'-dimethoxybenzoin acetate.<sup>27</sup> This is unusual in and of itself in the context of the development of prominent classes such as 2-NB and coumarins. More commonly various derivatives are synthesized for improvement of photochemical properties before or alongside practical application. This difference may be due to the exceptional baseline properties of the original molecule. Over time other classes of PPGs have been continuously improved, while the benzoin class has remained unchanged. In contrast, interest in the benzoin class has been hyper-focused on determination of the mechanism of photorelease since the late 1990s. While mechanistic interest is not inherently negative, the majority of literature in this area is contradictory and involves speculation on extremely short-lived intermediates. The complexity of this system and the time scale on which photorelease takes place indicates that this mechanism will realistically remain unproven. The combination of these factors and their timing has likely resulted in the stagnancy of this class and its increasing decline in literature. The development of novel derivatives serves

first and foremost to improve and diversify the class, but insight into key intermediates and alternate pathways may also be a product of this work.

Additionally, the improvement of photochemical properties is subjective. While efficient release with  $>365$  nm light is preferred for biological systems, a 312 nm light source may be sufficient or preferred in others. This is where having a wide variety, or ‘toolbox’ of benzoin PPGs is useful. The molecules presented in Chapter 3 and Chapter 4 seek to expand this toolbox of benzoin PPGs available for application in a wide variety of settings.



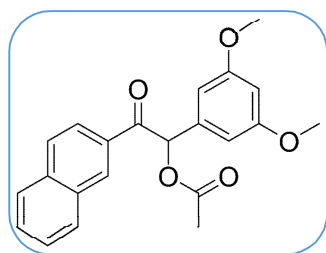
## Chapter 3. Preparation and Photochemistry of Polyaromatic Benzoin Acetate Photoremovable Protecting Groups

### 3.1. Abstract

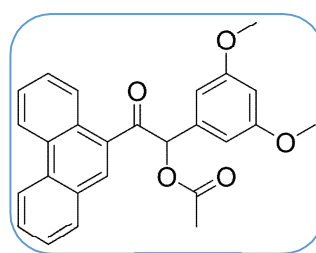
Two novel photoremovable protecting groups (PPGs) in the benzoin class have been prepared and their photochemistry investigated. These polyaromatic benzoin PPGs have significantly improved molar extinction coefficients with absorption extending towards 400 nm.

### 3.2. Introduction

In this work, two 3',5'-dimethoxybenzoin derivatives are synthesized for release of caged carboxylic acids with fluorescence reporting. The parent 3',5'-dimethoxybenzoin acetate is additionally prepared for comparative purposes. Successful release of acetic acid has been proven to translate well to the release of numerous functionalities, and thus this simple caged species is used here.<sup>11,21</sup> These molecules were developed via Strategy I, extension of conjugation. Additional conjugation is installed on the benzoyl ring, the moiety responsible for absorption of a photon to reach the excited state.<sup>42</sup> Extending conjugation of the benzoyl system is expected to increase probability of the molecule to absorb a photon as well as to induce a bathochromic shift of the primary absorption. The novel PPGs introduce naphthalene (**1a**) and phenanthrene (**1b**) aromatics into the benzoyl moiety. This structural modification does not introduce reactive functional groups and thus is unlikely to result in deviation from characteristic benzoin photochemistry. The novel PPGs are seen to react as the parent benzoin acetate **1P**, releasing acetic acid and yielding primarily the cyclization products, biologically inert and highly fluorescent benzofurans



**1a**



**1b**

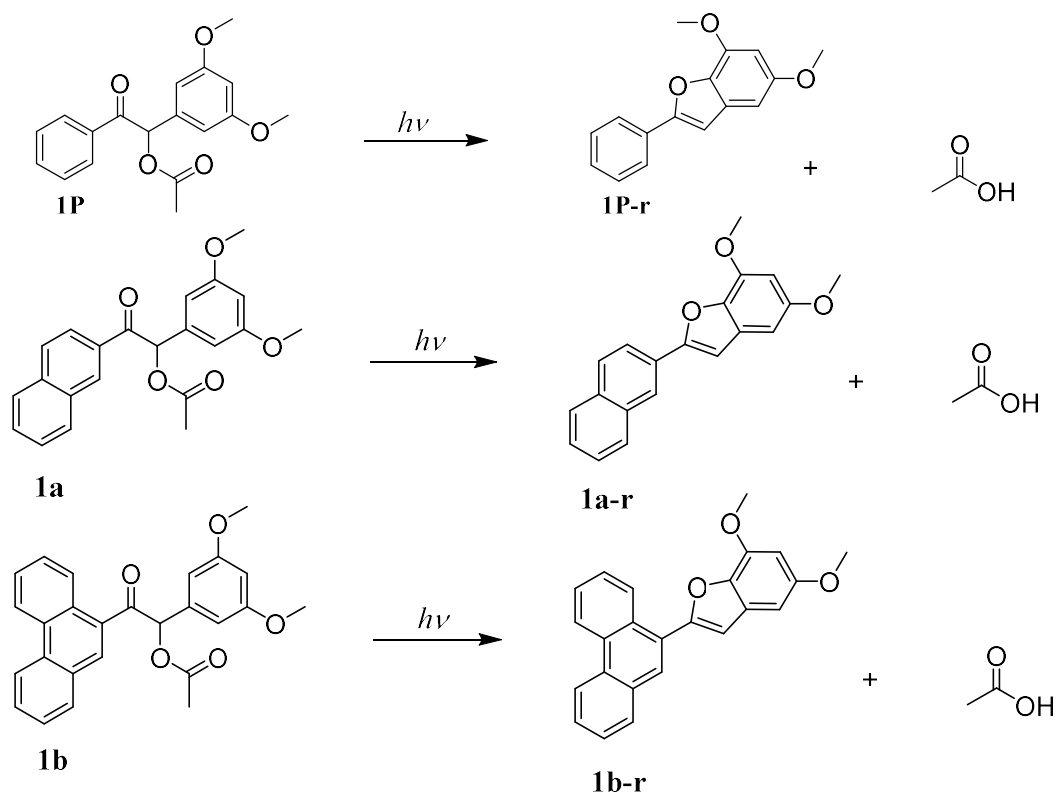
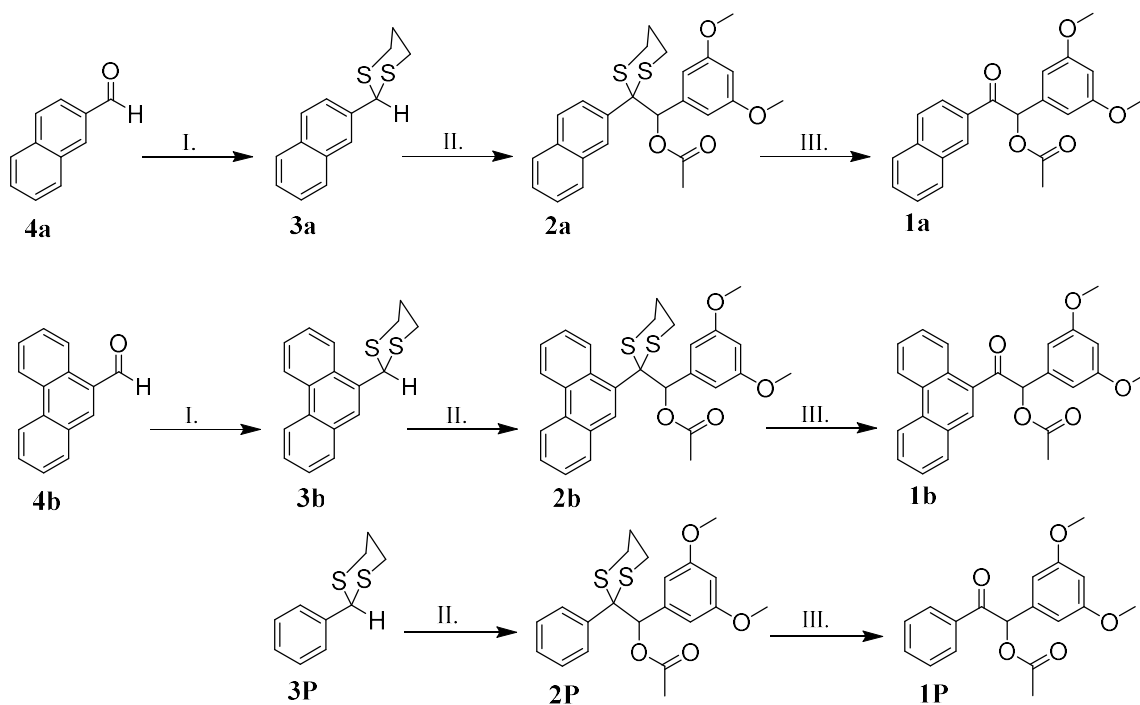


Figure 3-1 Photochemical release of acetic acid from compounds **1P**, **1a**, and **1b** with conversion to corresponding benzofuran cyclization products **1P-r**, **1a-r**, and **1b-r**.

PPGs **1a** and **1b** were synthesized in three steps. The commercially available aromatic aldehydes are first converted to their corresponding 1,3-propyldithianes. The robust propyl dithiane protecting group may be considered as a ‘safety catch’, preventing the molecule from becoming photoactive before the final synthetic step in which the protecting group is removed. This allows synthesis to proceed under normal light conditions until the final step without risk of premature photorelease. The aromatic dithianes then serve as nucleophiles in the Corey-Seebach umpolung reaction in which the benzoyl moiety is installed. While ambient light poses no risk to these compounds, direct UV irradiation results in degradation and minor release of acetic acid. Treatment with  $\text{Hg}(\text{ClO}_4)_2 \cdot 3\text{H}_2\text{O}$  in  $\text{CH}_3\text{CN}/\text{H}_2\text{O}$  rapidly removes the propyl dithiane group and generates the final chromophore. Parent **1P** was synthesized in two steps from the commercially available phenyl dithiane in the same manner as **1a** and **1b**, installation of the benzoyl moiety via the Corey-Seebach reaction and subsequent removal of the dithiane by  $\text{Hg}(\text{ClO}_4)_2 \cdot 3\text{H}_2\text{O}$ . Synthetic procedures and characterization are described in section 3.5, as well as details of the successful application of a mercury free deprotection procedure



- I. Propane dithiol,  $\text{Hf}(\text{OTf})_4$ ,  $\text{CH}_2\text{Cl}_2$ , R.T.  
 II. 1.  $n\text{-BuLi}$ , THF,  $0^\circ\text{C}$  2. 3,5-dimethoxybenzaldehyde, THF,  $0^\circ\text{C}$ -R.T. 3.  $\text{Ac}_2\text{O}$ , DMAP  
 III. 1.  $\text{Hg}(\text{ClO}_4)_2 \cdot 3\text{H}_2\text{O}$ ,  $\text{CH}_3\text{CN}/\text{H}_2\text{O}$ , R.T. 2. Sat.  $\text{NaHCO}_3(\text{aq})$

Figure 3-2 Synthesis of PPGs **1a**, **1b** from commercially available polyaromatic benzaldehydes and synthesis of parent **1P** from commercially available phenyl dithiane.

### 3.3. Results and Discussion

#### 3.3.1. Photochemical Properties of the Parent Benzoin Acetate: A Reinvestigation

Since its conception in 1971, 3',5'-dimethoxybenzoin acetate has been synthesized and investigated extensively. Past this significant initial publication, focus was primarily directed towards elucidating the mechanism of photorelease, release of diverse leaving groups, and to a lesser extent practical application. In this time period, no significant further characterization of the parent or the benzofuran product occurred, despite advances in instrumentation. Further understanding of the molecule is not only advanced by mechanistic understanding but through practical studies of photochemical characteristics. For this reason, the parent benzoin acetate was synthesized here and characterized in the same manner as novel derivatives **1a** and **1b**. Studies of **1P** alongside these derivatives allows for a more direct comparison novel molecules and their photochemical properties.

UV-Vis absorption studies done with broadband light from handheld UV lamps of three wavelengths (254, 312, and 356 nm) demonstrate both the significant self-filtering or ‘inner filter’ effect which is known to be associated with the parent as well as the minimal absorption past 300 nm. The benzofuran photoproduct, in comparison to the cage, is strongly absorbing. The associated absorption peak is centered at 302 nm. This highly absorbing photoproduct hampers reaction progress in what is often referred to as the inner-filter effect. As concentration of the cyclization product in solution increases, it competes for incident light in the near UV (300-400 nm). This results in decreased absorption of light by the cage, and thus increasingly slowed photorelease. The inner filter effect is most prominent in studies carried out with long wavelength incident light. The combination of poor absorption of **1P** in the near UV and this inner filter effect results in slow release with the 365 nm light source.

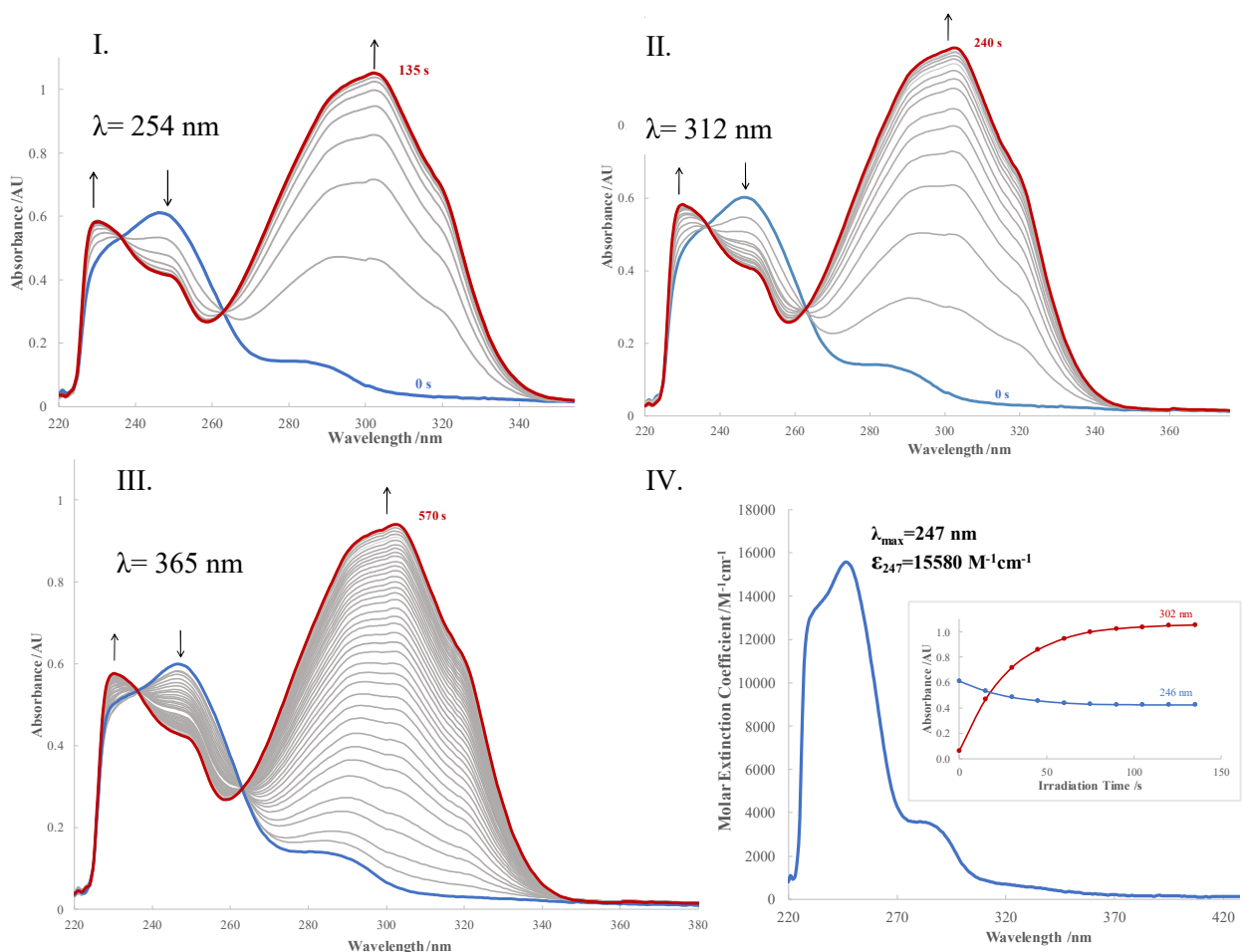


Figure 3-3 UV-Vis absorption spectra of photolysis of **1P** ( $3.82 \times 10^{-5} M$  in  $CH_2Cl_2$ ) with I. 254, II. 312, and III. 365 nm light. IV. Molar extinction coefficient plot of **1P** (Inset: Appearance of product at 302 nm and loss of **1P** at 246 nm with 254 nm irradiation).

When the solution is irradiated with short wave 254 nm light, the photorelease is complete within 135 seconds. With a light source centered at 312 nm, the reaction time nearly doubles to 240 seconds. With the 365 nm light source, the reaction progress is again significantly slowed, with completion in 570 seconds. Improving absorption of the cage in relation to the associated benzofuran is important in eliminating the inner filter effect and thus efficiency of release.

The presence of clear isosbestic points at 236 and 263 nm, the feature which first piqued the interest of Sheehan *et al.*, is indicative of conversion to the benzofuran with minimal formation of secondary photoproducts at this concentration scale and duration of irradiation.

Maximum absorption of the parent benzoin acetate occurs at 247 nm, a higher energy than what would be required for use in biological settings. Polyaromatic derivatives **1a** and **1b** seek to redshift this primary absorption peak and achieve efficient release with lower energy light sources. The molar extinction coefficient at 247 nm was calculated to be  $15680 \text{ M}^{-1}\text{cm}^{-1}$ , slightly higher than the  $14,250 \text{ M}^{-1}\text{cm}^{-1}$  reported by Sheehan.<sup>27</sup> Complete elimination of ethyl acetate from these compounds proved to be a challenge. Several cycles of dissolution in DCM and 24-hour drying periods with high-vacuum are required to remove the bulk of residual solvent. These cycles should total at minimum 7 days.

If removal of solvent is not complete the true mass of compound weighed is unknown and thus the uncertainty in determined concentrations and resulting extinction coefficients is high. This may account for discrepancy in extinction coefficients reported for these molecules as well as varying descriptions of texture/appearance of the material, which is a tacky solid before the described cycles of drying. Satisfactory drying should yield a fine powder which can be easily weighed and transferred quantitatively. Additionally, while the use of amber vials and glassware can provide a secondary layer of protection from ambient light, they are not appropriate as a primary defense. Full coverage of all vials, NMR tubes, and volumetric glassware with aluminum foil is necessary to prevent premature photorelease in these highly sensitive PPGs. When NMR tubes uncovered for analysis, room lights must be switched off and blinds drawn.

While  $^1\text{H}$  NMR spectra of these compounds exist in literature, use of NMR to monitor reaction progress has not been fully utilized. If long-lived intermediates are involved in the reaction, these may be observed in such NMR studies. This is not the case in the rapid reaction of **1P**, in which the benzoin acetate is quickly cyclized with no observable intermediates. However, there is value in observing the course of these reaction via NMR spectroscopy. Minor photoproducts may be identified, and the extent of release and cyclization is easily estimated.

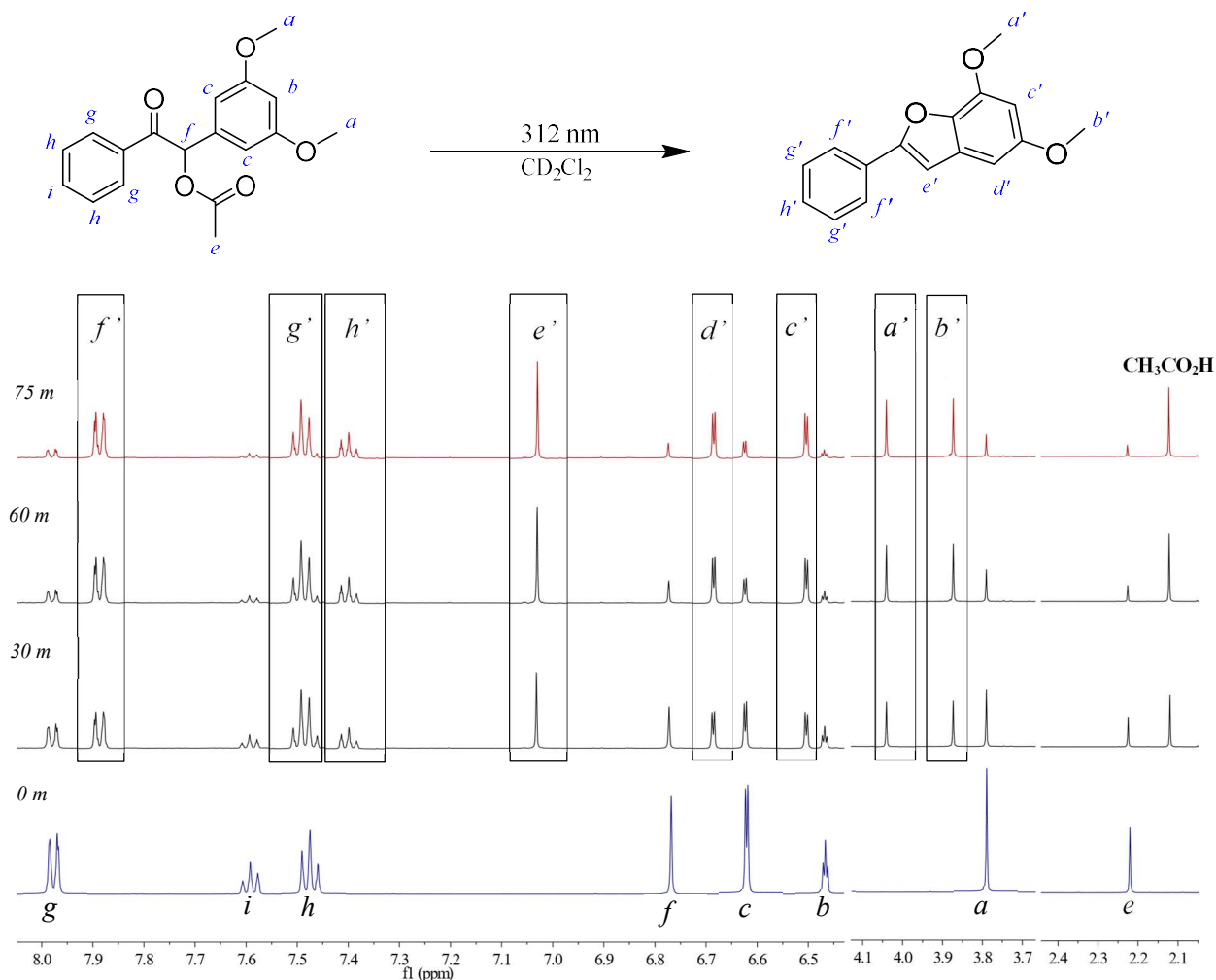


Figure 3-4 Evolution of selected regions of  $^1\text{H}$  NMR spectra throughout duration of irradiation of **1P** with 312 nm light.

NMR spectra at various intervals throughout the photolysis are presented in Figure 3-4. At the outset of the reaction, lack of release is clearly indicated by the absence of the characteristic acetic acid peak at 2.1 ppm. Complete elimination of all ambient light in purification and subsequent analyses is needed due to the extremely rapid nature of this photorelease.

In the structure of **1P** the 3' and 5' methoxy groups are chemically equivalent. As the reaction proceeds, this six proton peak at 3.75 ppm decreases, and two new three proton signals appear at 3.8 and 4.0. When cyclization occurs, the methoxy groups become chemically inequivalent due to proximity of the furan, pushing the 3' methoxy signal *a'* downfield. Release of acetate is confirmed by decrease of the three proton 2.15 ppm peak which is accompanied by the appearance and subsequent increase of the 2.1 ppm acetic acid signal.

Signals 6.48 and 6.65 correspond to protons *b* and *c* on the non-conjugated ring of **1P**. With cyclization to **1P-r**, two proton *c* peak is replaced by a one proton signal at 6.68 ppm. Its coupling partner *b* is similarly replaced by the slightly shifted 6.50 ppm doublet corresponding to *c'*. Additionally, the 6.75 ppm singlet, corresponding to proton *f*, decreases to a minimum throughout the reaction. This is accompanied by the appearance of a new singlet at 7.05 ppm which may be assigned to proton *e'* of the benzofuran.  $^4J$  coupling on the ring between protons *c'* and *d'* is observed, but *d'* does not couple with neighbour *e'*.

The displayed reactions on the  $^1\text{H}$  NMR scale were pushed to ~75%. This extent is more than sufficient for the identification of photoproducts without risk of decomposition. Taking release to >90%, while easily achievable on a UV-Vis  $\mu\text{M}$  concentration scale, is extremely time consuming at mM concentrations.

The chosen light source, medium wave UV light, is ideal for accomplishing relatively efficient release while avoiding the risk of degradation that comes with the use of high energy 254 nm light.

The cyclization product may be separated from the photolysis solution via flash column chromatography. Isolation of a significant amount of this molecule allowed for full characterization and structural confirmation. This benzofuran is not photosensitive, and thus may be handled in normal light conditions. Its strong fluorescence allows for visual confirmation of release.  $^1\text{H}$  and  $^{13}\text{C}$  NMR spectra of the photoproduct were obtained, as well as a UV-Vis spectrum. As seen in Figure 3.4, the  $^1\text{H}$  NMR spectrum of parent benzofuran **1P-r** matches well with that of the final photolyzed solution.

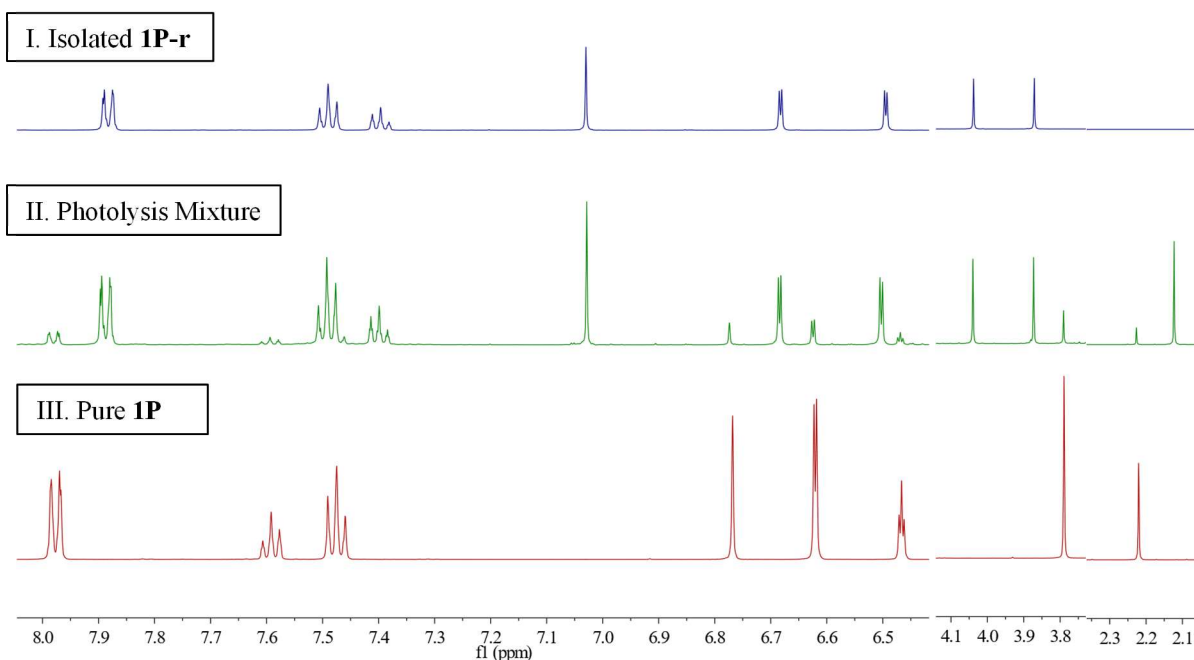


Figure 3-5  $^1\text{H}$  NMR comparison of (I) Isolated benzofuran, (II) Photolysis mixture-75 m, and (III) Photocage 0 m.

A 30  $\mu\text{M}$  solution of this molecule was prepared and analyzed by UV Vis spectroscopy. The UV-Vis spectra of the photoproduct and final photolyzed solution are essentially identical (Figure 3-6), suggesting nearly quantitative release and cyclization with these specific reaction conditions.

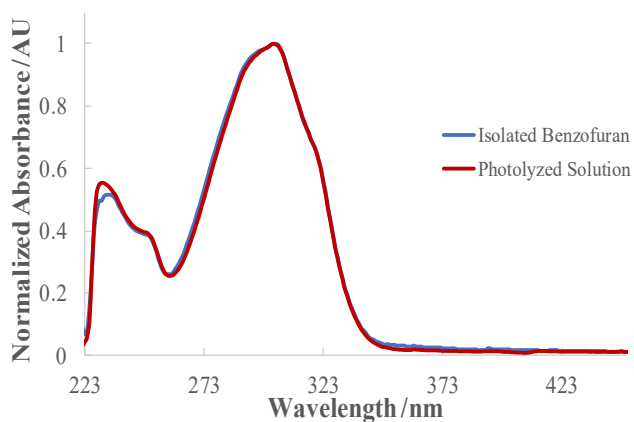


Figure 3-6 Normalized UV-Vis absorbance spectra of isolated benzofuran (30  $\mu\text{M}$  in DCM) and photolyzed solution of **1P**.



### 3.3.2. Polyaromatic Derivatives

The two polyaromatic derivatives were prepared with the intention to extend conjugation of the benzoyl moiety. Results of this structural modification are discussed here within the context of new data on the parent benzoin acetate **1P**.

#### 3.4.2.1 Naphthalene (1-(3,5-dimethoxyphenyl)-2-(naphthalen-2-yl)-2-oxoethyl acetate)

UV-Vis absorption spectra of solutions of **1a** in DCM at various stages of photorelease were obtained.

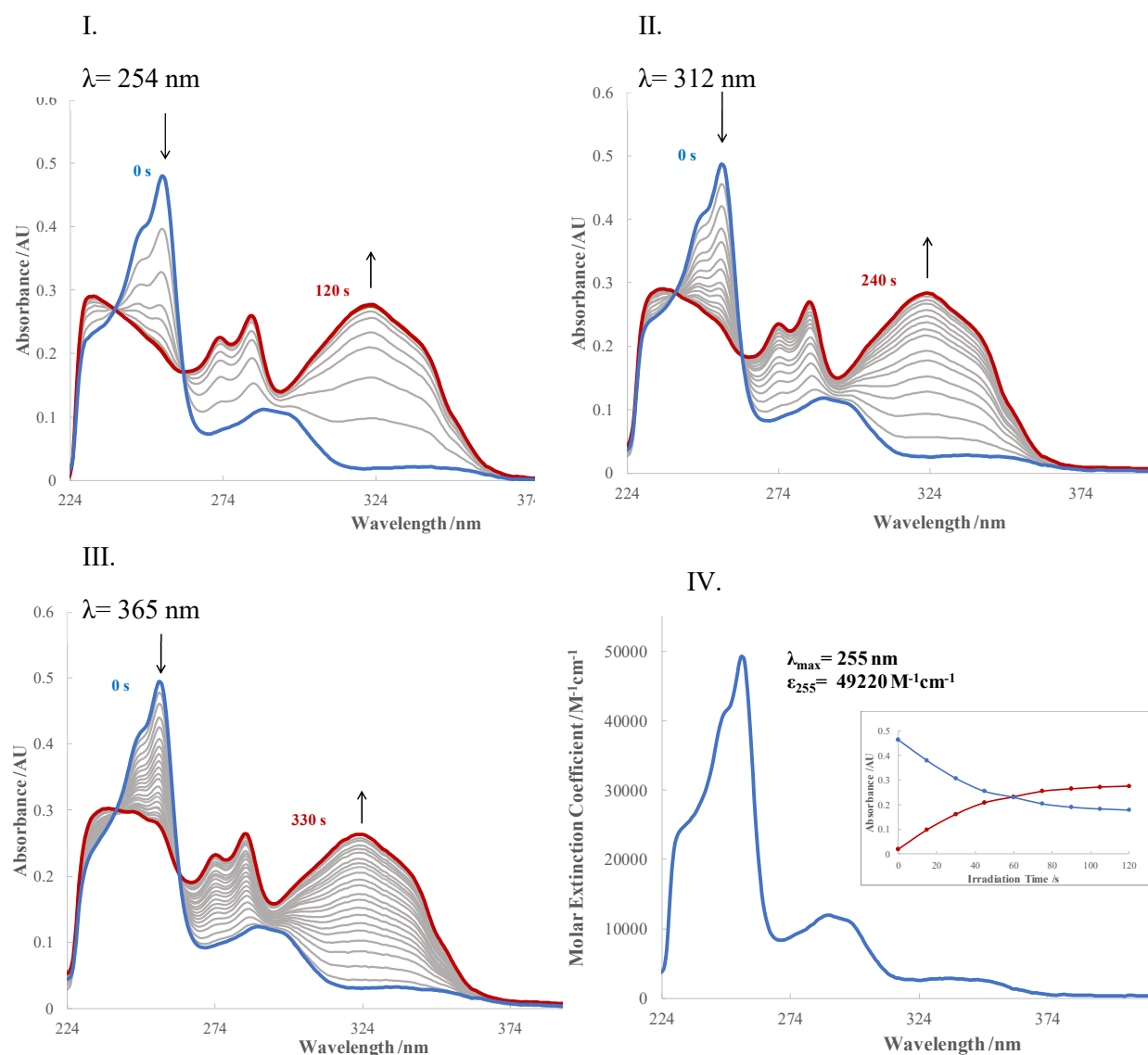


Figure 3-7 UV-Vis absorption spectra of photolysis of **1a** ( $9.88 \times 10^{-6} \text{ M}$  in  $\text{CH}_2\text{Cl}_2$ ) with I. 254, II. 312, and III. 365 nm light. IV. Molar extinction coefficient plot of **1a** (Inset: Appearance of product at 323 nm and loss of **1a** at 255 nm with 254 nm irradiation).

As presented in Figure 3-7, three primary absorptions are exhibited by the starting material. A sharp peak at 254 nm is the strongest absorption. In comparison to the primary absorption of **1P** at 247 nm, this represents a 7 nm redshift. The next absorptions are broadly from 270 to 315 nm (peak centered at 290), and from 320 to 365 nm. As the solution was irradiated in 15 second intervals, the 254 nm peak decreased significantly. Three new peaks gradually appeared as the reaction proceeded. Two peaks, appearing to be partially coalesced, were present at 273 and 282 nm. A broad absorption centered at 321 nm also appeared. Isosbestic points are present at 240 and 262 nm.

When the study was carried out with a 254 nm lamp, photolysis was complete within 120 seconds. Reaction times increased to 240 and 330 seconds in studies with 312 and 365 nm lamps, respectively. These kinetics followed the same pattern as **1P**, as would be suggested by the comparable absorption profiles. However, the margins between these times are significantly smaller than in the equivalent studies of **1P**. The extinction coefficients were calculated to be  $49200 \text{ M}^{-1}\text{cm}^{-1}$  at 255 nm and  $1050 \text{ M}^{-1}\text{cm}^{-1}$  at 365 nm. These coefficients are a much improved in comparison to **1P**, 316% at the primary  $\sim 250$  nm peak and, more significantly, 504% at 365 nm.

The photolysis of **1a** in  $\text{CD}_2\text{Cl}_2$  was then monitored by  $^1\text{H}$  NMR. Due to the number of aromatic protons in this molecule, multiplets appear in the aromatic region from 7.50-8.0. However, protons *b*, *c* (on the dimethoxy ring) and *f* are well resolved, as in the case of **1P**. Again, methoxy protons *a* are equivalent in the cage molecule, and appear as a 6H signal at 3.75. As photolysis occurs and **1a** is converted to **1a-r**, the methoxy groups become inequivalent and this signal decreases as two new 3H signals at 4.05 and 3.90 appear, corresponding to the 3' and 5' protons respectively. As acetic acetate is released, the signal corresponding to proton *e* of the leaving group decreases in intensity as the characteristic acetic acid signal at 2.1 ppm appears. As cyclization occurs, signal *f* decreases as the 7.15 ppm benzofuran proton *e'* increases. The furthest downfield signal, *g* at 8.55, decreases in intensity as the equivalent *f'* in **1a-r** appears slightly upfield at 8.40 ppm.

The benzofuran photoproduct was then isolated via flash column chromatography. As seen in Figure 3-9, the  $^1\text{H}$  NMR spectrum of this compound matches well with that of the photolyzed solution.

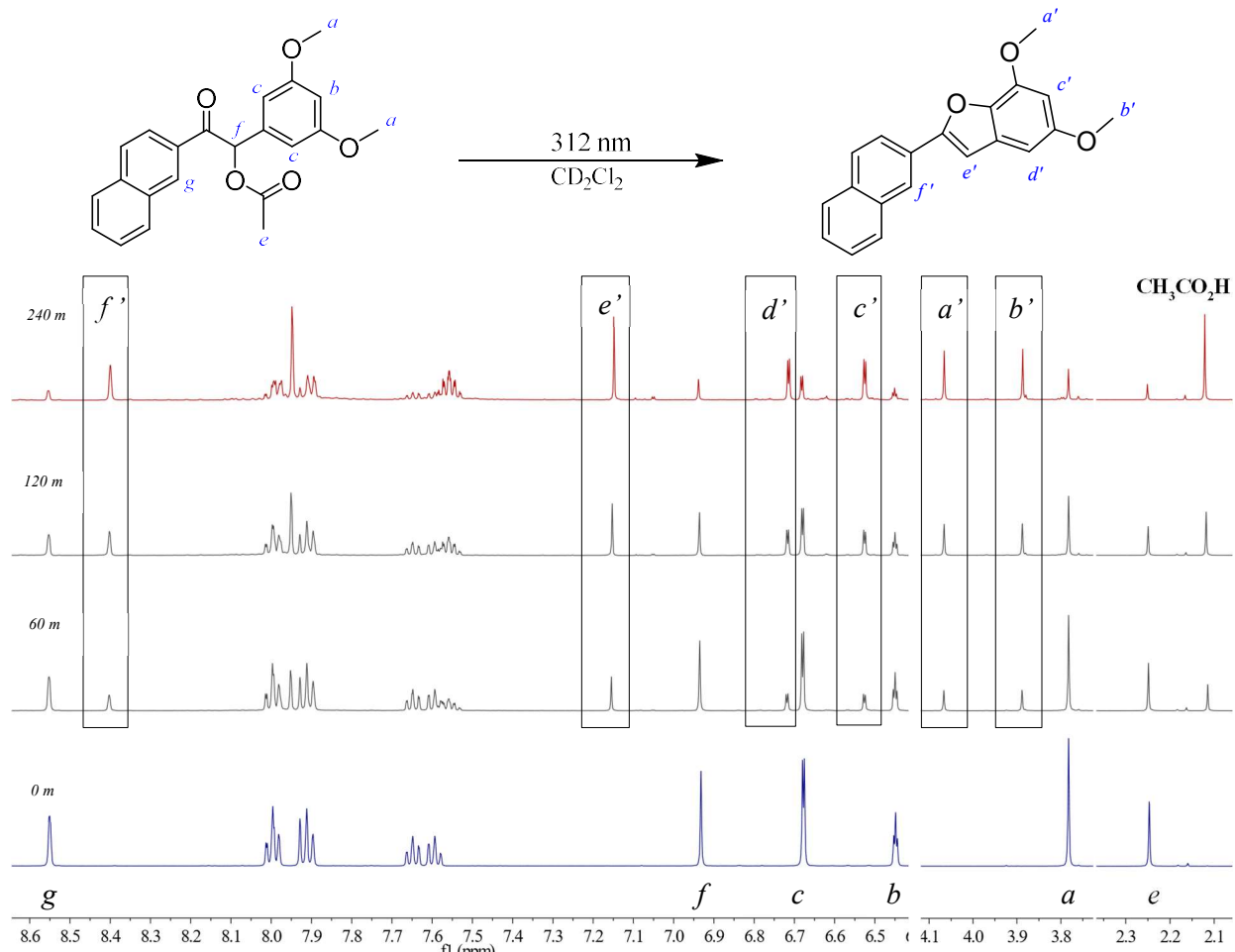


Figure 3-8 Evolution of selected regions of  $^1\text{H}$  NMR spectra throughout duration of irradiation of **1a** with 312 nm light.

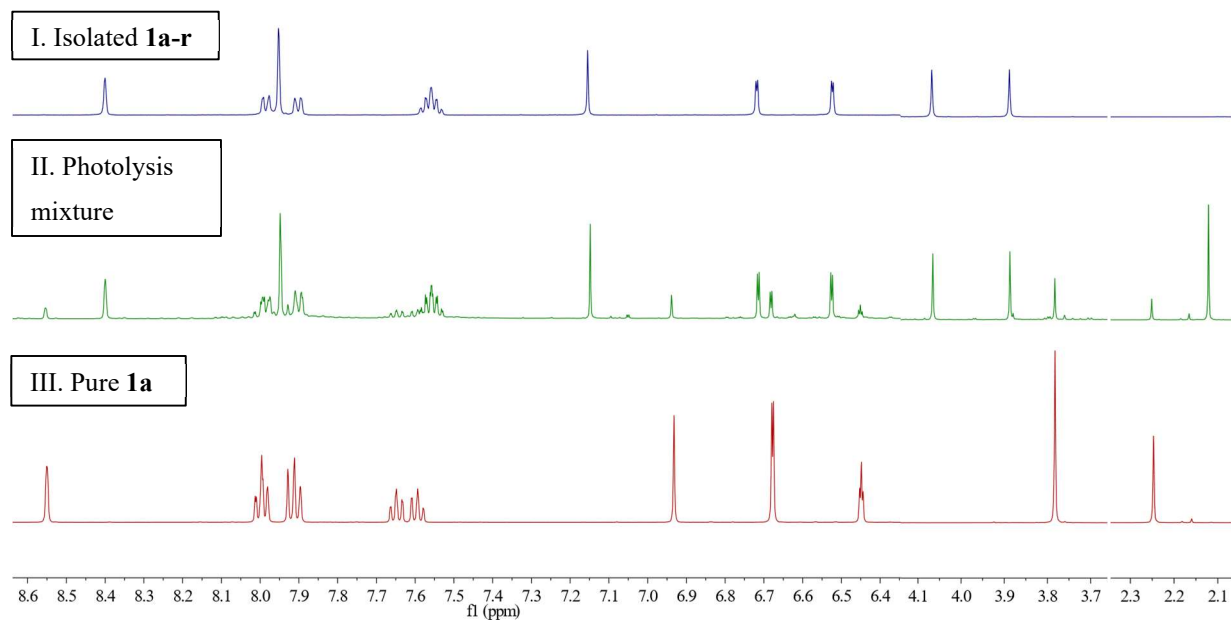


Figure 3-9  $^1\text{H}$  NMR comparison of (I) Isolated benzofuran (II) Photolysis mixture- 240 m, and (III) Photocage **1a**

### 3.4.2.2 Phenanthrene (1-(3,5-dimethoxyphenyl)-2-oxo-2-(phenanthrene-9-yl)ethyl acetate)

UV-Vis absorption spectra of solutions of **1b** in DCM at various stages of photorelease were obtained. The UV-Vis progression differs from those observed for molecules **1a** and **1P**. The primary absorption is centered at 250 nm, with a 230 nm shoulder. This absorption is broad with a gradual taper in intensity until approximately 400 nm. Upon exposure to UV light, this 250 nm peak begins to slightly decrease and give way to a redshifted absorption at 256 nm.

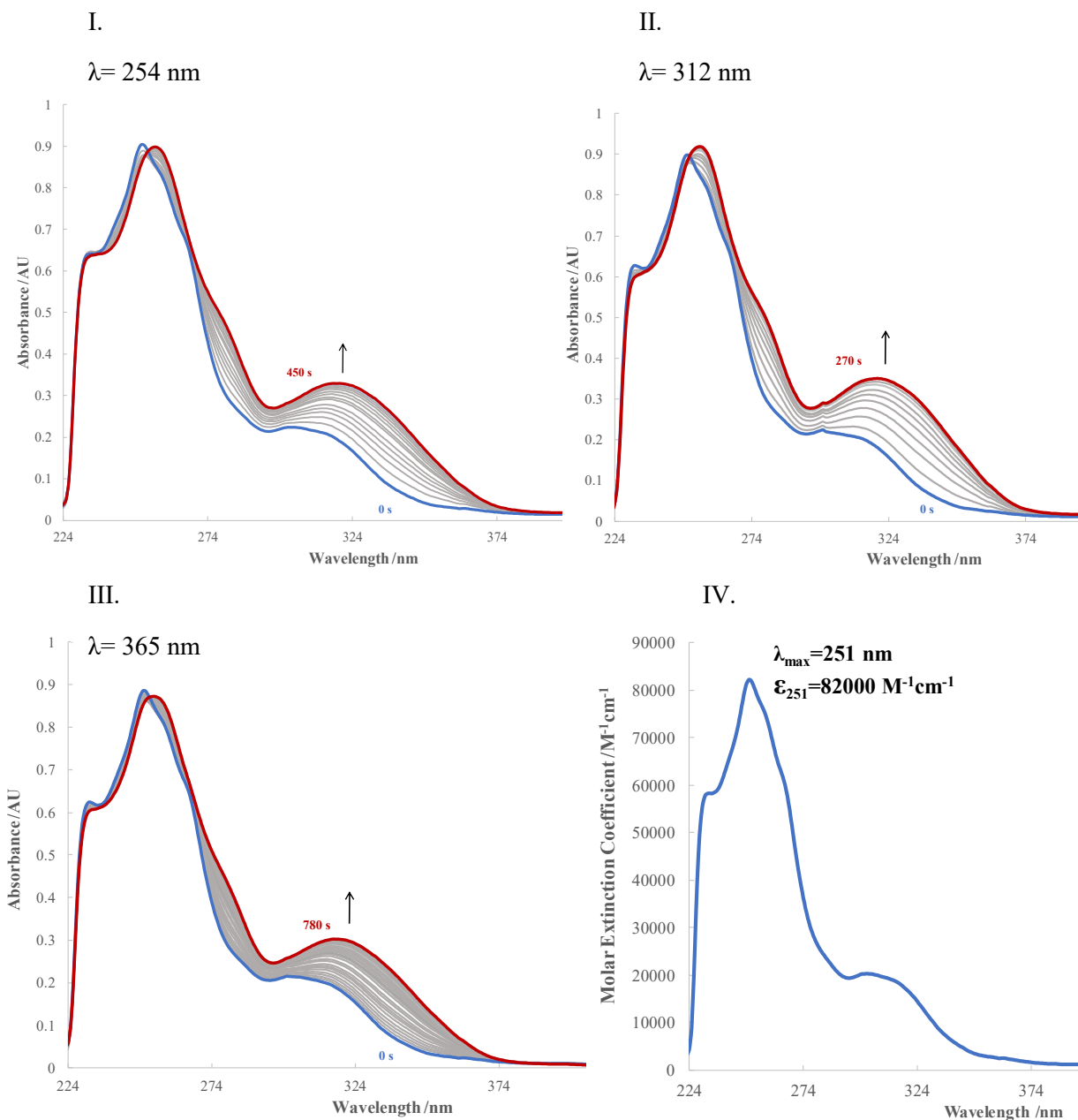


Figure 3-8 UV-Vis absorption spectra of photolysis of **1b** ( $11.0 \times 10^{-6} M$  in  $CH_2Cl_2$ ) with I. 254 II. 312 nm and III. 365 nm light. IV. Molar extinction coefficient plot of **1b**.

The area between 300 and 380 nm increases, giving way to a moderate peak centered at 325 nm. Isobestic points are not present, indicating one or more minor photoproducts.

Exhaustive removal of solvent from samples of **1b** allows for relatively accurate determination of extinction coefficients, an exceptional  $82,000 \text{ M}^{-1}\text{cm}^{-1}$  at 251 nm and  $2460 \text{ M}^{-1}\text{cm}^{-1}$  at 365 nm. In reference to **1P**, this represents a 530% increase at 251 nm, and a 780% increase at 365 nm. The differing absorption profiles of **1b** and the associated benzofuran may account for this interesting behaviour.

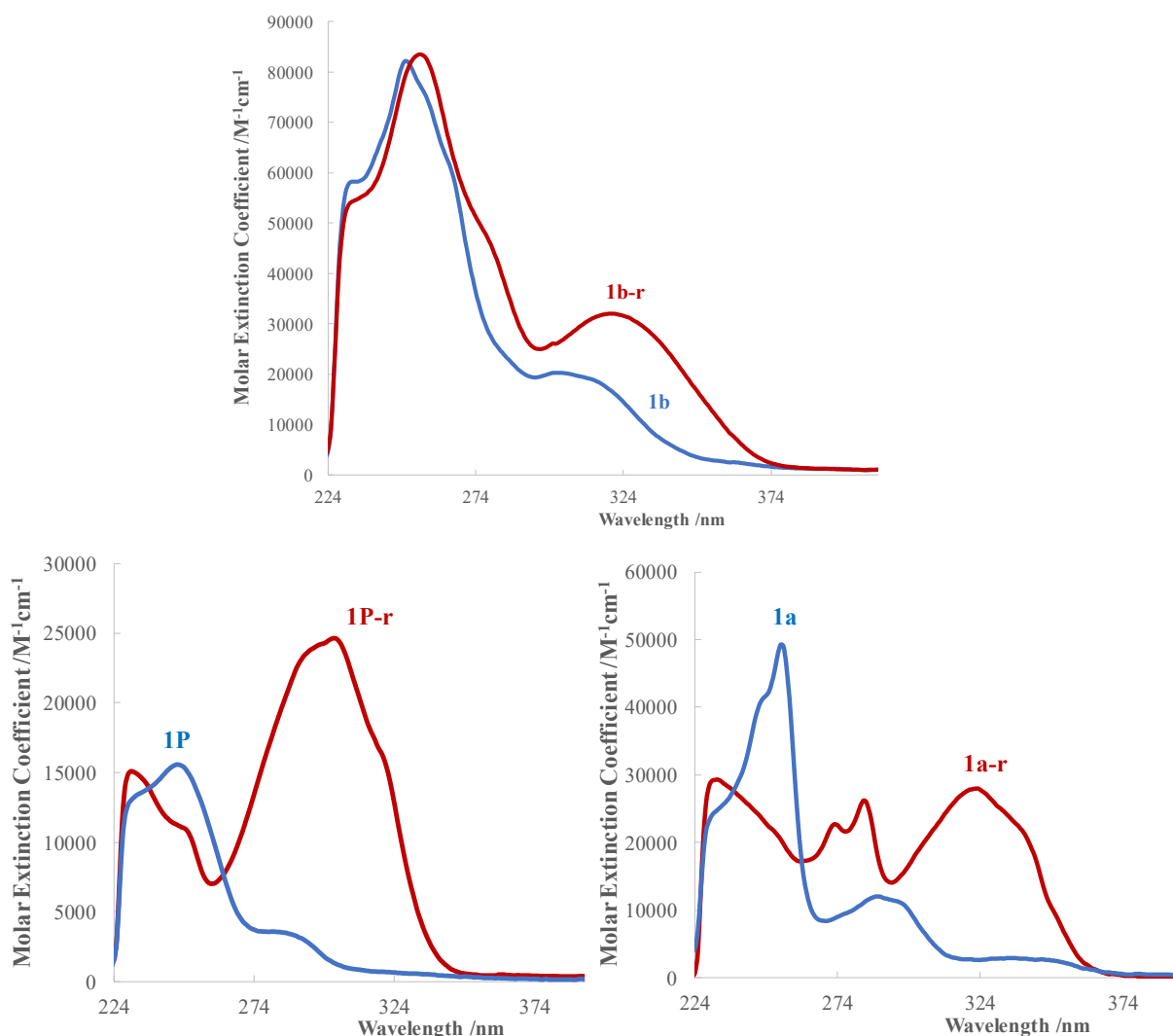


Figure 3-9 Comparative molar extinction coefficient plots of **1P**, **1a**, **1b** and their corresponding benzofurans

For **1P** and **1a**, release gives rise to strong and moderately absorbing bands (respectively) in the 300-400 nm region, with moderate or minimal absorption at 200-300 nm. As a result, a light source centered where the benzofurans do not absorb competitively (254 nm), is most effective for efficient release. In the case of **1b**, where the benzofuran has a similar absorption profile with a strong band in the 250 nm region, release with 254 nm is slow. The broad nature of this product band means that irradiation with 312 nm is similarly slowed but to a lesser extent. This is a departure from the wavelength dependent kinetics exhibited by **1P** and mirrored by **1a**, where 254 nm irradiation is most efficient. In this case 312 nm irradiation is preferable to 254 nm. The lesser absorption of **1b** at 365 nm as well as the appearance of a small band in this region result in significantly slower release with a 365 nm light sources. Photolysis of the 11.0  $\mu\text{M}$  solution was complete within 450 seconds with the 254 nm light source, 270 seconds with 312 nm, and finally 800 seconds with 365 nm.

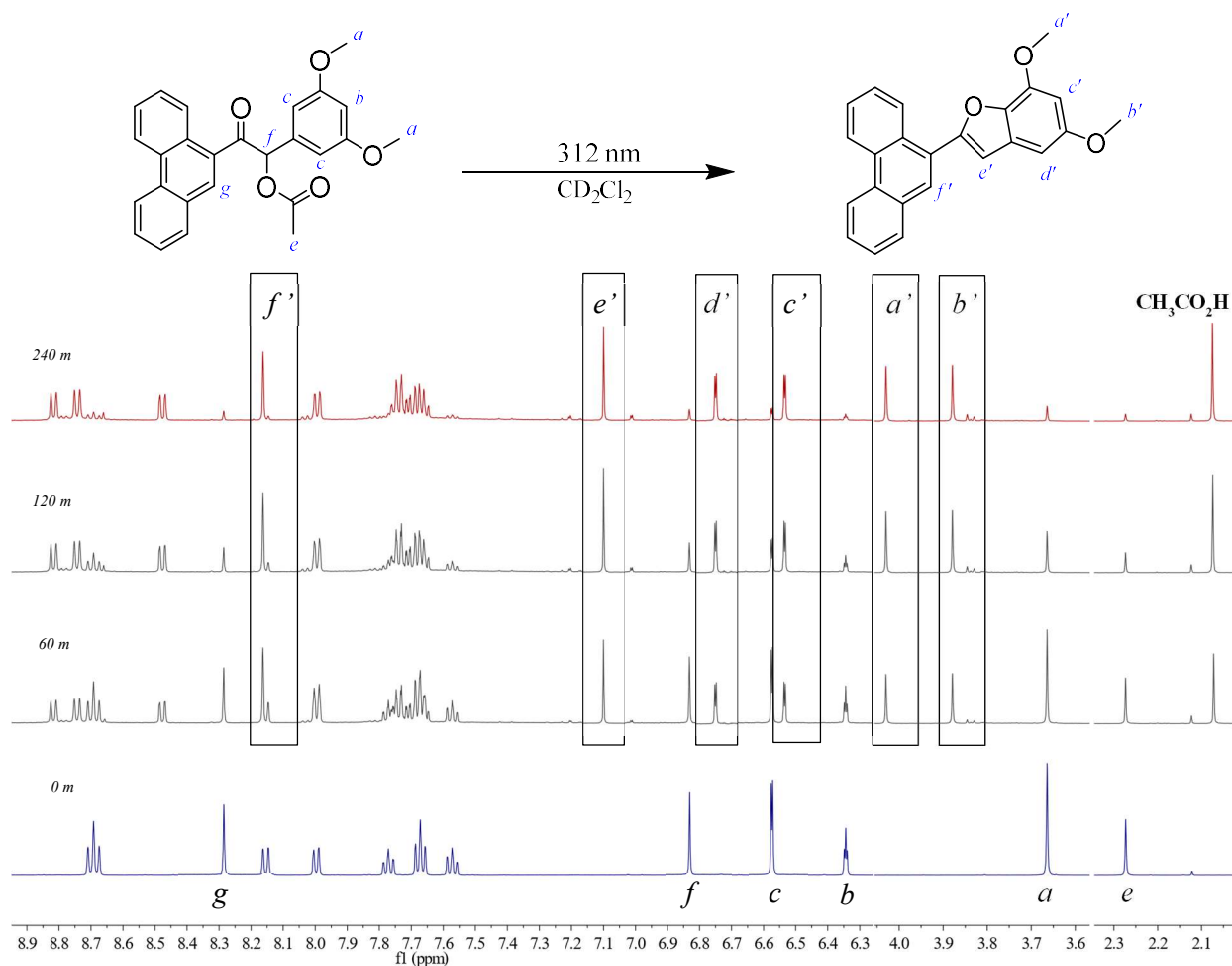


Figure 3-10 Evolution of selected regions of  $^1\text{H}$  NMR spectra throughout duration of irradiation of **1b** with 312 nm light.

The photolysis of **1b** in CD<sub>2</sub>Cl<sub>2</sub> was monitored by <sup>1</sup>H NMR in the same fashion as **1P** and **1a**. Progression of <sup>1</sup>H NMR spectra throughout the duration of photolysis is presented in Figure 3-12. A second minor unidentified photoproduct is visible in these spectra. Further work is required to characterize this product and determine the pathways from which it results.

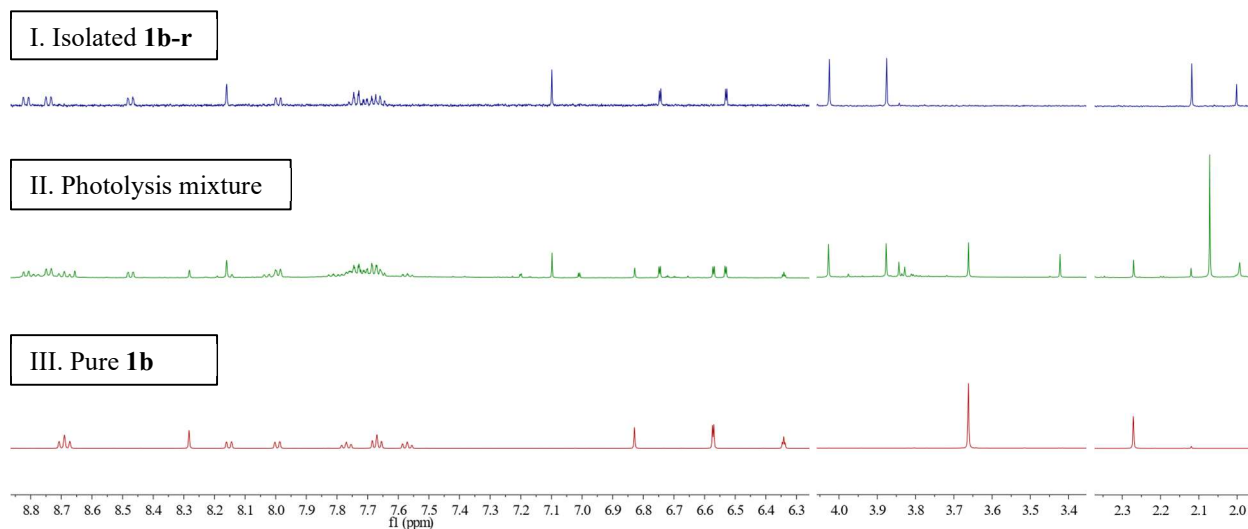


Figure 3-11 <sup>1</sup>H NMR comparison of (I) Isolated benzofuran (II) Photolysis mixture- 240 m, and (III) Photocage **1b**

The associated benzofuran was isolated via flash column chromatography. Its <sup>1</sup>H NMR spectrum is presented in Figure 3-13 and is seen to match that of the final photolyzed solution, indicating that the benzofuran is the major photoproduct.

While the benzofuran photoproduct has been reported to be highly fluorescent, there is minimal data associated with this observation. Here we seek to confirm that the strong fluorescence of the photolysis solutions is due solely to the photoproduct and not associated with the caged molecule, as suggested by Sheehan *et al.* in their 1971 publication.<sup>27</sup> A 1 μM solution of **1b** in DCM was prepared and kept protected from any possible sources of ambient light. This sample was analyzed by fluorescence emission spectroscopy. The starting solution, unexposed to UV light and thus comprised only of **1b**, did not exhibit any significant emission, as seen in Figure 3-14. Irradiation of this solution was carried out with a single 312 nm lamp in 30 second intervals. The result was the rapid appearance and increase of an emission peak centered at 409 nm. This is a reasonable result given that photolyzed solutions were seen to fluoresce blue. The confirmation of fluorescence as a property of the photoproduct is ideal given the practicality of release and report fluorescence for the monitoring of photorelease.

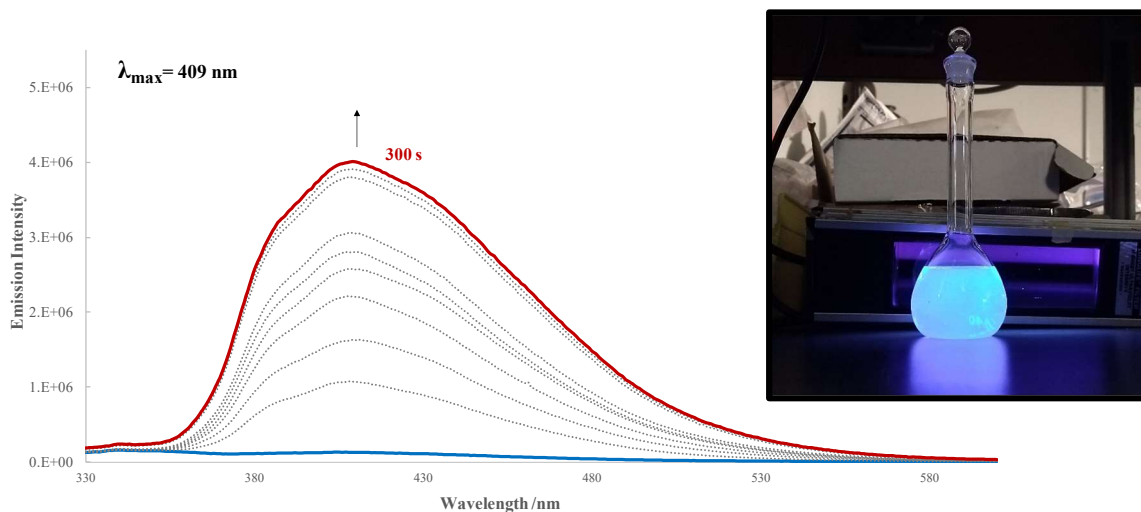


Figure 3-12 Progression of fluorescence emission spectra of a 1  $\mu$ M solution of **1b**. Inset: A photolyzed 10  $\mu$ M solution of **1a** is illuminated by a 312 nm handheld UV lamp.

### 3.3.3. Presence of Minor Photoproducts

Reaction of benzoin PPGs has long been touted as a clean conversion from cage to benzofuran with release of the caged compound of interest. While this appears to be the case in UV-Vis studies, on a micromolar scale with short intervals of irradiation totalling under 5 minutes, it is not applicable for other experimental conditions. The presence of additional photoproducts observed in NMR studies does not invalidate the exceptionally clean conversion of the benzoin acetate, as the major product (>85%) is the desired benzofuran. However, identification and acknowledgement of secondary photoproducts and/or degradation products has value, either in understanding minor reaction pathways or identifying at which point degradation begins.

In NMR studies of **1P**, **1a**, and **1b**, a 9.89 ppm peak appears in all cases after 60 minutes of irradiation. Investigation of the dimethylamino derivative discussed in Chapter 4 confirmed the identify of this species as 3,5-dimethoxybenzaldehyde. This aldehyde is not expected to be produced from the highly photostable benzofuran and was not observed in NMR samples of isolated benzofuran exposed to UV and ambient light sources.



Thus, this species is likely to be derived from the starting caged compounds, via a minor reaction pathway in quantities that are only resolvable after extended reaction times. The cage may begin to fragment after extended UV light exposure, likely via  $\alpha$ -scission into two free radical intermediates (Norrish type I). However, the second radical fragmentation products (phenyl, naphthyl, or phenanthryl aldehydes) are not observed. Further examination of this pathway may prove useful in gaining understanding of key intermediates.

The aldehyde is produced in higher quantities in reaction of **1b**, in part accounting for the lack of isosbestic points in UV-Vis photolysis studies, along with the aforementioned unidentified product. Interestingly, the dimethoxybenzaldehyde has been observed in small quantities by a previous study but has essentially never been discussed.<sup>39</sup> This is perhaps due to the intense focus on the mechanism of benzofuran formation and the reputation of this photorelease as exceptionally clean. By all standards reaction of benzoin PPGs is extremely clean, yielding primarily the desired benzofuran with release of the caged molecule. Acknowledgment of and investigation into minor photoproducts does not negate this and may prove to be unexpectedly valuable.

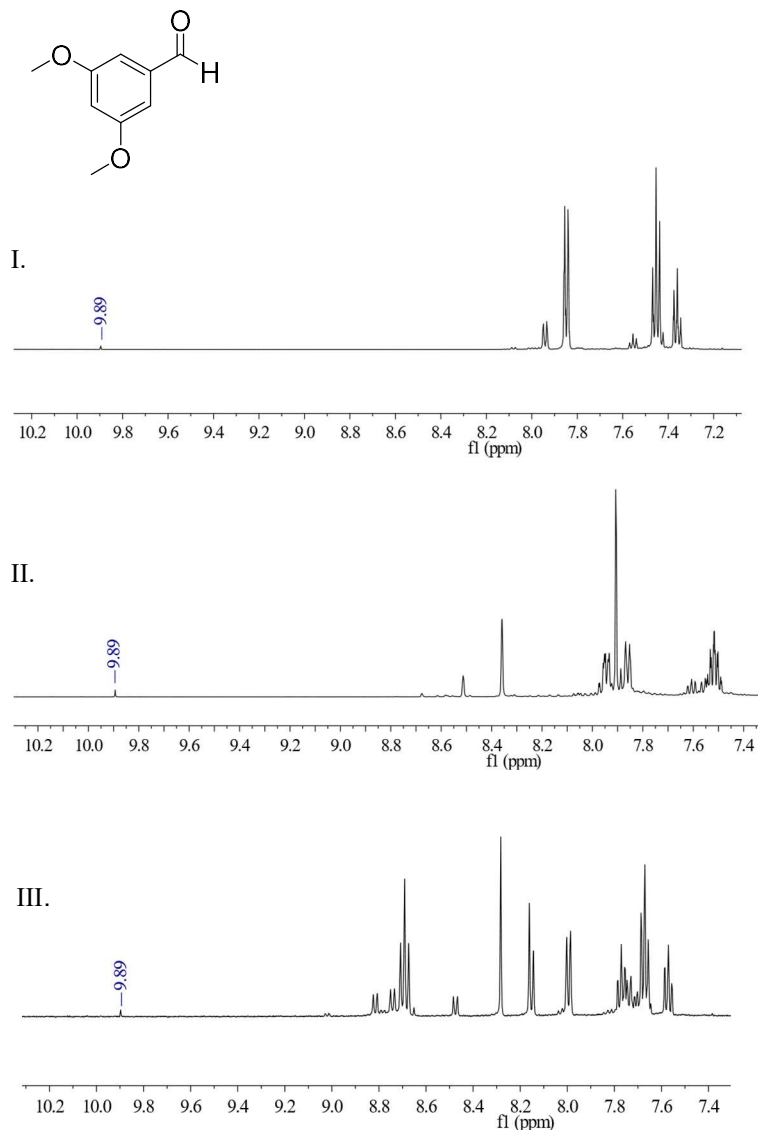


Figure 3-13 Minor photoproduct 3,5-dimethoxybenzaldehyde is observed in photolyzed solutions of I. **1P**, II. **1a**, and III. **1b**.

### 3.4. Conclusions

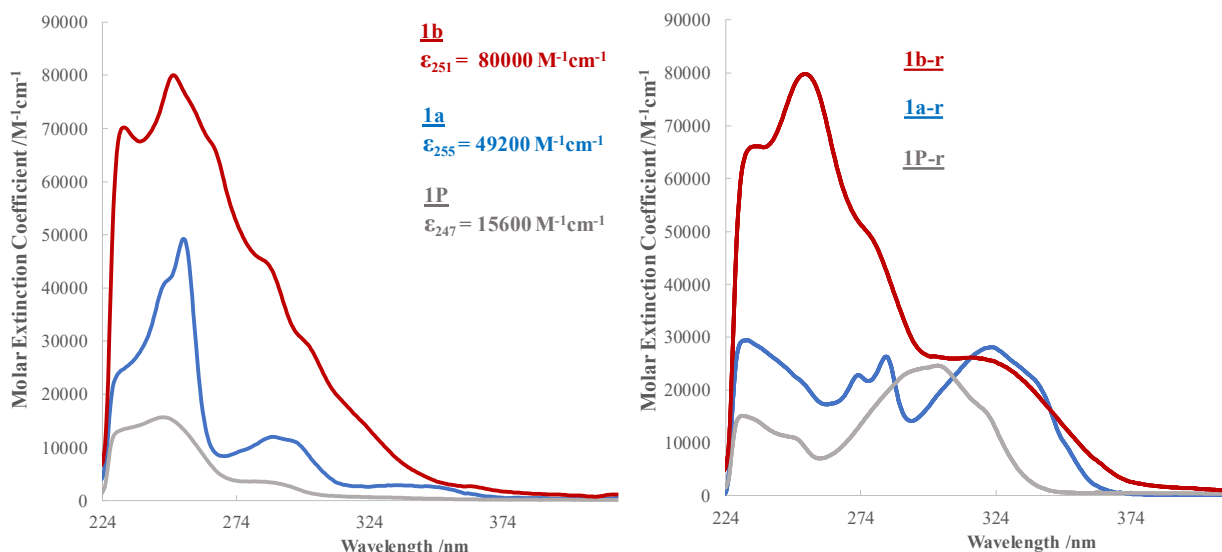


Figure 3-14 Molar Extinction Coefficient comparison of photocages **1a**, **1b**, and **1P** (left) and corresponding benzofurans (right).

A comparison of molar extinction coefficients of the novel polyaromatic PPGs and parent benzoin acetate is presented in Figure 3-16. In the case of derivatives **1a** and **1b**, extending conjugation on the benzoyl moiety red shifted the primary absorption by 8 nm and 5 nm, respectively. More significantly, these bands are broader and absorption extends towards 400 nm. These compounds were seen to be strongly absorbing with higher extinction coefficients at 365 nm. In the case of molar absorptivity at both the primary ~250 nm peak and at 365 nm, phenanthrene derivative **1b** is superior to its naphthalene analogue **1a**.

The novel PPGs maintain the characteristic photochemistry of **1P**, including the highly fluorescent benzofuran photoproduct and overall exceptional release rate, while also exhibiting improvement in absorptivity.

PPG	$\lambda_{\max}$ /nm	$\epsilon_{\lambda_{\max}}$ /M <sup>-1</sup> cm <sup>-1</sup>	$\epsilon_{365}$ /M <sup>-1</sup> cm <sup>-1</sup>	UV-Vis Release			
				Concentration / $\mu$ M	254 Lamp $t_r$ /s	312 Lamp $t_r$ /s	365 Lamp $t_r$ /s
<b>1P</b>	247	15600	210	38.2	135	240	570
<b>1a</b>	255	49200	1050	9.88	120	240	330
<b>1b</b>	251	80000	2460	11.0	450	270	780

Table 3-1 Summarized properties of **1P**, **1a**, and **1b**.

In order to quantitatively compare release rates, rate constants were calculated. When efficiency of release is discussed this may refer to a variety of factors including the one photon uncaging cross section ( $\phi \cdot \epsilon_{\lambda_{irr}}$ ), rate constant for appearance of the substrate, or extent of release with a specific irradiation dose. Here, first order rate constants for the disappearance of the cage or appearance of benzofuran are calculated from UV-Vis photolysis studies. The disappearance of the primary ~250 nm band is easily monitored. Appearance of the ~300 nm product bands may be separately tracked, but these rate constants differ from those derived from appearance of the product and are less relevant in this context.

With a short wave 254 nm light source **1a** is superior to **1P**, while release is significantly slower from **1b**. In the case of release with 312 nm, **1P** and **1a** are comparable, while the rate constant for release from **1b** is an order of magnitude lower. When the light source is a 365 nm lamp, most relevant for application in biological settings, the rate constant for **1a** is over double that of **1P**. Again, **1b** is an order of magnitude lower. These results highlight that high molar extinction coefficients do not always translate to fast release, as the absorption profile of the photoproduct(s) is also a factor. PPG **1a** balances improved extinction coefficients of the cage with a moderately absorbing benzofuran product and as a result releases with exceptional rate constants.

Cage	Rate Constant /s <sup>-1</sup>		
	254 Lamp	312 Lamp	365 Lamp
<b>1P</b>	0.007 ± 0.0008	0.005 ± 0.0004	0.00084 ± 0.000022
<b>1a</b>	0.01 ± 0.0007	0.0045 ± 0.00017	0.002 ± 0.00005
<b>1b</b>	0.0004 ± 0.00006	0.0005 ± 0.00004	0.0002 ± 0.000006

Table 3-2 First order rate constants of uncaging

While the absorption properties of **1b** are excellent in the 200-300 nm range, this does not translate to efficient release due to the strong absorption from **1b-r**. Additionally, the increased concentration of secondary photoproducts is a disadvantage. PPG **1a** is an excellent alternative to the **1P** for use in studies requiring release with medium long wave UV light. For contexts in which high energy light is appropriate, **1P** and **1a** are equally suitable.

## 3.5. Experimental

### 3.5.1. General Methods

All solvents and reagents used for synthesis, chromatography, UV-vis spectroscopy and photochemical studies were purchased from Aldrich, Anachemia, Caledon Labs, Fisher Scientific or Alfa Aesar, and used as received. THF was dried and degassed by passage through steel columns containing activated alumina under nitrogen using an MBraun solvent purification system. Solvents for NMR analysis were purchased from Cambridge Isotope Laboratories and used as received. Column chromatography was performed using silica gel 60 (230–400 mesh) from Silicycle Inc.  $^1\text{H}$  and  $^{13}\text{C}$  NMR characterizations were performed on a Bruker Avance-500 instrument with a 5 mm inverse probe operating 125.76 MHz for  $^{13}\text{C}$  NMR unless stated otherwise. Chemical shifts ( $\delta$ ) are reported in parts per million (ppm) relative to tetramethylsilane using the residual solvent peak as a reference, and splitting patterns are designated as s (singlet), d (doublet), t (triplet) and m (multiplet). Coupling constants ( $J$ ) are reported in Hertz. UV-vis absorption spectra were recorded on a Shimadzu UV-3600 Plus spectrophotometer. Fluorescence measurements were performed on a PTI Quantamaster spectrofluorometer. High Resolution Mass Spectroscopy (HRMS) measurements were performed using an Agilent 6210 TOF LC/MS in ESI-(+) mode.

### 3.5.2. Photochemical Studies

All irradiations and analyses were completed in a scare-light setting to ensure no interference from ambient light sources. Handheld Spectroline® E-Series UV lamps with broadband light centered at three wavelengths (254, 312, and 365 nm) were used.

#### *$^1\text{H}$ NMR Studies*

To trace the uncaging process with  $^1\text{H}$  NMR, approximately 1 mg of the chromophore was dissolved in 0.5 mL  $\text{CD}_2\text{Cl}_2$  and pipetted into an NMR tube. Irradiation was carried out with two handheld UV lamps, one on either side of the upright NMR tube.  $^1\text{H}$  NMR spectra were obtained at each time interval until no further spectral changes were observed.

### *UV-Vis Studies*

Solutions of the indicated concentrations were prepared with the use of amber volumetric flasks and volumetric pipettes. Irradiation was carried out in a quartz cuvette by a single handheld UV lamp.

### *Bulk Photolysis*

Approximately 50 mg of the given photocage was dissolved in 10 mL dichloromethane in a glass vial and irradiated with a handheld 312 nm lamp. The photolysis was observed by TLC and continued until the strong fluorescent top spot dominates, typically 120 minutes. The sample was then dry loaded onto a short column and eluted with 1:3 ethyl acetate/hexanes

### **3.5.3. Synthetic Procedures and Characterization**

***Synthesis of 2-(naphthalen-2-yl)-1,3-dithiane (3a)*** A solution of 2-naphthaldehyde (2.25 g, 14.42 mmol) in CH<sub>2</sub>Cl<sub>2</sub> (25 mL) was treated with 1,3-propanedithiol (1.45 ml, 14.42 mmol). After stirring for 5 min, the mixture was treated with Hf(OTf)<sub>4</sub> (55.9 mg, 0.072 mmol). The resulting colourless solution was stirred for 12 h, at which time it was filtered through a pad of Celite. The Celite was rinsed repeatedly with CH<sub>2</sub>Cl<sub>2</sub> and the combined filtrates were evaporated under reduced pressure. Recrystallization from a 1:1 mixture of hexanes and acetone yielded 2.18 g (51%) of **3a** as a white crystalline solid.

<sup>1</sup>H NMR (CD<sub>2</sub>Cl<sub>2</sub>, 500 MHz) δ: 7.94 (s, 1H), 7.82-7.79 (m, 3H), 7.57-7.55 (m, 1H), 7.47-7.45 (m, 2H), 5.34 (s, 1H), 3.14-3.09 (m, 2H), 2.98-2.94 (m, 2H), 2.24-2.18 (m, 1H), 2.04-1.94 (m, 1H)

<sup>13</sup>C NMR (CD<sub>2</sub>Cl<sub>2</sub>, 126 MHz) δ: 137.43, 133.87, 128.91, 128.50, 128.15, 127.19, 126.87, 126.23, 54.43, 54.22, 54.00, 53.78, 53.57, 52.01, 32.68, 25.82.

HRMS (ESI<sup>+</sup>) Anal. Calc. for C<sub>14</sub>H<sub>14</sub>NaS<sub>2</sub> (M+Na)<sup>+</sup> 269.0429 Found: (M+Na)<sup>+</sup> 269.0424

***Synthesis of (3,5-dimethoxyphenyl)(2-(naphthalen-2-yl)-1,3-dithian-2-yl)methyl acetate (2a)*** A flame dried flask under N<sub>2</sub> was charged with 2-(naphthalen-2-yl)-1,3-dithiane (961 mg, 3.90 mmol) and dry THF (50 mL). The system was cooled to 0°C in an ice bath before the dropwise addition of 1.6 M *n*-BuLi solution in hexanes (2.70 mL, 4.29 mmol). The resulting deep brown solution was stirred 10 min, at which time the septum was briefly removed and 3,5-

dimethoxybenzaldehyde (712 mg, 4.29 mmol) was added resulting in an abrupt colour change to pale yellow. The mixture was then purged with N<sub>2</sub> and allowed to warm to room temperature over a period of 45 min, at which time it was treated with acetic anhydride (0.42 mL, 4.29 mmol) and DMAP (524 mg, 4.29 mmol). After stirring at room temperature for 20 h, the solution was poured into water and extracted with EtOAc (10 mL). After three additional extractions with EtOAc, the combined organic layers were dried over MgSO<sub>4</sub> and the solvent was removed under reduced pressure. The crude mixture, a yellow oil, was purified by flash column chromatography on a column of moderate length with a solvent system of 1:6 EtOAc /hexanes. The product was isolated as a colourless oil that foamed into a fine white powder under high-vacuum (750 mg, 42%).  
<sup>1</sup>H NMR (500 MHz, CD<sub>2</sub>Cl<sub>2</sub>) δ 8.28 (s, 1H), 8.04 (dd, *J* = 8.7, 2.0 Hz, 1H), 7.94 – 7.82 (m, 3H), 7.60 – 7.50 (m, 2H), 6.34 (t, *J* = 2.3 Hz, 1H), 6.14 (s, 1H), 6.06 (d, *J* = 2.3 Hz, 2H), 3.47 (s, 6H), 2.83 – 2.65 (m, 4H), 2.12 (s, 3H), 1.94 (tt, *J* = 9.2, 4.2 Hz, 2H).  
<sup>13</sup>C NMR (126 MHz, CD<sub>2</sub>Cl<sub>2</sub>) δ 169.82, 160.15, 137.83, 135.34, 133.61, 133.13, 131.57, 128.91, 128.79, 127.91, 127.69, 127.07, 126.57, 107.12, 101.22, 81.01, 63.83, 27.98, 27.87, 25.26, 21.22.  
HRMS (ESI<sup>+</sup>) Anal. Calc. for C<sub>25</sub>H<sub>26</sub>NaO<sub>4</sub>S<sub>2</sub> (M+Na)<sup>+</sup> 477.1163 Found: (M+Na)<sup>+</sup> 477.1165

**Synthesis of 1-(3,5-dimethoxyphenyl)-2-(naphthalen-2-yl)-2-oxoethyl acetate (1a)** Under scarce light conditions a solution of (3,5-dimethoxyphenyl)(2-(naphthalen-2-yl)-1,3-dithian-2-yl)methyl acetate (95 mg, 0.21 mmol) in a mixture of 1:9 H<sub>2</sub>O/CH<sub>3</sub>CN (10 mL) was treated with Hg(ClO<sub>4</sub>)<sub>2</sub>·H<sub>2</sub>O (290 mg, 0.73 mmol) in one portion. After stirring for 25 min, the reaction mixture was quenched with sat. NaHCO<sub>3</sub> and vacuum filtered. The filtrate was extracted with EtOAc and the layers separated. After three more extractions of the aqueous layer, the combined organic extracts were dried over MgSO<sub>4</sub> and the solvent was removed under reduced pressure. The crude mixture was dry loaded onto a short column and eluted with 1:3 EtOAc/hexanes to yield 60 mg (78%) of **1a** as a white solid.

<sup>1</sup>H NMR (CD<sub>2</sub>Cl<sub>2</sub>, 500 MHz) δ: 8.51 (s, 1H), 7.97-7.86 (m, 4H), 7.63-7.54 (m, 2H), 6.89 (s, 1H), 6.64 (d, *J*=2.28 Hz, 2H), 6.41 (t, *J*=2.28 Hz, 1H), 3.74 (s, 6H), 2.21 (s, 3H)  
<sup>13</sup>C NMR (CD<sub>2</sub>Cl<sub>2</sub>, 126 MHz) δ: 193.99, 170.88, 161.88, 136.35, 136.24, 132.91, 132.56, 131.06, 130.17, 129.39, 129.12, 128.28, 127.50, 124.60, 107.22, 101.40, 100.56, 78.21, 55.98, 21.14  
HRMS (ESI<sup>+</sup>) Anal. Calc. for C<sub>22</sub>H<sub>20</sub>NaO<sub>5</sub>(M+Na)<sup>+</sup> 387.1208 Found: (M+Na)<sup>+</sup> 387.1203

**Synthesis of 2-(phenanthren-9-yl)-1,3-dithiane (3b)** A solution of phenanthrene-9-carbaldehyde (2.75 g, 13.31 mmol) in CH<sub>2</sub>Cl<sub>2</sub> (25 mL) was treated with 1,3-propanedithiol (1.34 mL, 13.34 mmol). After stirring for 5 min, the mixture was treated with Hf(OTf)<sub>4</sub> (55.9 mg, 0.072 mmol). The resulting colourless solution was stirred for 12 h, at which time it was filtered through a pad of Celite. The Celite was rinsed repeatedly with CH<sub>2</sub>Cl<sub>2</sub> and the combined filtrates were evaporated under reduced pressure. Recrystallization from a 1:1 mixture of hexanes and acetone yielded 2.18 g (51%) of **3b** as a white crystalline solid.

<sup>1</sup>H NMR (500 MHz, CD<sub>2</sub>Cl<sub>2</sub>) δ 8.80 – 8.73 (m, 1H), 8.68 (d, *J* = 8.3 Hz, 1H), 8.39 (s, 1H), 8.08 (s, 1H), 7.93 (d, *J* = 8.0 Hz, 1H), 7.74 – 7.65 (m, 3H), 7.63-7.59 (m, 1H), 5.96 (s, 1H), 3.30 – 3.22 (m, 2H), 3.05 – 2.98 (m, 2H), 2.32 – 2.24 (m, 1H), 2.08 – 1.95 (m, 1H).

<sup>13</sup>C NMR (126 MHz, CD<sub>2</sub>Cl<sub>2</sub>) δ 134.26, 131.83, 131.26, 130.77, 129.50, 129.33, 127.77, 127.76, 127.44, 127.25, 127.22, 124.61, 123.87, 122.98, 54.43, 54.22, 54.00, 53.78, 53.57, 33.30, 26.24.

HRMS (ESI<sup>+</sup>) Anal. Calc. for C<sub>18</sub>H<sub>16</sub>NaS<sub>2</sub> (M+Na)<sup>+</sup> 319.0591 Found: (M+Na)<sup>+</sup> 319.0586

**Synthesis of (3,5-dimethoxyphenyl)(2-(phenanthrene-9-yl)-1,3-dithian-2-yl)methyl acetate (2b)**

A flame dried flask under N<sub>2</sub> was charged with 2-(phenanthren-9-yl)-1,3-dithiane (810 mg, 2.73 mmol) and dry THF (50 mL). The system was cooled to 0°C in an ice bath before the dropwise addition of 1.6 M *n*-BuLi solution in hexanes (1.90 mL, 3.01 mmol). The resulting deep brown solution was stirred 10 min, at which time the septum was briefly removed and 3,5-dimethoxybenzaldehyde (50 mg, 3.01 mmol) was added resulting in an abrupt colour change to pale yellow. The mixture was then purged with N<sub>2</sub> and allowed to warm to room temperature over a period of 45 min, at which time it was treated with acetic anhydride (0.30 mL, 3.01 mmol) and DMAP (368 mg, 3.01 mmol). After stirring at room temperature for 20 h, the solution was poured into water and extracted with EtOAc (10 mL). After three additional extractions with EtOAc, the combined organic layers were dried over MgSO<sub>4</sub> and the solvent was removed under reduced pressure. The crude mixture, a yellow oil, was purified by flash column chromatography on a column of moderate length with a solvent system of 1:6 EtOAc /hexanes. The product was isolated as a colourless oil that foamed into a fine white powder under high-vacuum (551 mg, 40%).

<sup>1</sup>H NMR (500 MHz, CD<sub>2</sub>Cl<sub>2</sub>) δ 9.41 – 9.26 (m, 1H), 8.93 – 8.82 (m, 1H), 8.72 (d, *J* = 8.3 Hz, 1H), 8.45 (s, 1H), 7.89 (d, *J* = 7.8 Hz, 1H), 7.80 – 7.68 (m, 3H), 7.68 – 7.58 (m, 1H), 7.12 (s, 1H), 6.25 (s, 1H), 6.08 (s, 2H) 3.39 (s, 6H), 3.15 – 2.59 (m, 4H), 2.36 – 2.09 (m, 4H), 2.05-1.86 (m, 2H).

<sup>13</sup>C NMR (126 MHz, CD<sub>2</sub>Cl<sub>2</sub>) δ 160.12, 138.36, 133.67, 132.65, 131.97, 131.46, 131.02, 130.48,

129.82, 128.55, 127.48, 126.80, 126.15, 124.18, 122.77, 100.76, 55.44, 28.45, 27.90, 24.70, 21.34.  
HRMS (ESI<sup>+</sup>) Anal. Calc. for C<sub>29</sub>H<sub>28</sub>NaO<sub>4</sub>S<sub>2</sub> (M+Na)<sup>+</sup> 527.1327 Found: (M+Na)<sup>+</sup> 527.1321

**Synthesis of 1-(3,5-dimethoxyphenyl)-2-oxo-2-(phenanthrene-9-yl)ethyl acetate (1b)** Under scarce light conditions a solution of (3,5-dimethoxyphenyl)(2-(phenanthrene-9-yl)-1,3-dithian-2-yl)methyl acetate (112 mg, 0.22 mmol) in a mixture of 1:20 H<sub>2</sub>O/CH<sub>3</sub>CN (10 mL) was treated with Hg(ClO<sub>4</sub>)<sub>2</sub>·H<sub>2</sub>O (268 mg, 0.67 mmol) in one portion. After stirring for 25 min, the reaction mixture was quenched with sat. NaHCO<sub>3</sub> and vacuum filtered. The filtrate was extracted with EtOAc and the layers separated. After three more extractions of the aqueous layer, the combined organic extracts were dried over MgSO<sub>4</sub> and the solvent was removed under reduced pressure. The crude mixture was dry loaded onto a short column and eluted with 1:3 EtOAc/hexanes to yield 75 mg (82%) of **1c** as a white solid.

<sup>1</sup>H NMR (500 MHz, CD<sub>2</sub>Cl<sub>2</sub>) δ 8.69 (t, *J* = 9.0 Hz, 2H), 8.29 (s, 1H), 8.16 (d, *J* = 8.4 Hz, 1H), 7.99 (d, *J* = 8.0 Hz, 1H), 7.84-7.78 (m, 1H), 7.74-7.68 (m, 2H), 7.64-7.58 (m, 1H), 6.84 (s, 1H), 6.58 (d, *J* = 2.3 Hz, 2H), 6.35 (t, *J* = 2.2 Hz, 1H), 3.66 (s, 6H), 2.28 (s, 3H).

<sup>13</sup>C NMR (126 MHz, CD<sub>2</sub>Cl<sub>2</sub>) δ 197.40, 171.09, 161.71, 135.31, 133.88, 132.26, 131.16, 130.48, 130.34, 130.01, 129.59, 128.92, 128.00, 127.84, 127.82, 126.45, 123.36, 123.22, 106.85, 101.51, 80.34, 55.92, 54.43, 54.22, 54.00, 53.78, 53.57, 21.19.

HRMS (ESI<sup>+</sup>) Anal. Calc. for C<sub>26</sub>H<sub>22</sub>NaO<sub>5</sub> (M+Na)<sup>+</sup> 437.1365 Found: (M+Na)<sup>+</sup> 437.1359

**Synthesis of (3,5-dimethoxyphenyl)(2-phenyl-1,3-dithian-2-yl)methyl acetate (2P)** A flame dried flask under N<sub>2</sub> was charged with 2-phenyl-1,3-dithiane (327 mg, 1.67 mmol) and dry THF (15 mL). The system was cooled to 0°C in an ice bath before the dropwise addition of 2.5 M *n*-BuLi solution in hexanes (0.68 mL, 3.01 mmol). The resulting deep brown solution was stirred 10 min, at which time the septum was briefly removed and 3,5-dimethoxybenzaldehyde (309 mg, 1.84 mmol) was added resulting in an abrupt colour change to pale yellow. The mixture was then purged with N<sub>2</sub> and allowed to warm to room temperature over a period of 45 min, at which time it was treated with acetic anhydride (0.20 mL, 1.84 mmol) and DMAP (225 mg, 1.84 mmol). After stirring at room temperature for 18 h, the solution was poured into water and extracted with EtOAc (10 mL). After three additional extractions with EtOAc, the combined organic layers were dried over MgSO<sub>4</sub> and the solvent was removed under reduced pressure. The crude mixture, a yellow oil, was purified by flash column chromatography on a column of moderate length with a solvent



system of 1:6 EtOAc /hexanes. The product was isolated as a colourless oil that foamed into a fine white powder under high-vacuum (493.7 mg, 73%). Synthesized by CJ Carling in 2010. Purified on a short column, 1:3 EtOAc/hexanes, for use in 2019.

$^1\text{H}$  NMR (500 MHz,  $\text{CD}_2\text{Cl}_2$ )  $\delta$  7.78 (dd,  $J = 7.3, 1.8$  Hz, 1H), 7.38 – 7.26 (m, 2H), 6.31 (t,  $J = 2.3$  Hz, 1H), 6.02 (d,  $J = 2.4$  Hz, 2H), 3.59 (s, 3H), 2.77 – 2.55 (m, 3H), 2.07 (s, 2H), 1.89 (h,  $J = 4.6, 4.1$  Hz, 1H).

$^{13}\text{C}$  NMR ( $\text{CDCl}_3$ , 100 MHz)  $\delta$ : 169.61, 159.68, 137.36, 137.16, 131.22, 128.20, 127.77, 106.77, 101.19, 80.51, 63.53, 55.35, 27.56, 27.43, 24.88, 21.16.

HRMS (ESI+) Anal. Calc. for  $\text{C}_{21}\text{H}_{24}\text{NaO}_4\text{S}_2$  ( $\text{M}+\text{Na}$ ) $^+$  427.1000 Found: ( $\text{M}+\text{Na}$ ) $^+$ 427.1008

**Synthesis of 1-(3,5-dimethoxyphenyl)-2-oxo-2-phenylethyl acetate (1P)** Under scarce light conditions a solution of 3,5-dimethoxyphenyl(2-phenyl-1,3-dithian-2-yl)methyl acetate (134 mg, 0.33 mmol) in a mixture of 1:9  $\text{H}_2\text{O}/\text{CH}_3\text{CN}$  (10 mL) was treated with  $\text{Hg}(\text{ClO}_4)_2 \cdot \text{H}_2\text{O}$  (463 mg, 1.16 mmol) in one portion. After stirring for 25 min, the reaction mixture was quenched with sat.  $\text{NaHCO}_3$  and vacuum filtered. The filtrate was extracted with EtOAc and the layers separated. After three more extractions of the aqueous layer, the combined organic extracts were dried over  $\text{MgSO}_4$  and the solvent was removed under reduced pressure. The crude mixture was dry loaded onto a short column and eluted with 1:3 EtOAc/hexanes to yield 78 mg (75%) of **1P** as a white solid

$^1\text{H}$  NMR (500 MHz,  $\text{CD}_2\text{Cl}_2$ )  $\delta$  8.01 – 7.95 (m, 2H), 7.63 – 7.55 (m, 1H), 7.48 (dd,  $J = 8.4, 7.2$  Hz, 2H), 6.77 (s, 1H), 6.62 (d,  $J = 2.3$  Hz, 2H), 6.47 (t,  $J = 2.3$  Hz, 1H), 3.79 (s, 6H), 2.22 (s, 3H).  
 $^{13}\text{C}$  NMR (126 MHz,  $\text{CD}_2\text{Cl}_2$ )  $\delta$  193.99, 170.79, 161.87, 136.21, 135.23, 134.08, 129.24, 129.19, 107.19, 101.42, 78.21, 21.09.

### Isolated Photoproducts

#### **5,7-dimethoxy-2-(naphthalen-2-yl)benzofuran (1a-r)**

$^1\text{H}$  NMR (600 MHz,  $\text{CD}_2\text{Cl}_2$ )  $\delta$  8.36 (d,  $J = 1.3$  Hz, 1H), 8.01-7.92 (m, 2H), 7.93-7.88 (m, 1H), 7.60-7.52 (m, 2H), 7.16 (s, 1H), 6.71 (d,  $J = 2.2$  Hz, 1H), 6.52 (d,  $J = 2.2$  Hz, 1H), 4.06 (s, 3H), 3.89 (s, 3H).

$^{13}\text{C}$  NMR (151 MHz,  $\text{CD}_2\text{Cl}_2$ )  $\delta$  157.60, 156.89, 146.07, 140.02, 133.95, 133.75, 131.07, 128.99, 128.87, 128.24, 128.17, 127.22, 127.03, 124.01, 123.20, 103.09, 97.86, 94.83, 56.64, 56.29 HRMS (ESI $^+$ ) Anal. Calc. for  $\text{C}_{20}\text{H}_{17}\text{O}_3$  ( $\text{M}+\text{H}$ ) $^+$  305.1172 Found: 305.1171

### 5,7-dimethoxy-2-(phenanthren-9-yl)benzofuran (1b-r)

$^1\text{H}$  NMR (500 MHz,  $\text{CD}_2\text{Cl}_2$ )  $\delta$  8.85 (d,  $J = 8.9$  Hz, 1H), 8.78 (d,  $J = 8.2$  Hz, 1H), 8.51 (d,  $J = 8.1$  Hz, 1H), 8.20 (s, 1H), 8.03 (d,  $J = 7.7$  Hz, 1H), 7.82 – 7.71 (m, 4H), 7.14 (s, 1H), 6.78 (d,  $J = 2.2$  Hz, 1H), 6.57 (d,  $J = 2.2$  Hz, 1H), 4.06 (s, 3H), 3.91 (s, 3H).

HRMS (ESI $^+$ ) Anal. Calc. for  $\text{C}_{24}\text{H}_{19}\text{O}_3$  (M+H) $^+$  355.132 Found: 355.1324

### 5,7-dimethoxy-2-phenylbenzofuran (1P-r)

$^1\text{H}$  NMR (500 MHz,  $\text{CD}_2\text{Cl}_2$ )  $\delta$  7.94 – 7.83 (m, 2H), 7.49 (t,  $J = 7.7$  Hz, 2H), 7.44 – 7.35 (m, 1H), 7.03 (s, 1H), 6.68 (d,  $J = 2.3$  Hz, 1H), 6.49 (d,  $J = 2.3$  Hz, 1H), 4.04 (s, 3H), 3.87 (s, 3H).

$^{13}\text{C}$  NMR (151 MHz,  $\text{CD}_2\text{Cl}_2$ )  $\delta$  157.53, 156.85, 146.05, 139.86, 131.00, 130.89, 129.31, 129.04, 125.24, 102.42, 97.74, 94.79, 56.62, 56.27, 54.36, 54.22, 54.18, 54.05, 54.00, 53.82, 53.70, 53.64, 30.24.

HRMS (ESI $^+$ ) Anal. Calc. for  $\text{C}_{16}\text{H}_{14}\text{NaO}_3$  (M+Na) $^+$  277.083515 Found (M+Na) $^+$  277.084086

### 3.5.4. Mercury-Free Dethioacetalization Alternative

Mercury coordination continues to be the primary method for deprotection of thioacetals despite well documented risks.<sup>58</sup> Modern alternatives often employ expensive heterogenous catalysts and microwave irradiation, which is unsuitable for photosensitive materials. A lesser known protocol, developed by Mukaiyama *et al.* in 1972, was tested here.<sup>59</sup>

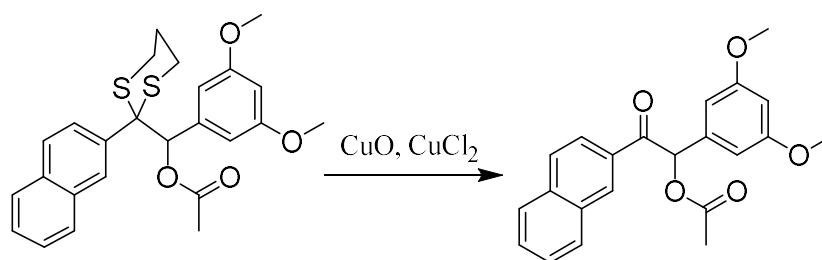


Figure 3-15 Copper mediated dethioacetalization of **2a**.

A solution of **2a** (1.10g, 2.42 mmol) in 100 mL acetone was prepared in scarce light conditions. Solid CuO (0.770 g, 968  $\mu\text{mol}$ ) and CuCl<sub>2</sub> (0.825 g, 4.84 mmol) were transferred to the solution of **2a** with the help of 1 mL water (final solution 99:1 acetone/water). The resulting solution was stirred at room temperature for 72 hours at which point it was filtered through a Celite

pad. The deep blue solution was concentrated under reduced pressure and subsequently dissolved in acetone. The acetone was evaporated under reduced pressure and this step was repeated twice. The concentrate was then dissolved in 15 mL ethyl acetate and an equal volume of 5% NaHCO<sub>3</sub> was added. The resulting aqueous layer was separated and extracted three times with 15 mL of ethyl acetate. The combined organic layers were dried over Na<sub>2</sub>SO<sub>4</sub> and concentrated. The crude mixture was dry loaded onto a column of moderate length with solvent system 1:4 Ethyl acetate/Hexanes. Compound **1a** was afforded as a colourless oil which foams to a fine white powder under high vacuum (0.750 g, 68%).

While this reaction proceeds slowly and requires more workup than those with mercury perchlorate, the yields are comparable. When the time required to put on layers of protective equipment required to handle mercury perchlorate and clean contaminated items is considered, these two reactions are equally time consuming. Most importantly, the reagents required pose less risk to human and environmental health and do not require specialized disposal services.

## Chapter 4. Preparation and Photochemistry of Novel Donor-Acceptor Benzoin Photoremovable Protecting Groups

### 4.1. Abstract

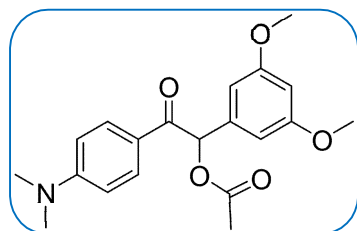
Two novel photoremovable protecting groups (PPGs) in the benzoin class have been prepared and their photochemistry investigated. Electron donating moieties in the para position of the benzoyl ring are introduced with the goal of red shifting absorption. The novel PPGs have improved molar extinction coefficients and release caged acetic acid at unprecedented rates.

### 4.2. Introduction

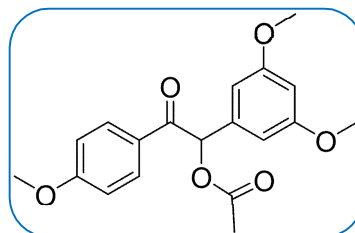
In this work, a set of two donor-acceptor 3',5'-dimethoxybenzoin derivatives are synthesized for release of caged carboxylic acids. These molecules were developed via Strategy II, the introduction of an electron donating moiety on the benzoyl ring. Two electron donating functionalities are used, dimethylamino (**1-DMA**) and methoxy (**1-OMe**). As with the polyaromatic derivatives presented in Chapter 3, these form a three-molecule series with the parent compound. The introduction of heteroatoms is more likely to alter the course of this photoreaction.

Novel PPG **1-OMe** is seen to react as the parent benzoin acetate **1P**, releasing acetic acid and yielding primarily the cyclization product.

While **1-DMA** releases caged acetic acid at extraordinary rates, the mixture of photoproducts is complex and primarily consists of two aldehydes. This may be attributed to the role of electron transfer chemistry.



**1-DMA**



**1-OMe**

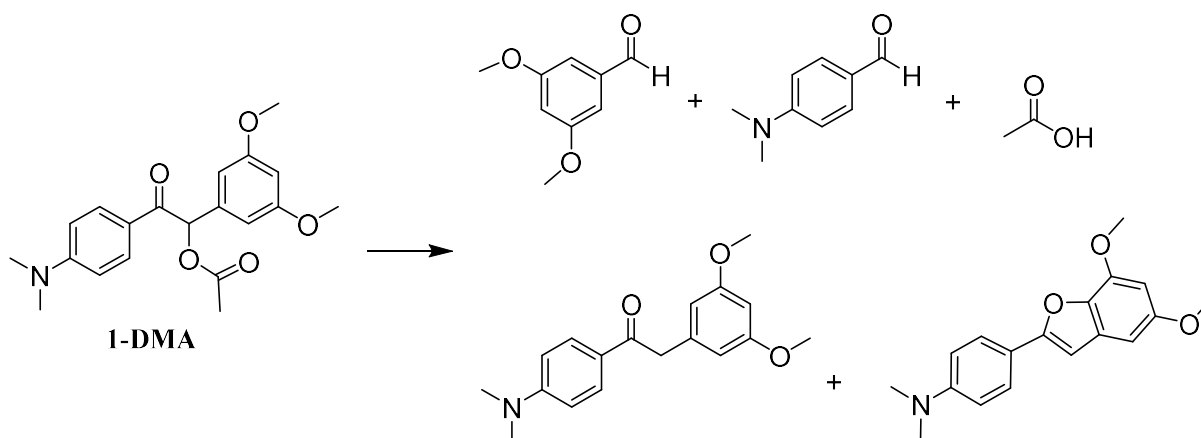


Figure 4-2 Photochemical release of acetic acid from **1-DMA**.

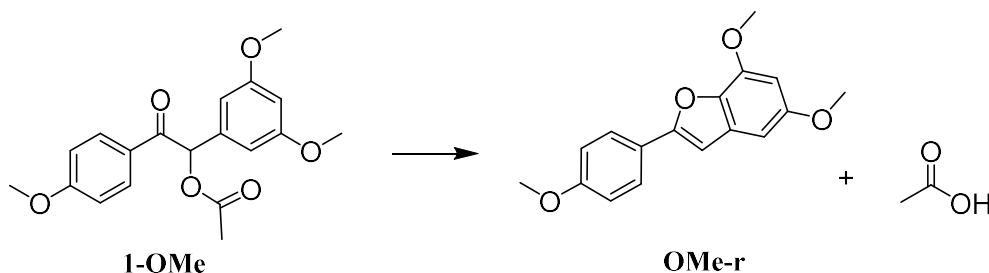


Figure 4-1 Photochemical release of acetic acid from **1-OMe** with conversion to cyclization product **OMe-r**.

PPGs **1-DMA** and **1-DMA** were synthesized in three steps. The commercially available aromatic aldehydes are first converted to their corresponding 1,3-propyldithianes. The aromatic dithianes then serve as nucleophiles in the Corey-Seebach umpolung reaction in which the benzoyl moiety is installed. While ambient light poses no risk to these compounds, direct irradiation results in degradation and release of acetic acid. Treatment with  $\text{Hg}(\text{ClO}_4)_2 \cdot 3\text{H}_2\text{O}$  in  $\text{CH}_3\text{CN}/\text{H}_2\text{O}$  was employed for dethioacetalization and the generation of chromophore **1-DMA**. The alternative deprotection procedure detailed in section 4.5 was used for deprotection of **2-OMe** to yield the final chromophore **1-OMe**. Detailed synthetic procedures and characterization are described in section 4.6.

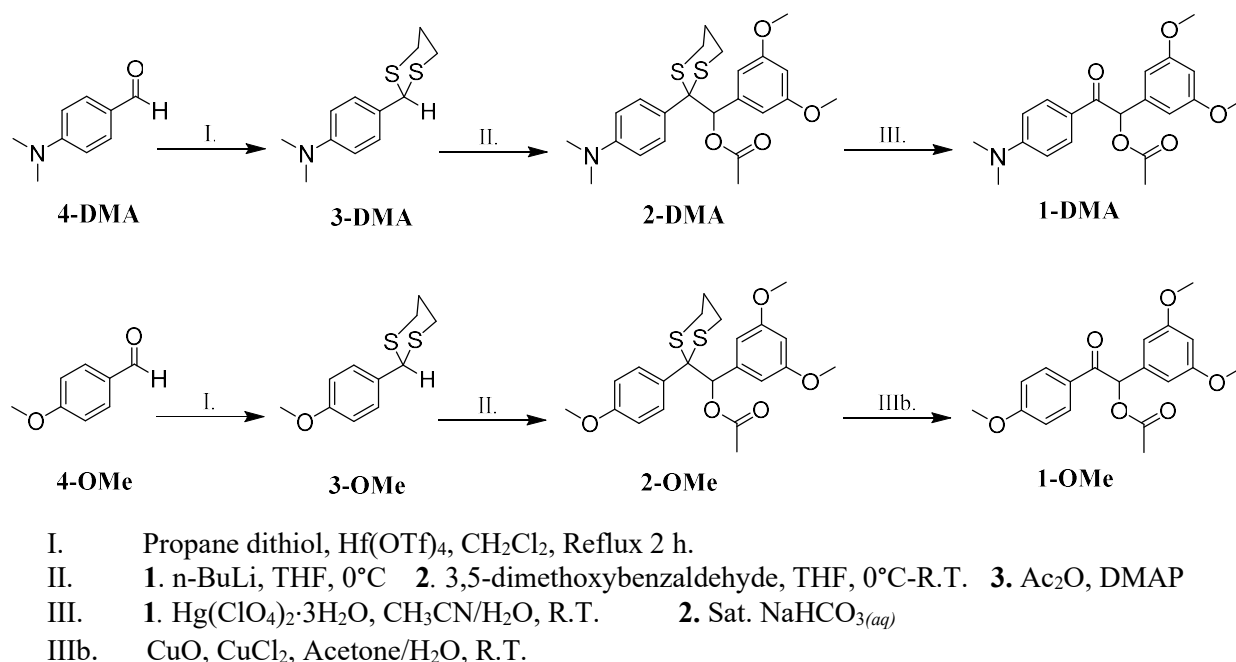


Figure 4-3 Synthesis of PPGs **1-DMA** and **1-OMe** from commercially available benzaldehydes.

## 4.3. Results and Discussion

### 4.3.1. 1-DMA [1-(3,5-dimethoxyphenyl)-2-(4-(dimethylamino)phenyl)-2-oxoethyl acetate]

UV-Vis absorption spectra collected in 15 second intervals throughout photolysis were the first indication of the unique behaviour of this novel PPG. As seen in Figure 4-4, the absorption profile of **1-DMA** differs significantly from both **1P** and the polyaromatic derivatives.

A small absorption is present near 250 nm, but the primary absorption is at 348 nm. This band is redshifted an astounding 100 nm. The extinction coefficient at 348 nm was calculated to be 42200 M<sup>-1</sup>cm<sup>-1</sup>.

With irradiation in 15 second intervals, the 348 nm band was quickly diminished as area between the 227 nm and 348 nm bands increased. A small increase of absorption at 250 nm was also observed. Interestingly, the final absorption profiles in studies carried out with 254, 312, and 365 nm lamps differ in the 250-330 nm range. In the 254 nm photolysis, a stronger moderate absorption centered at 320 nm appears. This absorption is not present in the 312 nm study and is extremely slight in the final absorption profile of the mixture photolyzed by the 365 nm light source.

This wavelength dependent reaction mixture is intriguing. NMR studies with these lamps show no major differences, suggesting minor photoproducts with high extinction coefficients. Most significantly, release with 312 and 365 nm is complete within 60 seconds. The rates of photorelease with medium and long wave UV light are exceptional. Photolysis with the 254 nm light source is slightly slowed, with completion in 120 seconds. After these time periods degradation is observed. There is no evidence of an inner-filter effect in these studies.

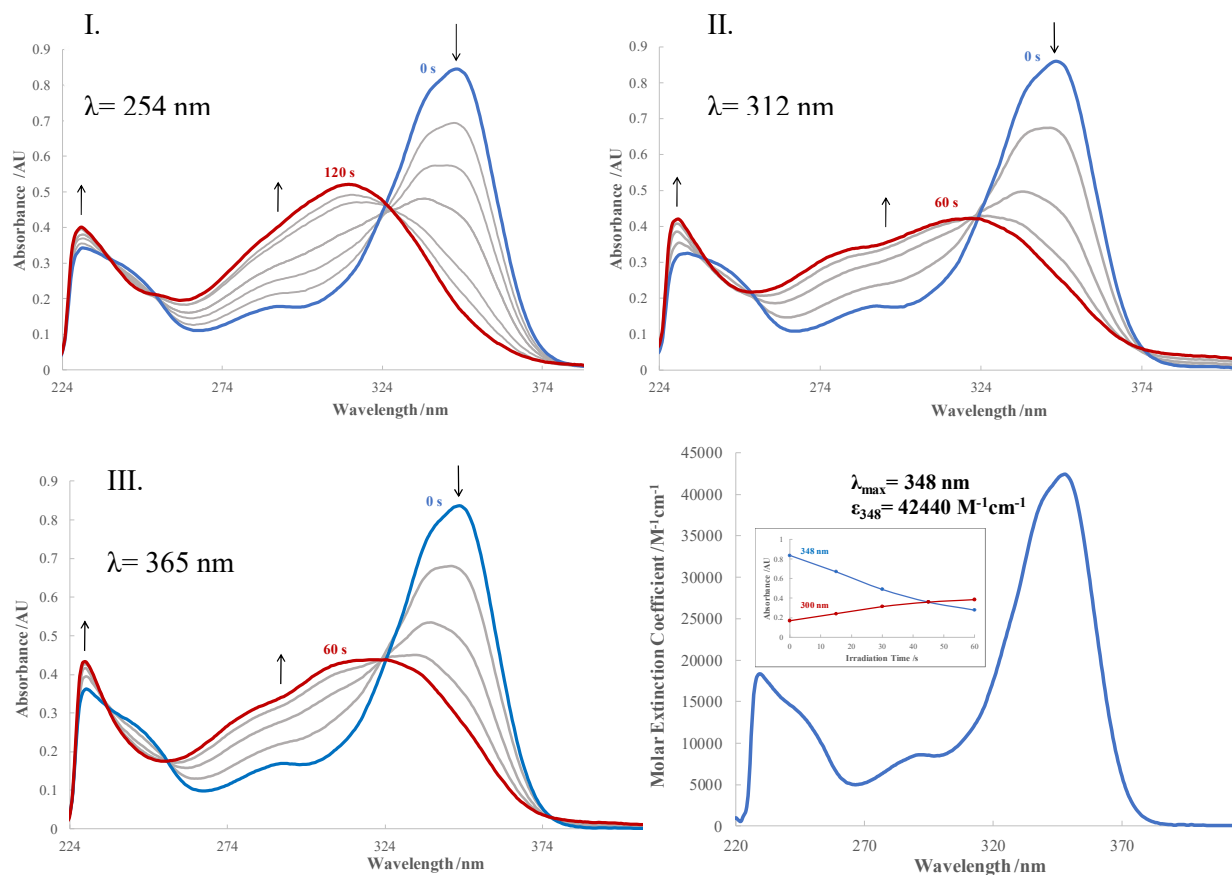


Figure 4-4 UV-Vis absorption spectra of photolysis of **1-DMA** ( $1.97 \times 10^{-5} M$  in  $CH_2Cl_2$ ) with I. 254, II. 312, and III. 365 nm light. IV. Molar extinction coefficient plot of **1-DMA**. (Inset: Appearance of product at 300 nm and loss of **1-DMA** at 348 nm with 356 nm irradiation).

The photolysis was then monitored via  $^1H$  NMR spectroscopy. Within one minute of irradiation with a single lamp, significant release was observed. Two signals, at 9.7 and 9.9 ppm, were observed. The characteristic acetic acid peak at 2.1 ppm increases as photolysis continues. At this concentration the photolysis is complete within 8 minutes. As was seen in UV-Vis studies, further irradiation past the point of completion results in significant degradation.

From the final NMR spectrum of the photolyzed solution it is clear that this photoreaction does not proceed in the same fashion as the parent benzoin acetate and the novel polyaromatic derivatives. The primary benzofuran photoproduct is not immediately evident in this mixture. The primary photoproducts of this reaction are two aldehydes.

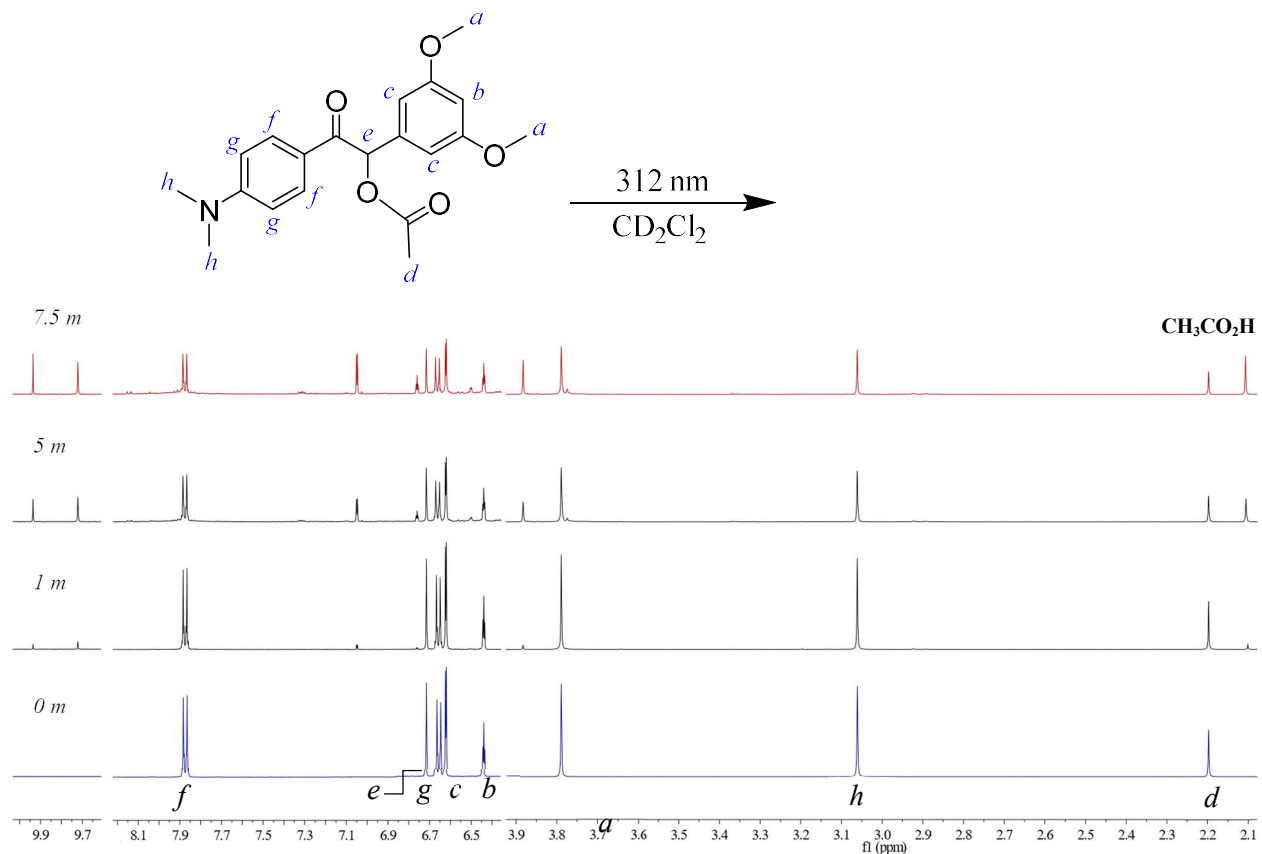
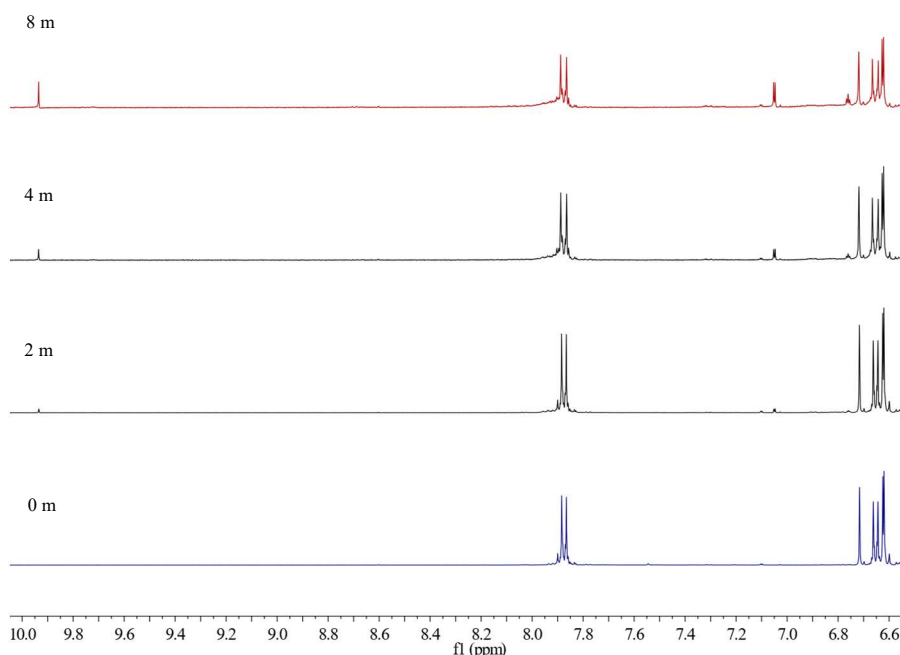


Figure 4-5 Evolution of selected regions of <sup>1</sup>H NMR spectra throughout duration of irradiation of **1-DMA** with 312 nm light.

The number of components in this mixture complicates identification of these photoproducts. Attempts to analyze solutions via LC-MS were unsuccessful. However, the preparation and analysis of the required solutions led to an interesting observation. Photolysis of these solutions was done in the same manner as <sup>1</sup>H NMR studies. The only difference in procedure was the opening of the NMR cap between periods of irradiation. This was required to obtain 1 μL aliquots of the solution to prepare the corresponding solution for LC-MS analysis. After each 1-minute irradiation a <sup>1</sup>H NMR spectrum was acquired. The result, displayed in Figure 4-6, shows that the 9.7 ppm aldehyde is not formed. Further investigation confirmed that this photoproduct forms until the point at which the NMR cap is removed.



At this point the peak does not disappear but rather remains at the same integration throughout the remaining duration of irradiation. This apparent quenching of a singular photoproduct is interesting and may provide insight into the mechanism of photorelease.



*Figure 4-6 Progression of selected region of  $^1\text{H}$  NMR spectra throughout duration of irradiation with 312 nm light with removal of NMR cap between cycles.*

In order to confirm the identify of both aldehydes and additional minor photoproducts, bulk photolysis was completed in an NMR tube. Constant monitoring via  $^1\text{H}$  NMR was required in order to push the reaction to near completion without degradation. These solutions were then dry loaded for separation via flash column chromatography. Column size and solvent systems were variable and unique to each separation. Numerous fractions were seen to be photosensitive and thus all further columns and analyses were completed in scarce light settings. When elution is monitored by thin layer chromatography, only the starting material is observed. It was quickly determined that standard TLC plating was not appropriate, as the majority of photoproduct spots were short lived. In order to observe the fluorescence, fractions were spotted individually and visualized with 312 nm immediately. The results of the separations are presented here.

### 3,5-Dimethoxybenzaldehyde

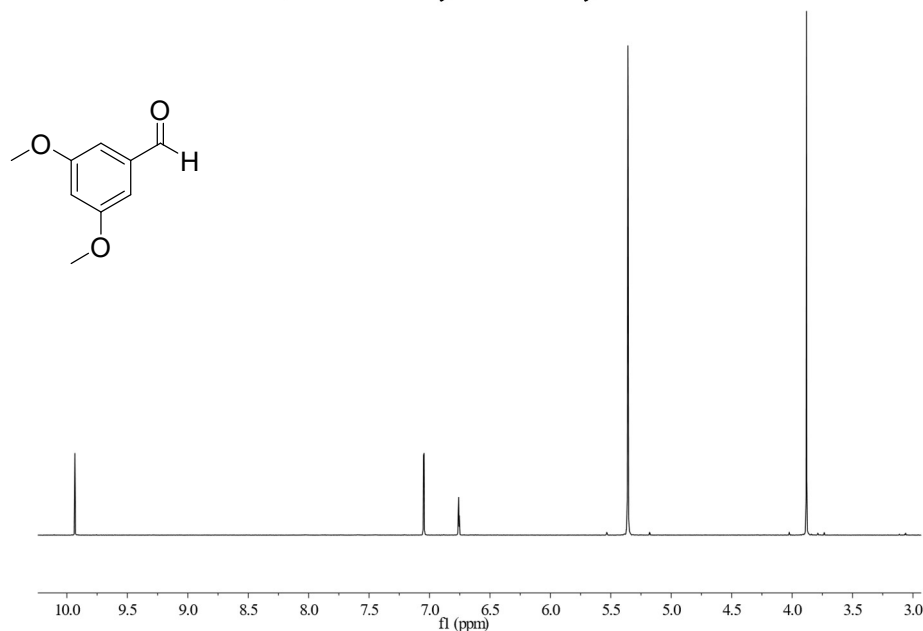


Figure 4-7. <sup>1</sup>H NMR (500 MHz, CD<sub>2</sub>Cl<sub>2</sub>) spectrum of isolated 3,5-dimethoxybenzaldehyde.

The 9.9 ppm aldehyde, alluded to in Chapter 3 (section 3.3.3) to be 3,5-dimethoxybenzaldehyde, was isolated in significant quantities. As is suggested by NMR studies, 3,5-dimethoxybenzaldehyde is one of two primary photoproducts. The secondary 9.9 ppm aldehyde could not be separated with reasonable purity. It may be assigned reasonably as 4-(dimethylamino)benzaldehyde based on existing NMR data.

The presence of aldehyde photoproducts is not necessarily detrimental. In some cases, exclusive release of aldehydes is sought after. The complex nature of this mixture and possibility of one or more of these products being biologically active/non-inert, particularly the aldehydes, is high. In the case of PPGs in the o-NB class, the presence of an aldehyde in the photoproduct mixture is problematic but has not prevented commercialization.

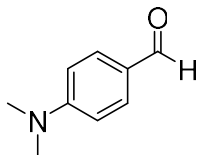
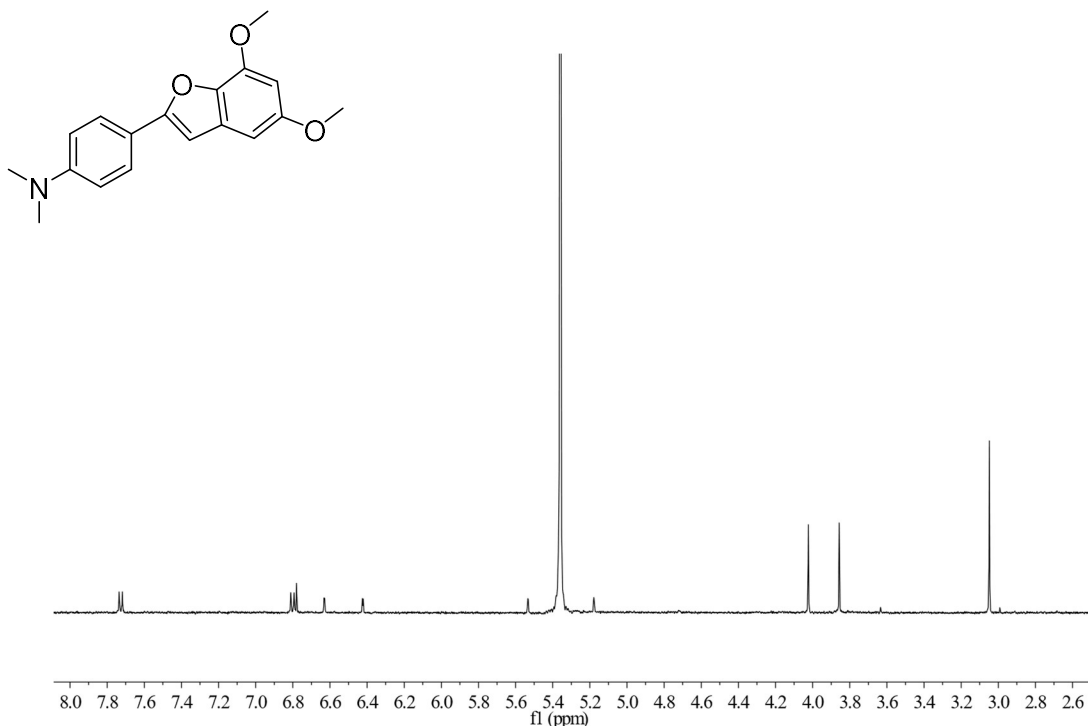


Figure 4-8 4-(dimethylamino) benzaldehyde.

*4-(5,7-dimethoxybenzofuran-2-yl)-N,N-dimethylaniline*



*Figure 4-9* <sup>1</sup>H NMR (500 MHz, CD<sub>2</sub>Cl<sub>2</sub>) of isolated 4-(5,7-dimethoxybenzofuran-2-yl)-N,N-dimethylaniline.

Unexpectedly, the corresponding benzofuran was obtained, albeit in small quantity. The isolation of this species implies that the mechanistic pathway associated with all other known benzoin PPGs is available here. Divergence from a single intermediate is not unfamiliar in modern investigations of the mechanism of benzoin PPG photorelease.

This benzofuran and 3,5-dimethoxybenzaldehyde are both fluorescent, and thus release may be monitored via optical methods despite the unusual photoproduct mixture.

2-(3,5-dimethoxyphenyl)-1-(4-(dimethylamino)phenyl)ethan-1-one

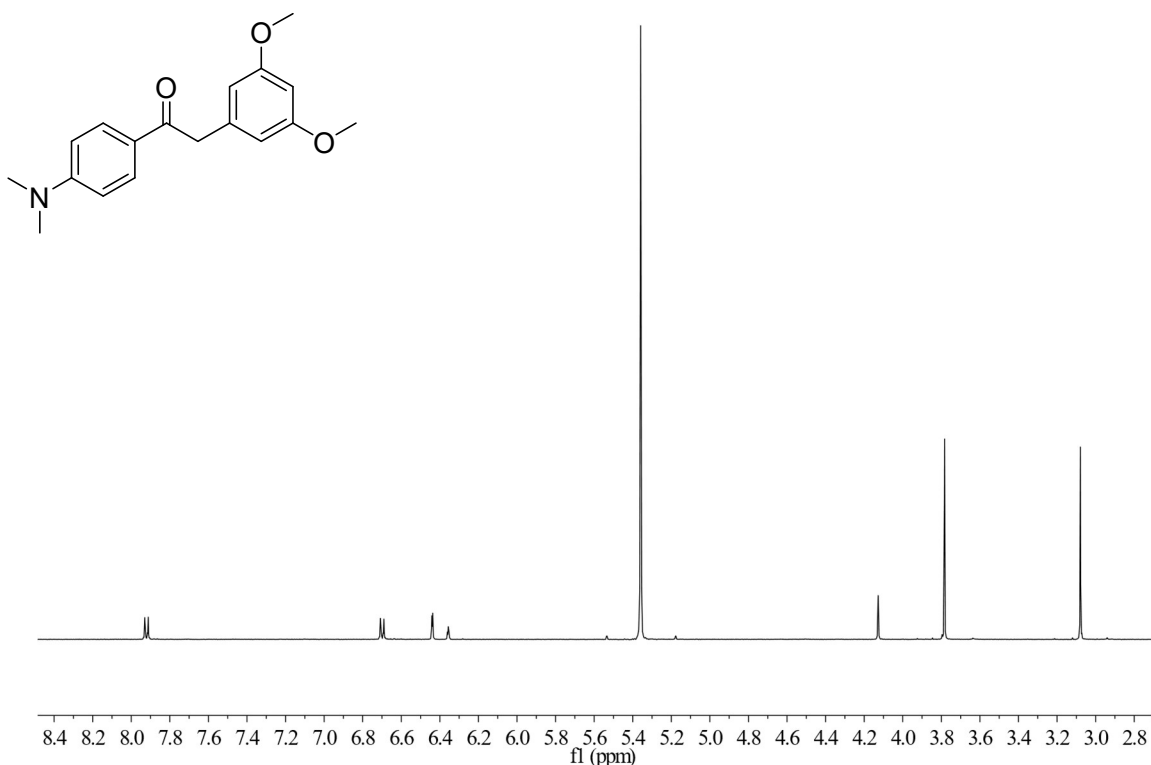


Figure 4-10 <sup>1</sup>H NMR (500 MHz, CD<sub>2</sub>Cl<sub>2</sub>) of isolated 2-(3,5-dimethoxyphenyl)-1-(4-(dimethylamino)phenyl)ethan-1-one.

Lastly, a novel deacetylated product was obtained. A related species was observed by Bisht *et al.* in their study of cross-acyloin derivatives modelled after 3,5-dimethoxybenzoin acetate for application in organic field effect transistors.<sup>60</sup> When irradiation was carried out in electron transfer conditions, in which triethylamine was added to solution, a mixture of the benzofuran and the deacetylated product was obtained. The authors proposed that this result suggested the participation of a photoinduced electron transfer process. The mechanism proposed based on these results is presented in Figure 4-11. While this mechanism is not supported by experimental work with ultrafast transient absorption spectroscopy, literature of this type concerning the benzoin class has been contradictory or inconclusive.

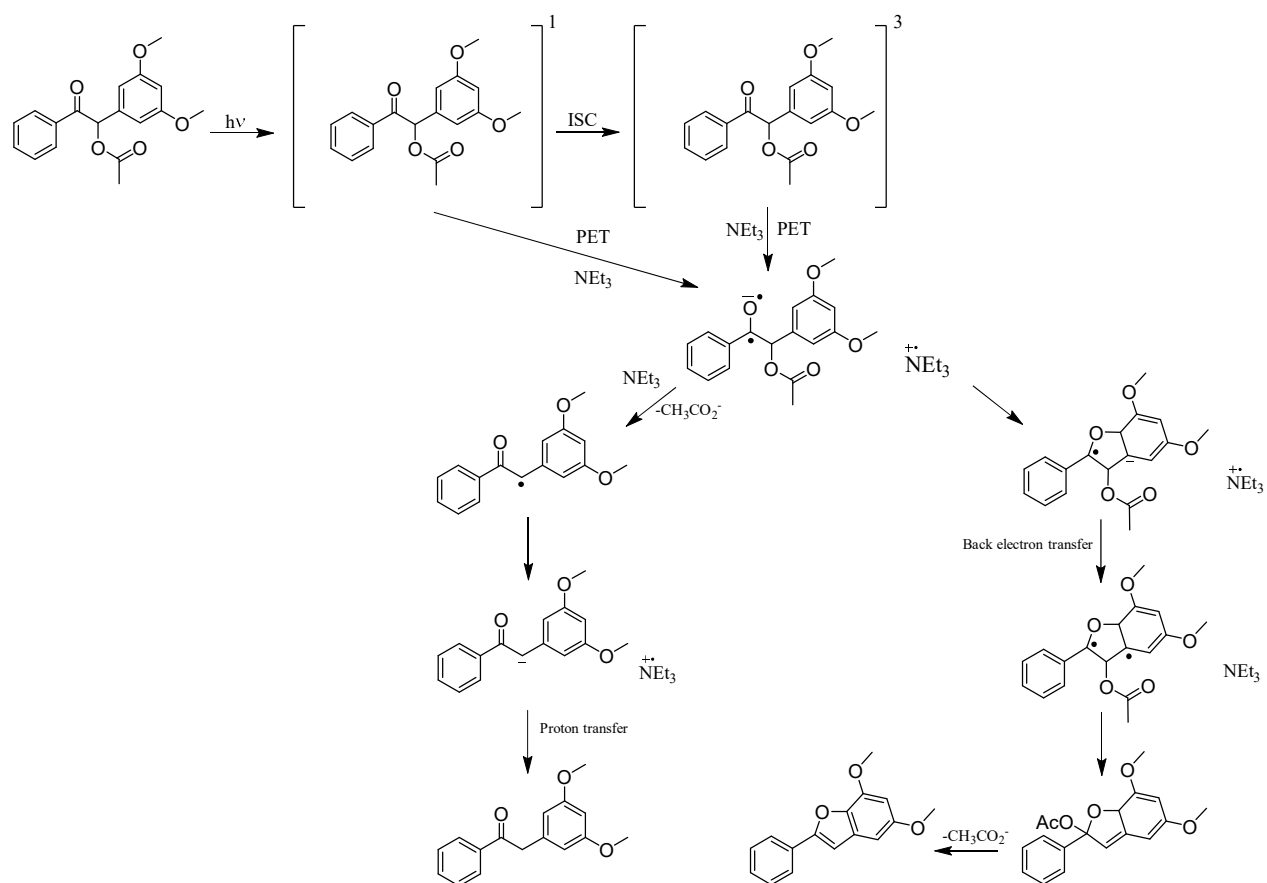


Figure 4-11 Pathways for formation of cyclized and deacetylated products in the presence of triethylamine proposed by Bisht et al in 2018.

In this mechanism, both the singlet and triplet excited states may interact with the electron donor triethylamine. Photoinduced electron transfer to either of these states results in a radical anion. This structure has precedence in literature, specifically in relation to the phenacyl PPG.<sup>61</sup> In the presence of a sensitizer, release from a phenacyl PPG is thought to begin with photoinduced electron transfer and the subsequent generation of a phenacyl anion radical. In the Bisht mechanism two pathways for reaction of the radical anion are possible. In the pathway which leads to the benzofuran, the anion attacks the 3',5'-dimethoxybenzyl moiety, yielding a cyclic radical anion. The subsequent diradical is generated by back electron transfer. The mechanism from this point onwards echoes that which was presented by Rock and Chan.<sup>41</sup>

In formation of the deacetylated product, the leaving group is first eliminated, affording the radical  $\alpha$ -carbonyl intermediate. Single electron transfer from triethylamine yields the  $\alpha$ -carbonyl anion. Proton transfer is the last step, resulting in the observed deacetylated species. The deacetylated product produced in the photolysis of **1-DMA** is expected to be a result of intramolecular photoinduced electron transfer. Two mechanisms are proposed here for the formation of this species. Reaction from both the triplet and singlet excited states are reflected. The basis of both mechanisms is photoinduced electron transfer resulting in the radical anion which is supported by phenacyl PPG literature.<sup>61</sup>

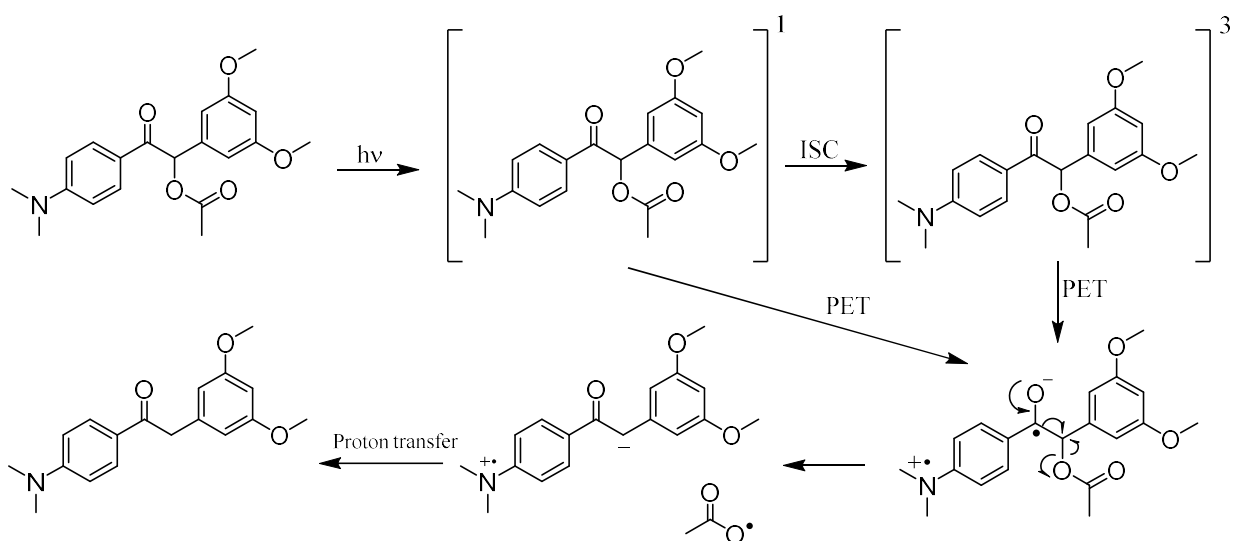


Figure 4-12 Mechanism I proposed for formation of deacetylated photoproduct.

In Mechanism I, Figure 4-12, the carbonyl reforms and the radical migrates to the alpha position. Simultaneously, the PPG-leaving group bond breaks homolytically to yield the radical precursor to acetic acid and the  $\alpha$ -anion. Proton transfer yields the observed product.

Mechanism II is less concise and more closely mirrors the Bischt mechanism. Here, the leaving group is first eliminated from the radical anion, affording the radical  $\alpha$ -carbonyl intermediate. Single electron transfer, which may be from a variety of sources including solvent or other species in solution or occur intramolecularly, yields the  $\alpha$ -carbonyl anion. As in Mechanism I, proton transfer is the last step.

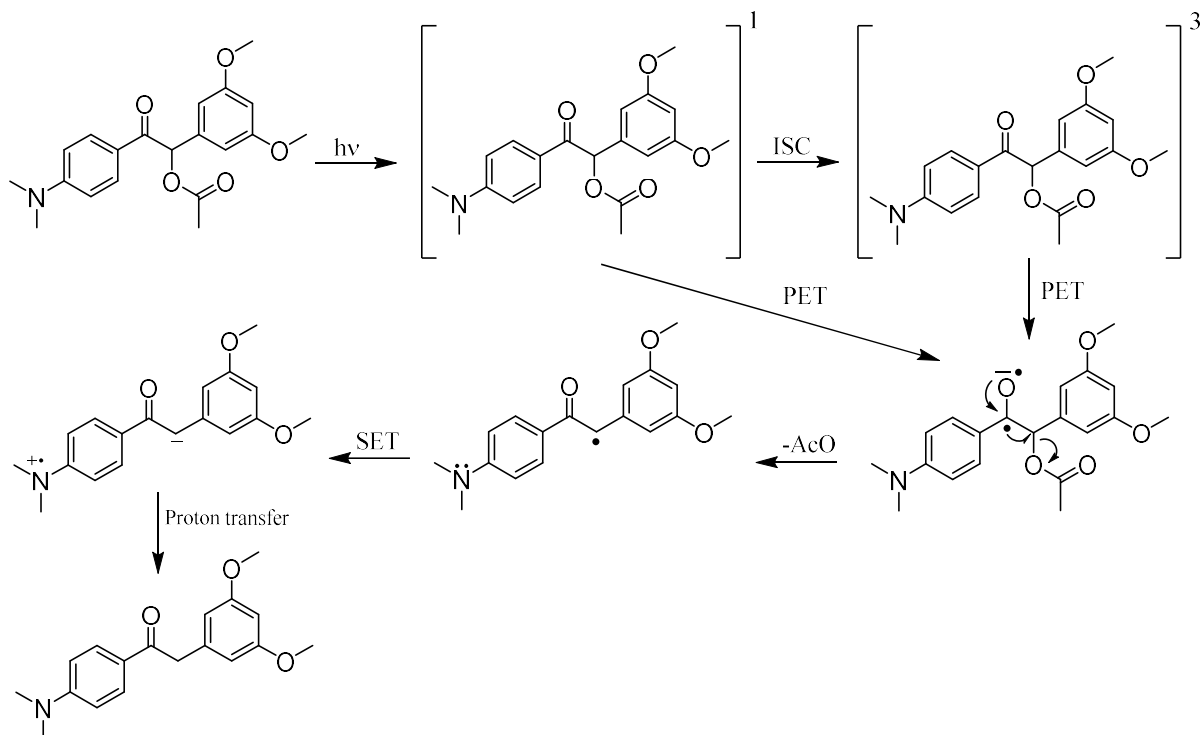


Figure 4-13 Mechanism II proposed for formation of deacetylated photoproduct.

Further work is required to ascertain whether benzofuran and aldehyde formation occurs on separate pathways from the proposed radical anion.

Preliminary quenching experiments with naphthalene indicate reaction from the triplet excited state. Additional work is again essential for the confirmation of this and other details of the photoreaction of this highly unusual PPG. The presence of an amine moiety in this molecule clearly results in a significant deviation from the characteristic photochemistry of the benzoin PPG. The formation of a single non-reactive photoproduct, such as the benzofuran, is preferable.

#### 4.3.2. 1-OMe [1-(3,5-dimethoxyphenyl)-2-(4-methoxyphenyl)-2-oxoethyl acetate

The second molecule in this series, **1-OMe**, seeks to significantly redshift absorption in the same manner as **1-DMA** while eliminating electron transfer photoproducts resulting from the amine functionality.

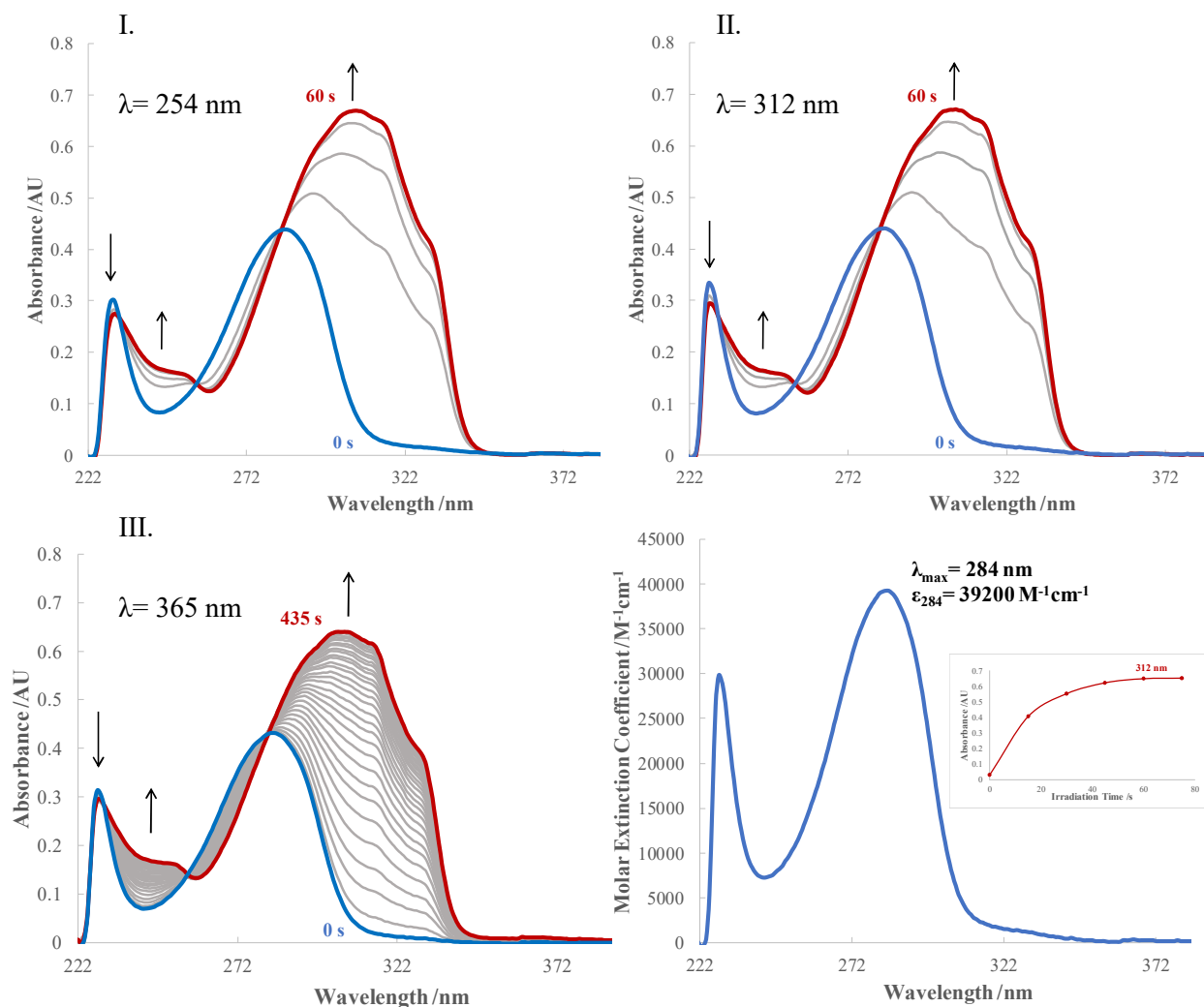


Figure 4-14 UV-Vis absorption spectra of photolysis of **1-OMe** (1.12 × 10<sup>-5</sup> M in CH<sub>2</sub>Cl<sub>2</sub>) with I. 254, II. 312, and III. 365 nm light. IV. Molar extinction coefficient plot of **1-OMe**. (Inset: Appearance of product at 312 nm with 312 nm irradiation).

The absorption profile of cage **1-OMe** mirrors that of **1-DMA**. The first absorption is centered at 230 nm and second at 284 nm. The extinction coefficient at 284 nm is 39,200 M<sup>-1</sup>cm<sup>-1</sup>, slightly less than that of **1-DMA**. This band represents a moderate 37 nm redshift from the primary absorption of **1P**. When these solutions are irradiated, the 284 nm band begins to shift bathochromically and increase in intensity. The area between 230 and 256 nm also begins to increase slightly. The primary absorption of the product is centered at 310 nm. Isosbestic points occur at 256 and 284 nm, indicating a clean conversion. The wavelength dependence of this photolysis is unique.



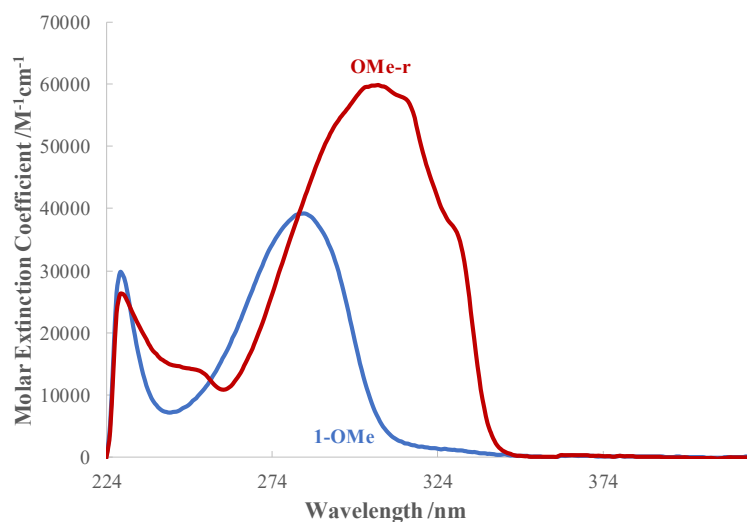


Figure 4-15 Molar extinction coefficient comparison of **1-OMe** and corresponding benzofuran **OMe-r**.

Photolysis of these 11  $\mu\text{M}$  solutions is complete within 60 seconds with both 254 and 312 nm light sources. Conversely, reaction progress lags with 365 nm irradiation, with the time of release increasing 730% to 435 seconds. The slow release rate with 365 nm may be partially rationalized by the absorption profiles of cage **1-OMe** and benzofuran **OMe-r**. Unlike polyaromatic derivatives **1a** and **1b**, absorption of the cage past 350 nm is extremely minimal. The benzofuran also absorbs minimally at 365 nm and as a result the inner filter effect should not be a factor. Interestingly, absorption of the benzofuran is centered near 312 nm and is more significant than that of the cage at this wavelength. In theory reaction progress should increasingly slow as concentration of the benzofuran increases and this species competitively absorbs incident light. Despite this, photorelease with 312 nm is exceptional. Further investigation into this phenomenon is required.

The photorelease was then monitored by  $^1\text{H}$  NMR spectroscopy. As would be suggested by the straightforward conversion demonstrated by UV-Vis studies, the reaction proceeded as parent **1P** with formation of the primary benzofuran photoproduct. Release of acetic acid is indicated by the appearance and increase of the characteristic 2.1 ppm signal

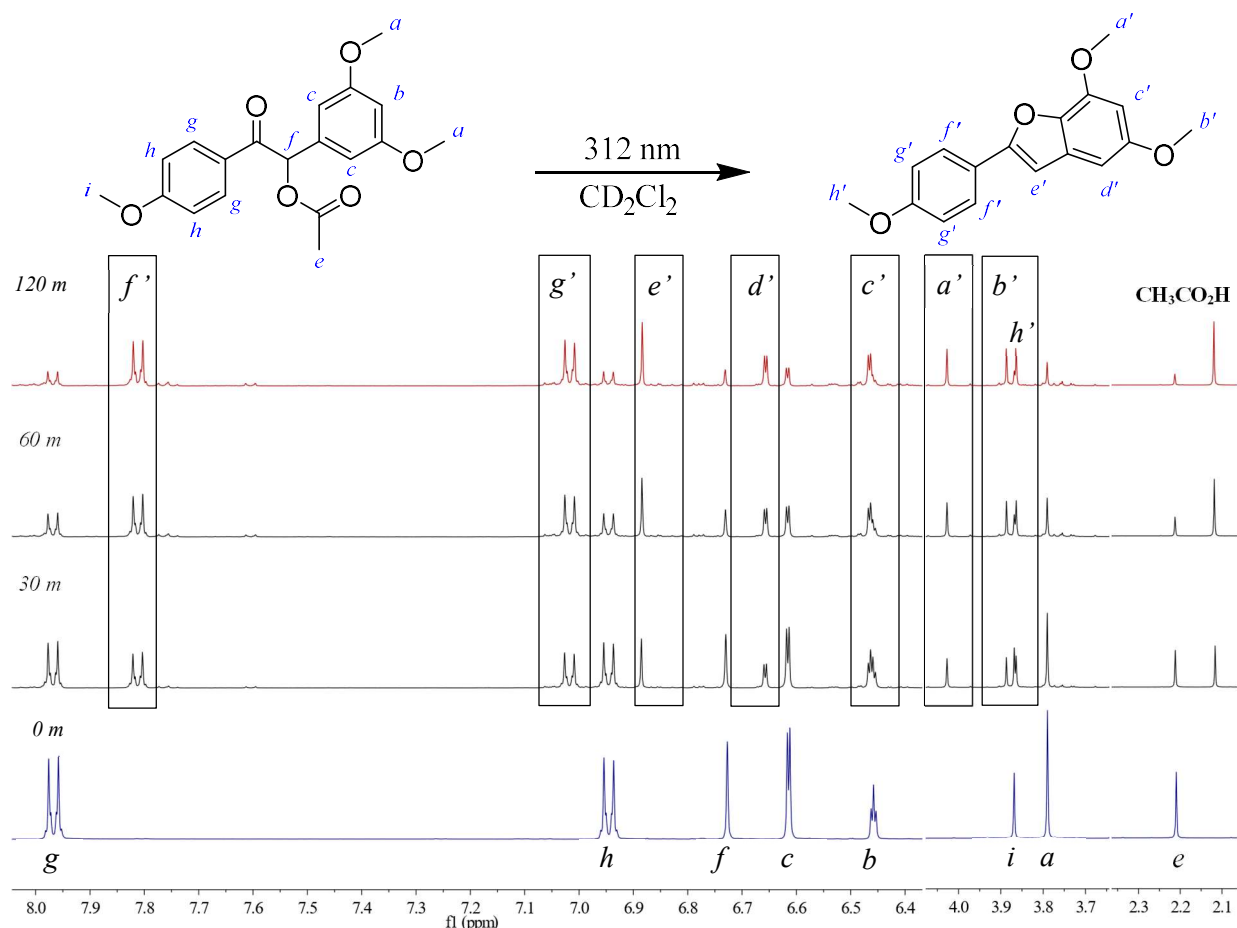


Figure 4-16 Evolution of selected regions of  $^1\text{H}$  NMR spectra throughout duration of irradiation of **1-OMe** with 312 nm light

The 3.7-4.0 ppm region is complicated by the presence of additional the additional methoxy group on the benzoyl moiety. As the photolysis proceeds, three proton signals *i* and *e*, corresponding to the para methoxy group and leaving group respectively, decrease. Six proton dimethoxy peak *a* is similarly diminished. The result is three new singlets in this region. Proton *a'* is pushed downfield to 3.98 ppm due to proximity to the newly formed furan. Protons *b'* and *h'* are present at 3.84 and 3.82 ppm, respectively. In the aromatic region, two proton signal *g* is replaced by *f'*, shifted upfield by loss of the carbonyl. The signal corresponding to proton *e'* at 6.83 ppm increases as *f* lessens. Unlike the case of **1-DMA**, the final mixture was seen to be photostable and did not degrade with further irradiation. Past 60 minutes a minor fraction of 3,5-dimethoxybenzaldehyde was seen to be produced. The quantity of this species was on par with that which is generated in the photorelease of **1P** at a similar concentration.

The photoproduct was isolated by flash column chromatography and confirmed by  $^1\text{H}$  and  $^{13}\text{C}$  NMR to be the corresponding benzofuran **OMe-r**. Comparison of the  $^1\text{H}$  NMR spectra of the final photolysis mixture and isolated benzofuran suggest nearly quantitative conversion. When a UV-Vis solution of the isolated product was analyzed and overlaid with the UV-Vis spectrum at 60s of irradiation (Figure 4-18), the are traces were seen to be essentially identical.

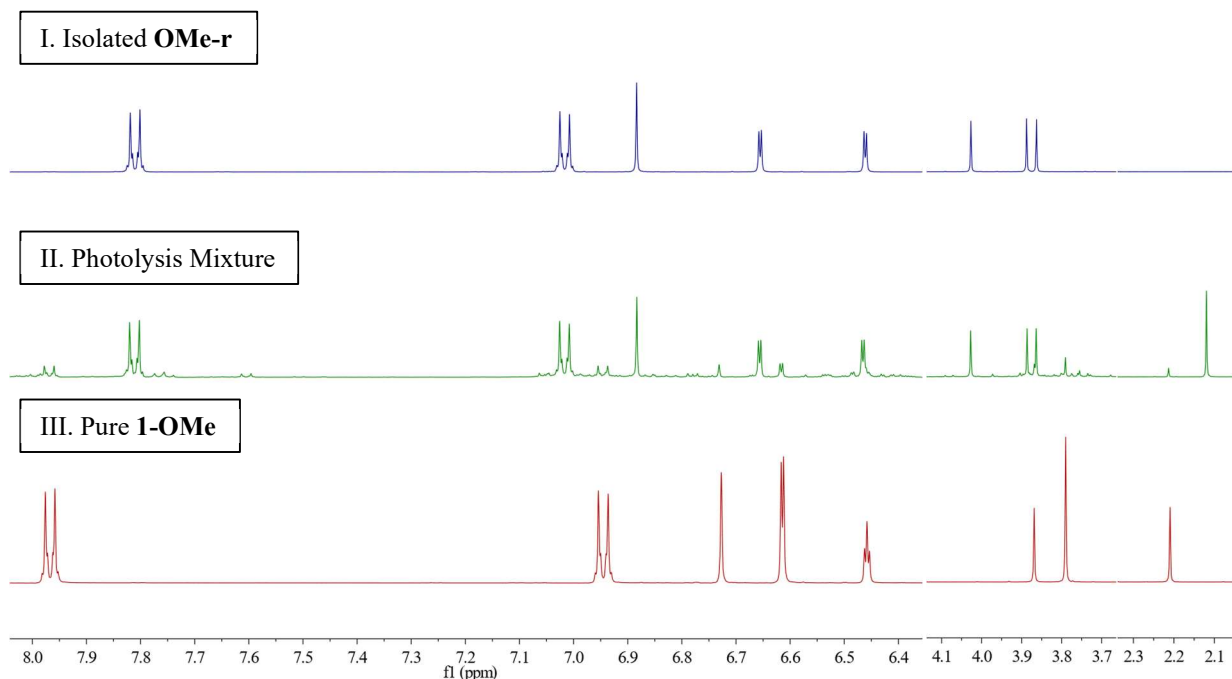


Figure 4-17  $^1\text{H}$  NMR comparison of (I) Isolated benzofuran, (II) Photolysis mixture-120 m, and (III) Photocage **1-OMe**.

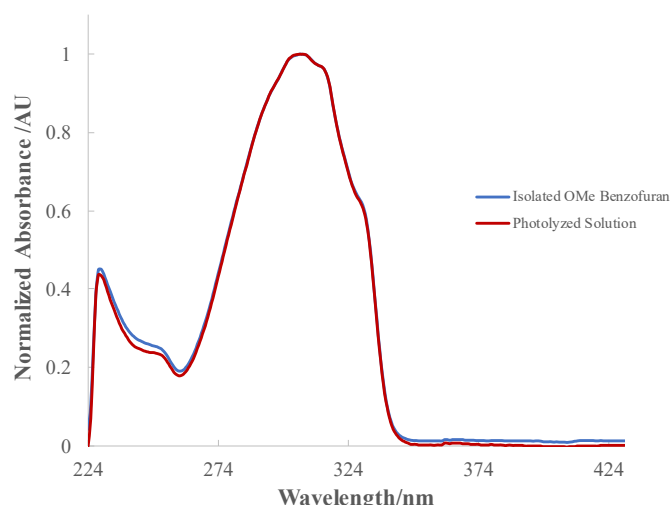


Figure 4-18 Normalized UV-Vis absorbance spectra of isolated benzofuran **OMe-r** and photolyzed solution of **1-OMe**.

#### 4.4. Conclusions

A comparison of molar extinction coefficients is presented in Figure 4-19. Both **1-OMe** and **1-DMA** are improved significantly from **1P** in this aspect.

The primary absorptions of **1-OMe** and **1-DMA** are 37 and 101 nm redshifted from **1P**, respectively. The properties of these PPGs are summarized in Table 4-1.

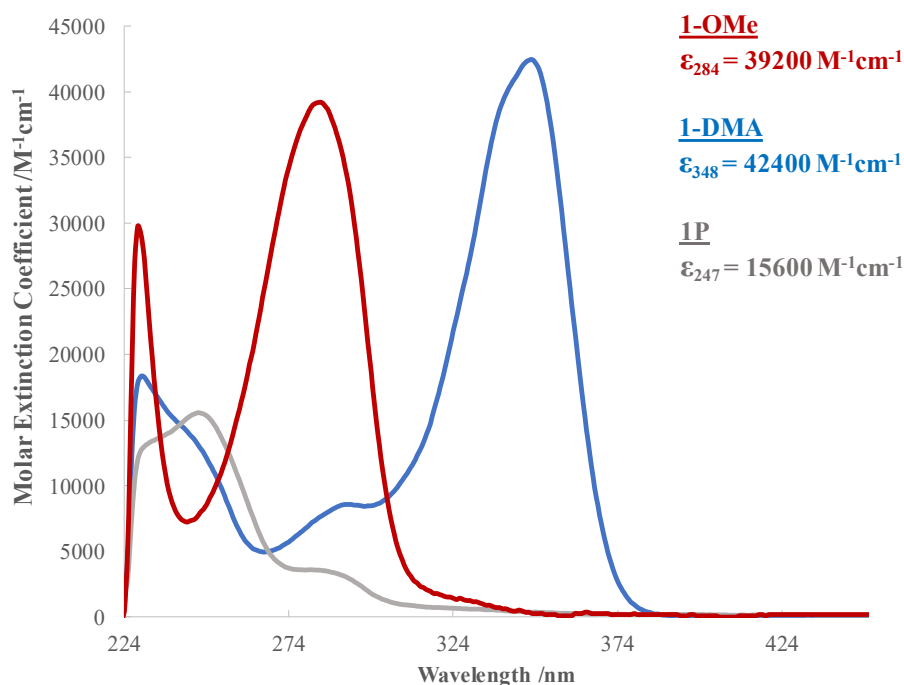


Figure 4-19 Molar Extinction coefficient comparison of photocages **1P**, **1-OMe**, and **1-DMA**.

Cage	$\lambda_{\max}$ /nm	$\epsilon_{\lambda_{\max}}$ /M <sup>-1</sup> cm <sup>-1</sup>	$\epsilon_{365}$ /M <sup>-1</sup> cm <sup>-1</sup>	UV-Vis Release			
				Concentration / $\mu$ M	254 Lamp t <sub>r</sub> /s	312 Lamp t <sub>r</sub> /s	365 Lamp t <sub>r</sub> /s
<b>1P</b>	247	15600	210	38.2	135	240	570
<b>1-DMA</b>	348	42400	13400	19.7	120	60	60
<b>1-OMe</b>	284	39200	360	11.2	90	60	435

Table 4-1 Summarized properties of **1P**, **1-DMA**, and **1-OMe**.

Rate constants for photorelease were calculated in the same manner as those in Table 3-2 (See Appendix B). Unfortunately, loss of **1-OMe** cannot be monitored by UV-Vis by disappearance of the ~250 nm band. As a result, comparison of this PPG is purely qualitative and does not involve determination of rate constants.

Cage	Rate Constant /s <sup>-1</sup>		
	254 Lamp	312 Lamp	365 Lamp
<b>1P</b>	0.007 ± 0.0008	0.005 ± 0.0004	0.00084 ± 0.000022
<b>1-DMA</b>	0.020 ± 0.0012	0.014 ± 0.00015	0.02 ± 0.0006

Table 4-2 First order rate constants for photorelease of acetic acid

For release with 254 nm, both donor-acceptor derivatives are superior to **1P**. In the case of **1-DMA**, this rate constant is nearly triple that of **1P**. The ability to release with medium and long wave UV light is extremely significant, as this is the primary deficiency of traditional 3',5'-dimethoxybenzoin systems. With a 312 nm light source, **1-DMA** releases with rate constants an order of magnitude larger than that of **1P**. Qualitatively, the rate constant of **1-OMe** is expected to be similar based on the corresponding reaction times. In studies carried out with a 365 nm lamp, the rate constant for release of acetic acid from **1-DMA** was calculated to be 3800% greater than that of **1P**. This is extremely significant. **1-OMe** maintains the characteristic photochemistry of the benzoin PPG, yielding a single benzofuran photoproduct. This PPG is an excellent alternative to **1P** in studies where 254 or 312 nm irradiation is preferred.

The unique photochemistry of **1-DMA** presents an opportunity to uncover mechanistic insights, much like the observation of the novel benzoin photoproduct by Rock and Chan.<sup>41</sup> In these systems where the concrete identification of extremely short-lived intermediates is elusive, these observations are particularly important. Further modification of the structural characteristics of the benzoin PPG is dually beneficial. Novel photoproducts and structure-reactivity relationships are bound to be uncovered in this process. These are valuable for critical evaluation of the numerous proposed mechanisms of photorelease. An expanded toolbox of PPGs in the benzoin class is crucial for a resurgence of their use in applied chemistry and biology. The molecules presented in this thesis are a solid starting point for the development of benzoin PPGs with improved and/or varied properties and demonstrate the exceptional sensitivity of these PPGs to structural modification.

## 4.5. Experimental

### 4.5.1. General Methods

All solvents and reagents used for synthesis, chromatography, UV-vis spectroscopy and photochemical studies were purchased from Aldrich, Anachemia, Caledon Labs, Fisher Scientific or Alfa Aesar, and used as received. THF was dried and degassed by passage through steel columns containing activated alumina under nitrogen using an MBraun solvent purification system. Solvents for NMR analysis were purchased from Cambridge Isotope Laboratories and used as received. Column chromatography was performed using silica gel 60 (230–400 mesh) from Silicycle Inc.  $^1\text{H}$  and  $^{13}\text{C}$  NMR characterizations were performed on a Bruker Avance-500 instrument with a 5 mm inverse probe operating 125.76 MHz for  $^{13}\text{C}$  NMR unless stated otherwise. Chemical shifts ( $\delta$ ) are reported in parts per million (ppm) relative to tetramethylsilane using the residual solvent peak as a reference, and splitting patterns are designated as s (singlet), d (doublet), t (triplet) and m (multiplet). Coupling constants ( $J$ ) are reported in Hertz. UV-Vis absorption spectra were recorded on a Shimadzu UV-3600 Plus spectrophotometer. Fluorescence measurements were performed on a PTI Quantamaster spectrofluorometer. High Resolution Mass Spectroscopy (HRMS) measurements were performed using an Agilent 6210 TOF LC/MS in ESI-(+) mode.

### 4.5.2. Photolysis

All irradiations and analyses were completed in a scarce-light setting to ensure no interference from ambient light sources. Handheld Spectroline® E-Series UV lamps with broadband light centered at three wavelengths (254, 312, and 365 nm) were used.

#### *Bulk Photolysis*

For **1-OMe**, 50 mg of the given photocage was dissolved in 10 mL dichloromethane in a glass vial and irradiated with a handheld 312 nm lamp. The photolysis was observed by TLC and continued until the strong fluorescent top spot dominates, typically 120 minutes. Samples of **1-DMA** were monitored by  $^1\text{H}$  NMR throughout the duration of photolysis to ensure complete release without significant degradation. The samples were then dry loaded onto short columns. The solvent system

for separation was 1:3 ethyl acetate/hexanes for photolyzed **1-OMe** solutions and 1:6 ethyl acetate/hexanes for photolyzed **1-DMA** solutions.

#### *<sup>1</sup>H NMR Studies*

To trace the uncaging process with <sup>1</sup>H NMR, approximately 1 mg of the chromophore was dissolved in 0.5 mL CD<sub>2</sub>Cl<sub>2</sub> and pipetted into an NMR tube. In the case of **1-OMe**, irradiation was carried out with two handheld UV lamps, one on either side of the upright NMR tube. Reactions of **1-DMA** were completed with a single handheld UV lamp placed over the horizontal NMR tube. <sup>1</sup>H NMR spectra were obtained at each time interval until either no further spectral changes or degradation was observed.

#### *UV-Vis Studies*

Solutions of the indicated concentrations were prepared with the use of amber volumetric flasks and volumetric pipettes. Irradiation was carried out in a quartz cuvette by a single handheld UV lamp.

### **4.5.3. Synthetic Procedures and Characterization**

**Synthesis of 4-(1,3-dithian-2-yl)-N,N-dimethylaniline (3-DMA)** A solution of 4-dimethylamino benzaldehyde (2.99 g, 20.0 mmol) in CH<sub>2</sub>Cl<sub>2</sub> (50 mL) was treated with 1,3-propanedithiol (2.10 ml, 20.9 mmol). After stirring for 5 min, the mixture was treated with Hf(OTf)<sub>4</sub> (51 mg, 0.0658 mmol). The resulting yellow solution was stirred for 2 h and subsequently refluxed for 4 h, at which time it was cooled and filtered through a pad of Celite. The Celite was rinsed repeatedly with CH<sub>2</sub>Cl<sub>2</sub> and the combined filtrates were evaporated under reduced pressure. The product was purified by flash column chromatography on with a solvent system of 1:3 EtOAc/hexanes, yielding 4.31 g (90%) of **3-DMA** as a white crystalline solid.

<sup>1</sup>H NMR (500 MHz, CDCl<sub>3</sub>) δ 7.37 – 7.27 (m, 2H), 6.71 – 6.62 (m, 2H), 5.12 (s, 1H), 3.06-2.98 (m, 2H), 2.94 (s, 6H), 2.94 – 2.84 (m, 2H), 2.20-2.12 (m, 1H), 1.90-1.75 (m, 1H).

<sup>13</sup>C NMR (126 MHz, CDCl<sub>3</sub>) δ 150.39, 128.36, 126.52, 112.24, 50.82, 40.34, 32.19, 25.04.

HRMS (ESI<sup>+</sup>) Anal. Calc. for C<sub>12</sub>H<sub>18</sub>NS<sub>2</sub> (M+H)<sup>+</sup> 240.0875 Found: 240.0872

**Synthesis of (3,5-dimethoxyphenyl)(2-(4-(dimethylamino)phenyl)-1,3-dithian-2-yl)methyl acetate (2-DMA)** A flame dried flask under N<sub>2</sub> was charged with 4-(1,3-dithian-2-yl)-N,N-dimethylaniline 810 mg, 3.38 mmol) and dry THF (50 mL). The system was cooled to 0°C in an ice bath before the dropwise addition of 1.6 M *n*-BuLi solution in hexanes (2.30 mL, 3.68 mmol). The resulting yellow solution was stirred 10 min, at which time the septum was briefly removed and 3,5-dimethoxybenzaldehyde (620 mg, 3.73 mmol) was added. The mixture was then purged with N<sub>2</sub> and allowed to warm to room temperature over a period of 45 min, at which time it was treated with acetic anhydride (0.65 mL, 5.90 mmol) and DMAP (208 mg, 1.70 mmol). After stirring at room temperature for 24 h, the solution was poured into water and extracted with EtOAc (10 mL). After three additional extractions with EtOAc, the combined organic layers were dried over MgSO<sub>4</sub> and the solvent was removed under reduced pressure. The crude mixture, an orange oil, was purified by flash column chromatography on a column of moderate length with a solvent system of 1:6 EtOAc /hexanes. The product was isolated as a colourless oil that foamed into a fine yellow powder under high-vacuum (954 mg, 63%).

<sup>1</sup>H NMR (500 MHz, CD<sub>2</sub>Cl<sub>2</sub>) δ 7.59 – 7.53 (m, 2H), 6.70 – 6.64 (m, 2H), 6.31 (t, *J* = 2.3 Hz, 1H), 6.04 (d, *J* = 2.3 Hz, 2H), 5.96 (s, 1H), 3.60 (s, 6H), 2.95 (s, 6H), 2.75 – 2.59 (m, 4H), 2.08 (s, 3H), 1.91 – 1.82 (m, 2H).

<sup>13</sup>C NMR (126 MHz, CD<sub>2</sub>Cl<sub>2</sub>) δ 169.37, 159.47, 149.87, 137.72, 131.65, 124.00, 111.51, 106.62, 100.45, 80.54, 55.11, 40.20, 27.32, 27.18, 24.94, 20.72.

HRMS (ESI<sup>+</sup>) Anal. Calc. for C<sub>23</sub>H<sub>29</sub>NNaO<sub>4</sub>S<sub>2</sub> (M+Na)<sup>+</sup> 470.1430 Found: 470.1435

**Synthesis of 1-(3,5-dimethoxyphenyl)-2-(4-(dimethylamino)phenyl)-2-oxoethyl acetate**

**(1-DMA)** Under scarce light conditions a solution of 3,5-dimethoxyphenyl(2-(4-(dimethylamino)phenyl)-1,3-dithian-2-yl)methyl acetate (310 mg, 0.69 mmol) in a mixture of 1:4 H<sub>2</sub>O/CH<sub>3</sub>CN (10 mL) was treated with Hg(ClO<sub>4</sub>)<sub>2</sub>·H<sub>2</sub>O (970 mg, 2.42 mmol) in one portion. After stirring for 30 min, the reaction mixture was quenched with sat. NaHCO<sub>3</sub> and vacuum filtered. The filtrate was extracted with EtOAc and the layers separated. After three more extractions of the aqueous layer, the combined organic extracts were dried over MgSO<sub>4</sub> and the solvent was removed under reduced pressure. The crude mixture was dry loaded onto a short column and eluted with 1:3 EtOAc/hexanes to yield 172 mg (70%) of **1-DMA** as a yellow solid.

<sup>1</sup>H NMR (500 MHz, CD<sub>2</sub>Cl<sub>2</sub>) δ 7.87 – 7.80 (m, 2H), 6.68 (s, 1H), 6.65 – 6.56 (m, 4H), 6.40 (t, *J* = 2.3 Hz, 1H), 3.75 (s, 6H), 3.02 (s, 6H), 2.16 (s, 3H).



$^{13}\text{C}$  NMR (151 MHz,  $\text{CD}_2\text{Cl}_2$ )  $\delta$  191.10, 170.74, 161.64, 154.24, 137.50, 131.28, 122.30, 111.11, 106.96, 101.02, 77.62, 55.92, 40.31, 21.20.

HRMS (ESI<sup>+</sup>) Anal. Calc. for  $\text{C}_{20}\text{H}_{24}\text{NO}_5$  (M+H)<sup>+</sup> 358.1654 Found: 358.1642

**Synthesis of 2-(4-methoxyphenyl)-1,3-dithiane (3-OMe)** p-Anisaldehyde (1.85 mL, 15.0 mmol) was dissolved in  $\text{CH}_2\text{Cl}_2$  (20 mL). 1,3-propanedithiol (1.50 mL, 15.0 mmol) was added, followed by  $\text{Hf}(\text{OTf})_4$  (35 mg, 0.045 mmol). The yellow solution was stirred for 24 hours at room temperature. The solution was filtered through a pad of Celite which was subsequently rinsed repeatedly with  $\text{CH}_2\text{Cl}_2$ . The solvent was evaporated under reduced pressure and the crude product was purified on a short column with solvent system 1:4 EtOAc/hexanes, yielding 1.36 g (40%) of **3-OMe** as a pale blue crystalline solid.

$^1\text{H}$  NMR (500 MHz,  $\text{CD}_2\text{Cl}_2$ )  $\delta$  7.96 – 7.91 (m, 2H), 7.34 – 7.28 (m, 2H), 5.60 (s, 1H), 4.24 (s, 3H), 3.57-3.45 (m, 2H), 3.38-3.28 (m, 2H), 2.66-2.56 (m, 1H), 2.38 – 2.23 (m, 1H).

$^{13}\text{C}$  NMR (126 MHz,  $\text{CD}_2\text{Cl}_2$ )  $\delta$  160.17, 132.13, 129.38, 114.52, 55.82, 54.43, 54.22, 54.00, 53.78, 53.57, 51.17, 32.73, 25.71.

HRMS (ESI<sup>+</sup>) Anal. Calc. for  $\text{C}_{11}\text{H}_{14}\text{NaOS}_2$  (M+Na)<sup>+</sup> 249.0378 Found: 249.0377

**Synthesis of (3,5-dimethoxyphenyl)(2-(4-methoxyphenyl)1,3-dithian-2-yl)methyl acetate (2-OMe)** A flame dried flask under  $\text{N}_2$  was charged with 2-(4-methoxyphenyl)-1,3-dithiane (800 mg, 3.23 mmol) and dry THF (50 mL). The system was cooled to 0°C in an ice bath before the dropwise addition of 1.6 M *n*-BuLi solution in hexanes (2.40 mL, 3.55 mmol). The resulting orange solution was stirred 10 min, at which time the septum was briefly removed and 3,5-dimethoxybenzaldehyde (590 mg, 3.55 mmol) was added. The mixture was then purged with  $\text{N}_2$  and allowed to warm to room temperature over a period of 45 min, at which time it was treated with acetic anhydride (0.36 mL, 3.81 mmol) and DMAP (435 mg, 3.56 mmol). After stirring at room temperature for 24 h, the solution was poured into water and extracted with EtOAc (10 mL). After three additional extractions with EtOAc, the combined organic layers were dried over  $\text{MgSO}_4$  and the solvent was removed under reduced pressure. The crude mixture, a red oil, was purified by flash column chromatography on a column of moderate length with a solvent system of 1:6 EtOAc /hexanes. The product was isolated as a colourless oil that foamed into a fine yellow powder under high-vacuum (280 mg, 20%)

$^1\text{H}$  NMR (500 MHz,  $\text{CD}_2\text{Cl}_2$ )  $\delta$  7.72 – 7.64 (m, 2H), 6.90 – 6.83 (m, 2H), 6.35 (t,  $J = 2.3$  Hz, 1H), 6.13 – 6.03 (m, 3H), 3.86 (d,  $J = 9.7$  Hz, 4H), 3.63 (s, 6H), 2.78 – 2.61 (m, 4H), 2.14 (s, 3H), 2.00 – 1.87 (m, 2H).

$^{13}\text{C}$  NMR (151 MHz,  $\text{CD}_2\text{Cl}_2$ )  $\delta$  169.32, 159.53, 159.05, 137.43, 132.25, 128.89, 113.06, 107.46, 106.56, 100.41, 80.33, 55.60, 55.27, 55.12, 53.82, 53.64, 53.46, 53.28, 53.14, 53.10, 29.69, 27.30, 27.16, 24.79, 20.70.

HRMS (ESI<sup>+</sup>) Anal. Calc. for  $\text{C}_{22}\text{H}_{26}\text{NaO}_5\text{S}_2$  (M+Na)<sup>+</sup> 457.1129 Found: 457.1114

**Synthesis of 1-(3,5-dimethoxyphenyl)-2-(4-methoxyphenyl)-2-oxoethyl acetate (1-OMe)** Under scarce light conditions a solution of (3,5-dimethoxyphenyl)(2-(4-methoxyphenyl)1,3-dithian-2-yl)methyl acetate (250 mg, 0.58 mmol) in a mixture of 1:100  $\text{H}_2\text{O}$ /Acetone (50 mL) was treated with CuO (183 mg, 2.30 mmol) and  $\text{CuCl}_2$  (196 mg, 1.15 mmol). The resulting solution was stirred at room temperature for 72 hours at which point it was filtered through a Celite pad. The deep blue solution was concentrated under reduced pressure and subsequently dissolved in acetone. The solvent was evaporated under reduced pressure and this step was repeated twice. The concentrate was then dissolved in 15 mL ethyl acetate. In a separation funnel an equal volume of 5%  $\text{NaHCO}_3$  was added. The resulting aqueous layer was separated and extracted three times with 15 mL of ethyl acetate. The combined organic layers were dried over  $\text{Na}_2\text{SO}_4$  and concentrated. The crude mixture was dry loaded onto a short column and eluted with 1:4 EtOAc/hexanes to yield 130 mg (65%) of **1-OMe** as a colourless oil.

$^1\text{H}$  NMR (500 MHz,  $\text{CD}_2\text{Cl}_2$ )  $\delta$  7.96 – 7.89 (m, 2H), 6.94 – 6.87 (m, 2H), 6.69 (s, 1H), 6.57 (d,  $J = 2.3$  Hz, 2H), 6.42 (t,  $J = 2.3$  Hz, 1H), 3.83 (s, 3H), 3.75 (s, 6H), 2.17 (s, 3H)

$^{13}\text{C}$  NMR (126 MHz,  $\text{CD}_2\text{Cl}_2$ )  $\delta$  192.24, 170.77, 164.46, 161.81, 136.71, 131.52, 127.93, 114.43, 107.11, 101.27, 77.94, 56.07, 55.95, 54.43, 54.22, 54.00, 53.78, 53.57, 21.12.

HRMS (ESI<sup>+</sup>) Anal. Calc. for  $\text{C}_{19}\text{H}_{20}\text{NaO}_6$  (M+Na)<sup>+</sup> 367.1152 Found: 367.1164

## Isolated Photoproducts

### *3,5-dimethoxybenzaldehyde*

$^1\text{H}$  NMR (500 MHz,  $\text{CD}_2\text{Cl}_2$ )  $\delta$  9.93 (s, 1H), 7.05 (d,  $J = 2.4$  Hz, 2H), 6.76 (t,  $J = 2.4$  Hz, 1H), 3.88 (s, 6H).

***4-(5,7-dimethoxybenzofuran-2-yl)-N,N-dimethylaniline***

<sup>1</sup>H NMR (500 MHz, CD<sub>2</sub>Cl<sub>2</sub>) δ 7.73 (d, *J* = 8.9 Hz, 2H), 6.83 – 6.76 (m, 3H), 6.63 (d, *J* = 2.2 Hz, 1H), 6.42 (d, *J* = 2.3 Hz, 1H), 4.02 (s, 3H), 3.86 (s, 3H), 3.05 (s, 6H)

HRMS (ESI<sup>+</sup>) Anal. Calc. for C<sub>18</sub>H<sub>20</sub>NO<sub>3</sub> (M+H)<sup>+</sup> 298.1438 Found: 298.1439

***2-(3,5-dimethoxyphenyl)-1-(4-(dimethylamino)phenyl)ethan-1-one***

<sup>1</sup>H NMR (500 MHz, CD<sub>2</sub>Cl<sub>2</sub>) δ 7.96 – 7.89 (m, 2H), 6.73 – 6.65 (m, 2H), 6.44 (d, *J* = 2.3 Hz, 2H), 6.36 (t, *J* = 2.3 Hz, 1H), 4.13 (s, 2H), 3.78 (s, 6H), 3.08 (s, 6H).

HRMS (ESI<sup>+</sup>) Anal. Calc. for C<sub>18</sub>H<sub>21</sub>NNaO<sub>3</sub> (M+Na)<sup>+</sup> 322.1414 Found: 322.1422

***5,7-dimethoxy-2-(4-methoxyphenyl)benzofuran (OMe-r)***

<sup>1</sup>H NMR (500 MHz, Methylene Chloride-*d*<sub>2</sub>) δ 7.81 – 7.71 (m, 2H), 7.02 – 6.93 (m, 2H), 6.84 (s, 1H), 6.61 (d, *J* = 2.2 Hz, 1H), 6.42 (d, *J* = 2.3 Hz, 1H), 3.99 (s, 3H), 3.85 (s, 3H), 3.82 (s, 3H).

HRMS (ESI<sup>+</sup>) Anal. Calc. for C<sub>17</sub>H<sub>16</sub>NaO<sub>4</sub> (M+Na)<sup>+</sup> 307.0940 Found 307.0941

## References

- (1) Kaplan, J. H.; Forbush, B.; Hoffman, J. F. Rapid Photolytic Release of Adenosine 5'-Triphosphate from a Protected Analog: Utilization by the Sodium:Potassium Pump of Human Red Blood Cell Ghosts. *Biochemistry* **1978**, *17* (10), 1929–1935.
- (2) Hoffmann, N. Photochemical Reactions of Aromatic Compounds and the Concept of the Photon as a Traceless Reagent. *Photochemical & Photobiological Sciences* **2012**, *11* (11), 1613.
- (3) Lester, H. A.; Nerbonne, J. M. Physiological and Pharmacological Manipulations with Light Flashes. *Annual Review of Biophysics and Bioengineering* **1982**, *11* (1), 151–175.
- (4) Barltrop, J.; Schofield, P. Photosensitive Protecting Groups. *Tetrahedron Letters* **1962**, *3* (16), 697–699.
- (5) Barltrop, J. A.; Plant, P. J.; Schofield, P. Photosensitive Protective Groups. *Chemical Communications (London)* **1966**, No. 22, 822.
- (6) Yousef, A.; Lee, J.-I.; Li, Conrad, P.; Givens, R. Photoremovable Protecting Groups. *CRC Handbook of Organic Photochemistry and Photobiology, Volumes 1 & 2, Second Edition* **2003**
- (7) Pelliccioli, A. P.; Wirz, J. Photoremovable Protecting Groups: Reaction Mechanisms and Applications. *Photochemical & Photobiological Sciences* **2002**, *1* (7), 441–458.
- (8) Cameron, J. F.; Frechet, J. M. J. Photogeneration of Organic Bases from o-Nitrobenzyl-Derived Carbamates. *Journal of the American Chemical Society* **1991**, *113* (11), 4303–4313.
- (9) Wang, P. Photolabile Protecting Groups: Structure and Reactivity. *Asian Journal of Organic Chemistry* **2013**, *2* (6), 452–464.
- (10) Singh, A. K.; Khade, P. K. 3-Nitro-2-Naphthalenemethanol: a Photocleavable Protecting Group for Carboxylic Acids. *Tetrahedron* **2005**, *61* (42), 10007–10012
- (11) Givens, R. S.; Athey, P. S.; Matuszewski, B.; Kueper, L. W.; Xue, J.; Fister, T. Photochemistry of Phosphate Esters: Alpha-Keto Phosphates as a Photoprotecting Group for Caged Phosphate. *Journal of the American Chemical Society* **1993**, *115* (14), 6001–6012
- (12) Schmidt, R.; Geissler, D.; Hagen, V.; Bendig, J. Mechanism of Photocleavage of (Coumarin-4-Yl)Methyl Esters. *The Journal of Physical Chemistry A* **2007**, *111* (26), 5768–5774.
- (13) Zimmerman, H. E.; Sandel, V. R. Mechanistic Organic Photochemistry. II. Solvolytic Photochemical Reactions. *Journal of the American Chemical Society* **1963**, *85* (7), 915–922.
- (14) Pincock, J. A. Photochemistry of Arylmethyl Esters in Nucleophilic Solvents: Radical Pair and Ion Pair Intermediates. *Accounts of Chemical Research* **1997**, *30* (1), 43–49.

- (15) Zimmerman, H. E. The Meta–Ortho Effect in Organic Photochemistry; Mechanistic and Exploratory Organic Photochemistry. *The Journal of Physical Chemistry A* **1998**, *102* (39), 7725–7725.
- (16) Sheehan, J. C.; Umezawa, K. Phenacyl Photosensitive Blocking Groups. *The Journal of Organic Chemistry* **1973**, *38* (21), 3771–3774.
- (17) Givens R.S.; Heger D.; Hellrung B.; Kamdzhilov Y.; Mac M.; Conrad P. G.; Lee E.; Cope J.I.; Mata-Segreda J. F.; Schowen R. L.; and Wirz J. The photo-Favorskii reaction of p-hydroxyphenacyl compounds is initiated by water-assisted, adiabatic extrusion of a triplet biradical, *J. Am. Chem. Soc.*, **2008**, *130* (11), 3307–3309.
- (18) Givens, R. S.; Park, C.-H. p-Hydroxyphenacyl ATP1: A New Phototrigger. *Tetrahedron Letters* **1996**, *37* (35), 6259–6262.
- (19) Zhang, K.; Corrie, J. E. T.; Munasinghe, V. R. N.; Wan, P. Mechanism of Photosolvolytic Rearrangement Of p-Hydroxyphenacyl Esters: Evidence for Excited-State Intramolecular Proton Transfer as the Primary Photochemical Step. *Journal of the American Chemical Society* **1999**, *121* (24), 5625–5632.
- (20) Conrad, P. G.; Givens, R. S.; Weber, J. F. W.; Kandler, K. New Phototriggers: Extending the p-Hydroxyphenacyl  $\pi$ – $\pi^*$  Absorption Range. *Organic Letters* **2000**, *2* (11), 1545–1547.
- (21) Sheehan, J. C.; Wilson, R. M. Photolysis of Desyl Compounds. A New Photolytic Cyclization. *Journal of the American Chemical Society* **1964**, *86* (23), 5277–5281.
- (22) Bochet, C. G. Wavelength-Selective Cleavage of Photolabile Protecting Groups. *Tetrahedron Letters* **2000**, *41* (33), 6341–6346.
- (23) Piloto, A. M.; Costa, S. P.; Gonçalves, M. S. T. Wavelength-Selective Cleavage of o-Nitrobenzyl and Polyheteroaromatic Benzyl Protecting Groups. *Tetrahedron* **2014**, *70* (3), 650–657.
- (24) Specht, A.; Bolze, F.; Donato, L.; Herbivo, C.; Charon, S.; Warther, D.; Gug, S.; Nicoud, J.-F.; Goeldner, M. The Donor–Acceptor Biphenyl Platform: A Versatile Chromophore for the Engineering of Highly Efficient Two-Photon Sensitive Photoremovable Protecting Groups. *Photochemical & Photobiological Sciences* **2012**, *11* (3), 578.
- (25) Khade, P. K.; Singh, A. K. A New Caging Phototrigger Based on a 2-Acetonaphthyl Chromophore. *Tetrahedron Letters* **2007**, *48* (39), 6920–6923.
- (26) Singh, A. K.; Khade, P. K. Anthracene-9-Methanol—a Novel Fluorescent Phototrigger for Biomolecular Caging. *Tetrahedron Letters* **2005**, *46* (33), 5563–5566.

- (27)Sheehan, J. C.; Wilson, R. M.; Oxford, A. W. Photolysis of Methoxy-Substituted Benzoin Esters. Photosensitive Protecting Group for Carboxylic Acids. *Journal of the American Chemical Society* **1971**, *93* (26), 7222–7228.
- (28)Tenney, L. P.; Boykin, D. W.; Lutz, R. E. Novel Photocyclization of a Highly Phenylated  $\beta,\gamma$ -Unsaturated Ketone to a Cyclopropyl Ketone, Involving Benzoyl Group Migration. *Journal of the American Chemical Society* **1966**, *88* (8), 1835–1836.
- (29)Padwa, A.; Gruber, R. Photochemical Transformations of Small-Ring Carbonyl Compounds. XXII. Observations on the Scope of the Photoinduced Ring Expansion of Aroylazetidines. *Journal of the American Chemical Society* **1970**, *92* (1), 100–107.
- (30)Corrie, J. E. T.; Trentham, D. R. Synthetic, Mechanistic and Photochemical Studies of Phosphate Esters of Substituted Benzoin. *Journal of the Chemical Society, Perkin Transactions I* **1992**, No. 18, 2409.
- (31)Givens, R. S.; Athey, P. S.; Kueper, L. W.; Matuszewski, B.; Xue, J. Y. Photochemistry of Alpha-Keto Phosphate Esters: Photorelease of a Caged CAMP. *Journal of the American Chemical Society* **1992**, *114* (22), 8708–8710.
- (32)Givens, R. S.; Athey, P. S.; Matuszewski, B.; Kueper, L. W.; Xue, J.; Fister, T. Photochemistry of Phosphate Esters: .Alpha.-Keto Phosphates as a Photoprotecting Group for Caged Phosphate. *Journal of the American Chemical Society* **1993**, *115* (14), 6001–6012.
- (33)Pirrung, M. C.; Shuey, S. W. Photoremovable Protecting Groups for Phosphorylation of Chiral Alcohols. Asymmetric Synthesis of Phosphotriesters of (-)-3',5'-Dimethoxybenzoin. *The Journal of Organic Chemistry* **1994**, *59* (14), 3890–3897.
- (34)Pirrung, M. C., & Bradley, J. (1995). Dimethoxybenzoin Carbonates: Photochemically-Removable Alcohol Protecting Groups Suitable for Phosphoramidite-Based DNA Synthesis. *The Journal of Organic Chemistry*, *60*(5), 1116-1117. doi:10.1021/jo00110a011
- (35)Pirrung, M. C.; Fallon, L.; Lever, D. C.; Shuey, S. W. Inverse Phosphotriester DNA Synthesis Using Photochemically-Removable Dimethoxybenzoin Phosphate Protecting Groups. *The Journal of Organic Chemistry* **1996**, *61* (6), 2129–2136.
- (36)Rock, R. S.; Chan, S. I. Synthesis and Photolysis Properties of a Photolabile Linker Based on 3'-Methoxybenzoin. *The Journal of Organic Chemistry* **1996**, *61* (4), 1526–1529.
- (37)Routledge, A.; Abell, C.; Balasubramanian, S. The Use of a Dithiane Protected Benzoin Photolabile Safety Catch Linker for Solid-Phase Synthesis. *Tetrahedron Letters* **1997**, *38* (7), 1227–1230.
- (38)Lee, H. B.; Balasubramanian, S. Studies on a Dithiane-Protected Benzoin Photolabile Safety Catch Linker for Solid-Phase Synthesis. *The Journal of Organic Chemistry* **1999**, *64* (15), 5728–5728.

- (39)Cano, M.; Ladlow, M.; Balasubramanian, S. Studies on the Chemical Stability and Functional Group Compatibility of the Benzoin Photolabile Safety-Catch Linker Using an Analytical Construct. *Journal of Combinatorial Chemistry* **2002**, *4* (1), 44–48.
- (40)Shi, Y.; Corrie, J. E. T.; Wan, P. Mechanism of 3',5'-Dimethoxybenzoin Ester Photochemistry: Heterolytic Cleavage Intramolecularly Assisted by the Dimethoxybenzene Ring Is the Primary Photochemical Step. *The Journal of Organic Chemistry* **1997**, *62* (24), 8278–8279.
- (41)Rock, R. S.; Chan, S. I. Preparation of a Water-Soluble “Cage” Based on 3',5'-Dimethoxybenzoin. *Journal of the American Chemical Society* **1998**, *120* (41), 10766–10767.
- (42)Rajesh, C. S.; Givens, R. S.; Wirz, J. Kinetics and Mechanism of Phosphate Photorelease from Benzoin Diethyl Phosphate: Evidence for Adiabatic Fission to an  $\alpha$ -Keto Cation in the Triplet State. *Journal of the American Chemical Society* **2000**, *122* (4), 611–618.
- (43)Pirrung, M. C.; Ye, T.; Zhou, Z.; Simon, J. D. Mechanistic Studies on the Photochemical Deprotection of 3',5'-Dimethoxybenzoin Esters. *Photochemistry and Photobiology* **2006**, *82* (5), 1258.
- (44)Boudebous, H.; Košmrlj, B.; Šket, B.; Wirz, J. Primary Photoreactions of the 3',5'-Dimethoxybenzoin Cage and Determination of the Release Rate in Polar Media. *The Journal of Physical Chemistry A* **2007**, *111* (15), 2811–2813.
- (45)Ma, C.; Du, Y.; Kwok, W. M.; Phillips, D. L. Femtosecond Transient Absorption and Nanosecond Time-Resolved Resonance Raman Study of the Solvent-Dependent Photo-Deprotection Reaction of Benzoin Diethyl Phosphate. *Chemistry - A European Journal* **2007**, *13* (8), 2290–2305.
- (46)Ma, C.; Kwok, W. M.; An, H.-Y.; Guan, X.; Fu, M. Y.; Toy, P. H.; Phillips, D. L. A Time-Resolved Spectroscopic Study of the Bichromophoric Phototrigger 3',5'-Dimethoxybenzoin Diethyl Phosphate: Interaction Between the Two Chromophores Determines the Reaction Pathway. *Chemistry - A European Journal* **2010**, *16* (17), 5102–5118.
- (47)Chen, X.; Ma, C.; Phillips, D. L.; Fang, W.-H. A Case of Fast Photocyclization: The Model of a Downhill Ladder Reaction Pathway for the Bichromophoric Phototrigger 3',5'-Dimethoxybenzoin Acetate. *Organic Letters* **2010**, *12* (22), 5108–5111.
- (48)Chan, W. S.; Ma, C.; Kwok, W. M.; Zuo, P.; Phillips, D. L. Resonance Raman Spectroscopic and Density Functional Theory Study of Benzoin Diethyl Phosphate. *The Journal of Physical Chemistry A* **2004**, *108* (18), 4047–4058.
- (49)Brieke, C.; Rohrbach, F.; Gottschalk, A.; Mayer, G.; Heckel, A. Light-Controlled Tools. *Angewandte Chemie International Edition* **2012**, *51* (34), 8446–8476.

- (50) Hoffman, A. S. The Origins and Evolution of “Controlled” Drug Delivery Systems. *Journal of Controlled Release* **2008**, *132* (3), 153–163.
- (51) Fan, N.-C.; Cheng, F.-Y.; Ho, J.-A. A.; Yeh, C.-S. Photocontrolled Targeted Drug Delivery: Photocaged Biologically Active Folic Acid as a Light-Responsive Tumor-Targeting Molecule. *Angewandte Chemie International Edition* **2012**, *51* (35), 8806–8810.
- (52) Carling, C.-J.; Viger, M. L.; Huu, V. A. N.; Garcia, A. V.; Almutairi, A. In Vivo Visible Light-Triggered Drug Release from an Implanted Depot. *Chemical Science* **2015**, *6* (1), 335–341.
- (53) Yan, B.; Boyer, J.-C.; Branda, N. R.; Zhao, Y. Near-Infrared Light-Triggered Dissociation of Block Copolymer Micelles Using Upconverting Nanoparticles. *Journal of the American Chemical Society* **2011**, *133* (49), 19714–19717.
- (54) McCoy, C. P.; Rooney, C.; Jones, D. S.; Gorman, S. P.; Nieuwenhuyzen, M. Rational Design of a Dual-Mode Optical and Chemical Prodrug. *Pharmaceutical Research* **2006**, *24* (1), 194–200.
- (55) McCoy, C. P.; Rooney, C.; Edwards, C. R.; Jones, D. S.; Gorman, S. P. Light-Triggered Molecule-Scale Drug Dosing Devices. *Journal of the American Chemical Society* **2007**, *129* (31), 9572–9573.
- (56) Carling, C.-J.; Nourmohammadian, F.; Boyer, J.-C.; Branda, N. R. Remote-Control Photorelease of Caged Compounds Using Near-Infrared Light and Upconverting Nanoparticles. *Angewandte Chemie* **2010**, *122* (22), 3870–3873.
- (57) Carling, C.-J. The use of upconverting nanoparticles to drive organic photoreactions. Ph.D. Dissertation, Simon Fraser University, Burnaby, BC, 2012.
- (58) Burghardt, T. E. Developments in the Deprotection of Thioacetals. *Journal of Sulfur Chemistry* **2005**, *26* (4-5), 411–427.
- (59) Mukaiyama, T.; Narasaka, K.; Furusato, M. Convenient Synthesis of 1,4-Diketones. Application to the Synthesis of Dihydrojasmane. *Journal of the American Chemical Society* **1972**, *94* (24), 8641–8642.
- (60) Bisht, R.; Singh, S.; Krishnamoorthy, K.; Nithyanandhan, J. Modulated Photochemical Reactivities of O-Acetylated (3',5'-Dimethoxyphenyl)Heteroaryl Acyloin Derivatives under Direct Irradiation and Photo-Induced Electron Transfer Conditions. *Photochemical & Photobiological Sciences* **2018**, *17* (6), 835–845.
- (61) Banerjee, A.; Lee, K.; Falvey, D. E. Photoreleasable Protecting Groups Based on Electron Transfer Chemistry. Donor Sensitized Release of Phenacyl Groups from Alcohols, Phosphates and Diacids. *Tetrahedron* **1999**, *55* (44), 12699–12710.



## Appendix A. NMR Characterization

### *NMR Spectra- Compounds from Chapter 3*

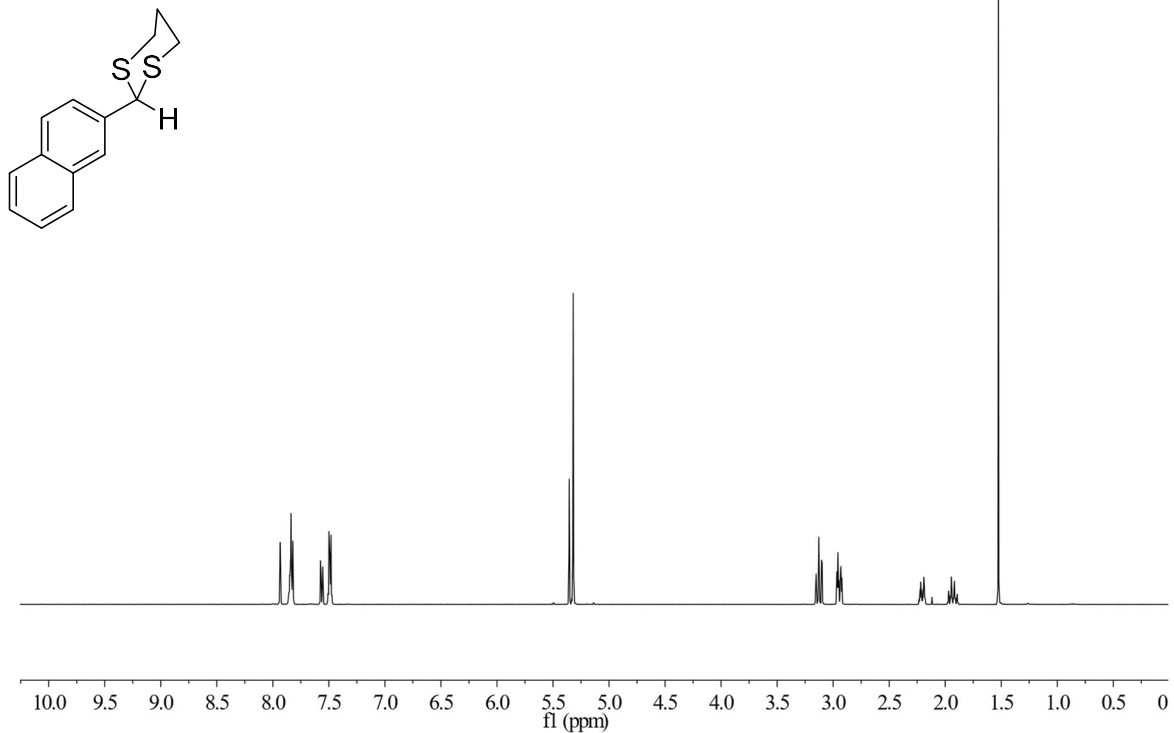


Figure A.1. <sup>1</sup>H NMR (500 MHz, CD<sub>2</sub>Cl<sub>2</sub>) spectrum of 2-(naphthalen-2-yl)-1,3-dithiane (**3a**)

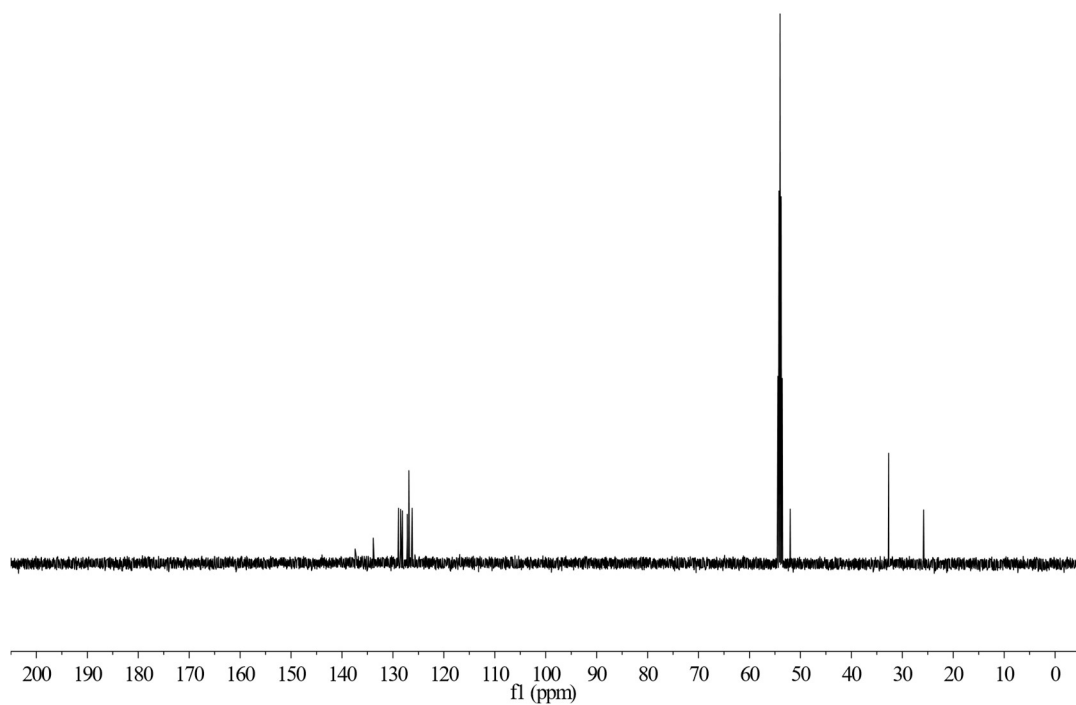


Figure A.2. <sup>13</sup>C NMR (126 MHz, CD<sub>2</sub>Cl<sub>2</sub>) spectrum of 2-(naphthalen-2-yl)-1,3-dithiane (**3a**)

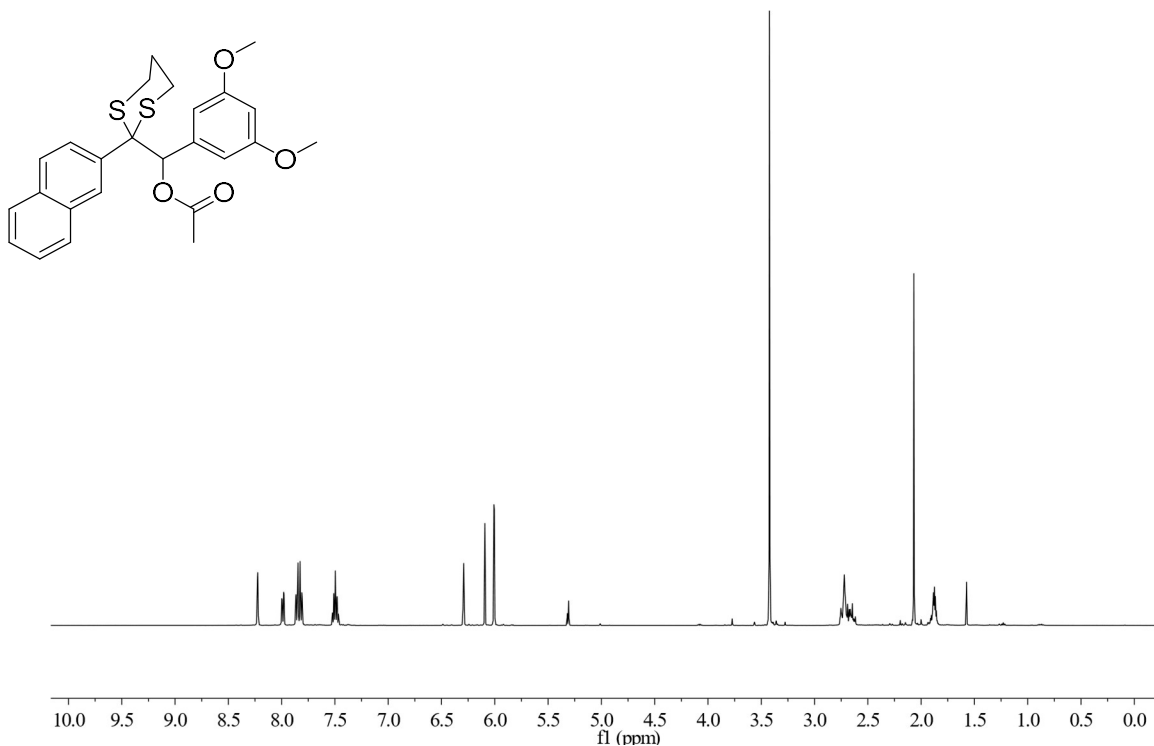


Figure A.3.  $^1\text{H}$  NMR (500 MHz,  $\text{CD}_2\text{Cl}_2$ ) spectrum of (3,5-dimethoxyphenyl)(2-(naphthalen-2-yl)-1,3-dithian-2-yl) methyl acetate (**2a**)

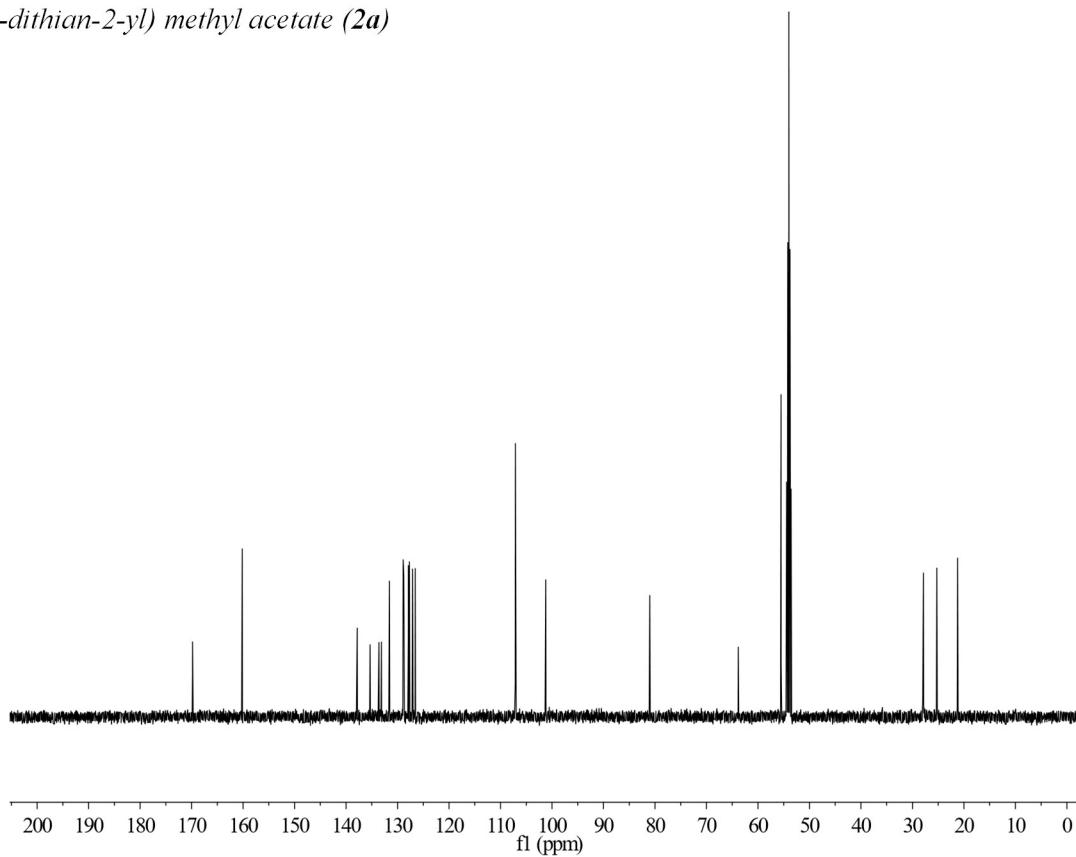


Figure A.4.  $^{13}\text{C}$  NMR (126 MHz,  $\text{CD}_2\text{Cl}_2$ ) spectrum of (3,5-dimethoxyphenyl)(2-(naphthalen-2-yl)-1,3-dithian-2-yl) methyl acetate (**2a**)

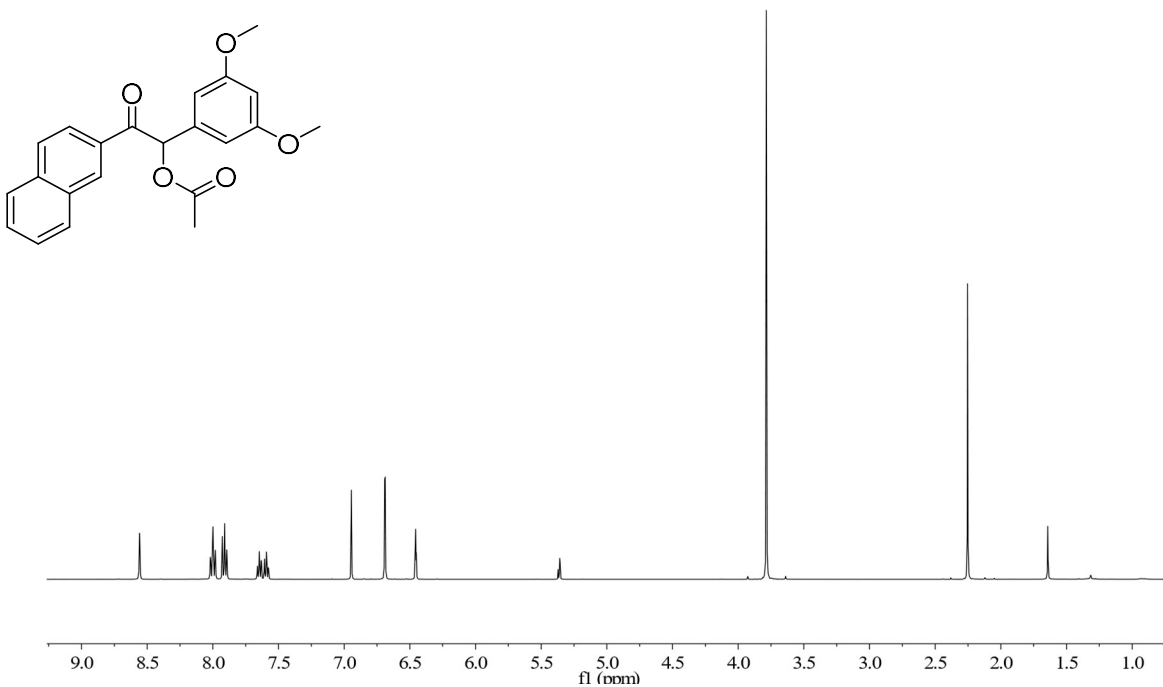


Figure A.5. <sup>1</sup>H NMR (500 MHz, CD<sub>2</sub>Cl<sub>2</sub>) spectrum of 1-(3,5-dimethoxyphenyl)-2-(naphthalen-2-yl)-2-oxoethyl acetate (**1a**)

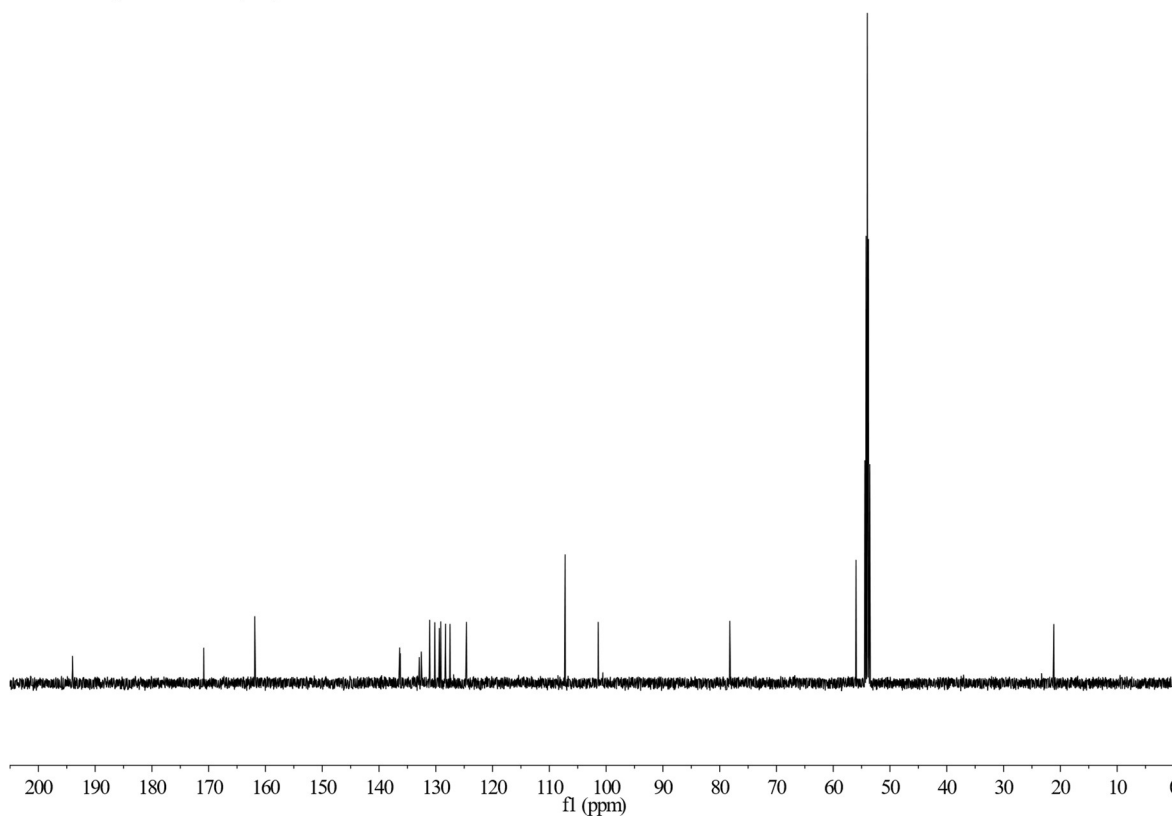


Figure A.6. <sup>13</sup>C NMR (126 MHz, CD<sub>2</sub>Cl<sub>2</sub>) spectrum of 1-(3,5-dimethoxyphenyl)-2-(naphthalen-2-yl)-2-oxoethyl acetate (**1a**)

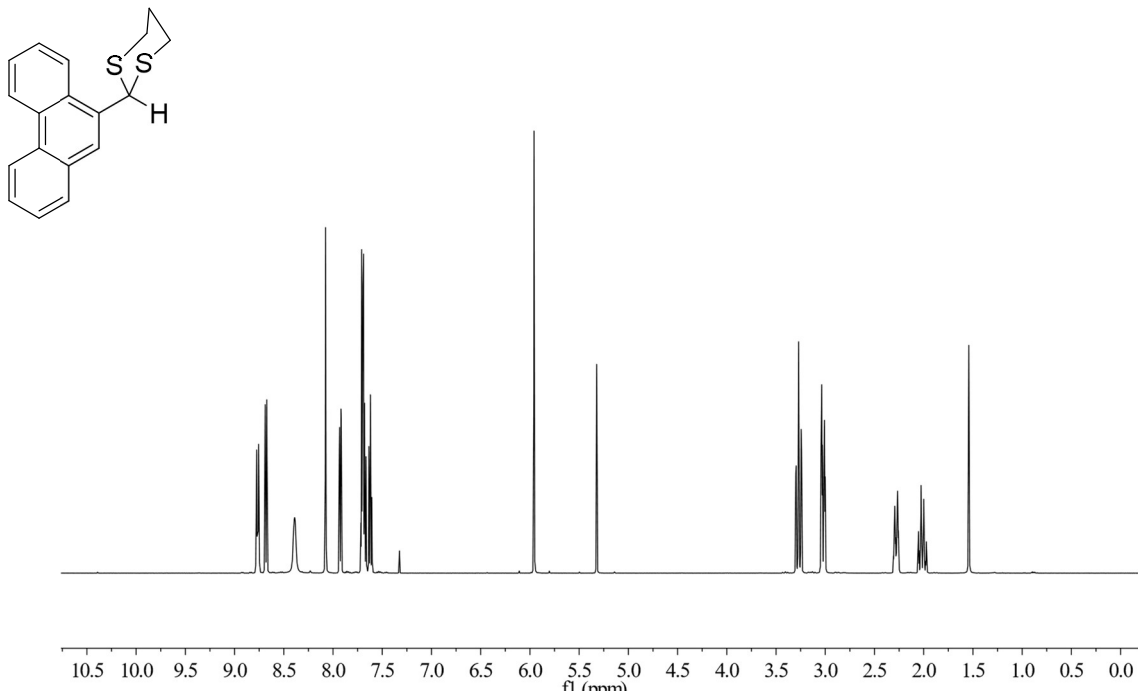


Figure A.7. <sup>1</sup>H NMR (500 MHz, CD<sub>2</sub>Cl<sub>2</sub>) spectrum of 2-(phenanthren-9-yl)-1,3-dithiane (**3b**)

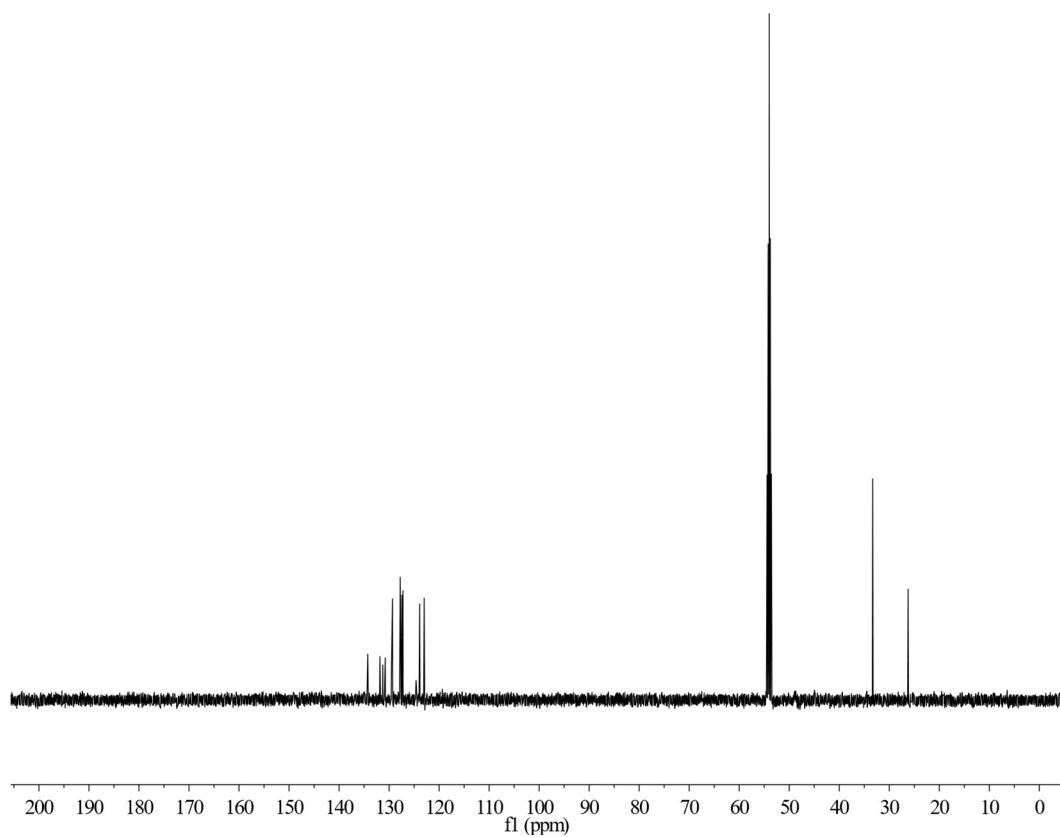


Figure A.8. <sup>13</sup>C NMR (126 MHz, CD<sub>2</sub>Cl<sub>2</sub>) spectrum of 2-(phenanthren-9-yl)-1,3-dithiane (**3b**)

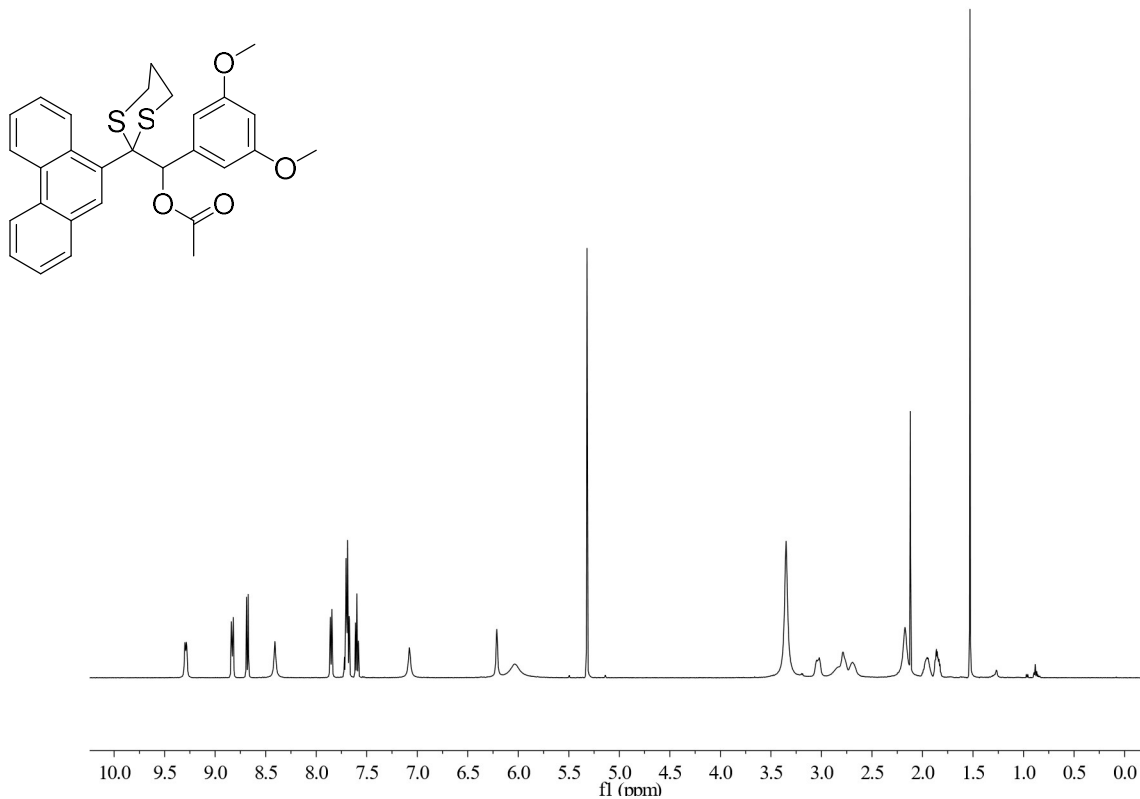


Figure A.9.  $^1\text{H}$  NMR (500 MHz,  $\text{CD}_2\text{Cl}_2$ ) spectrum of (3,5-dimethoxyphenyl)(2-(phenanthren-9-yl)-1,3-dithian-2-yl)methyl acetate (**2b**)

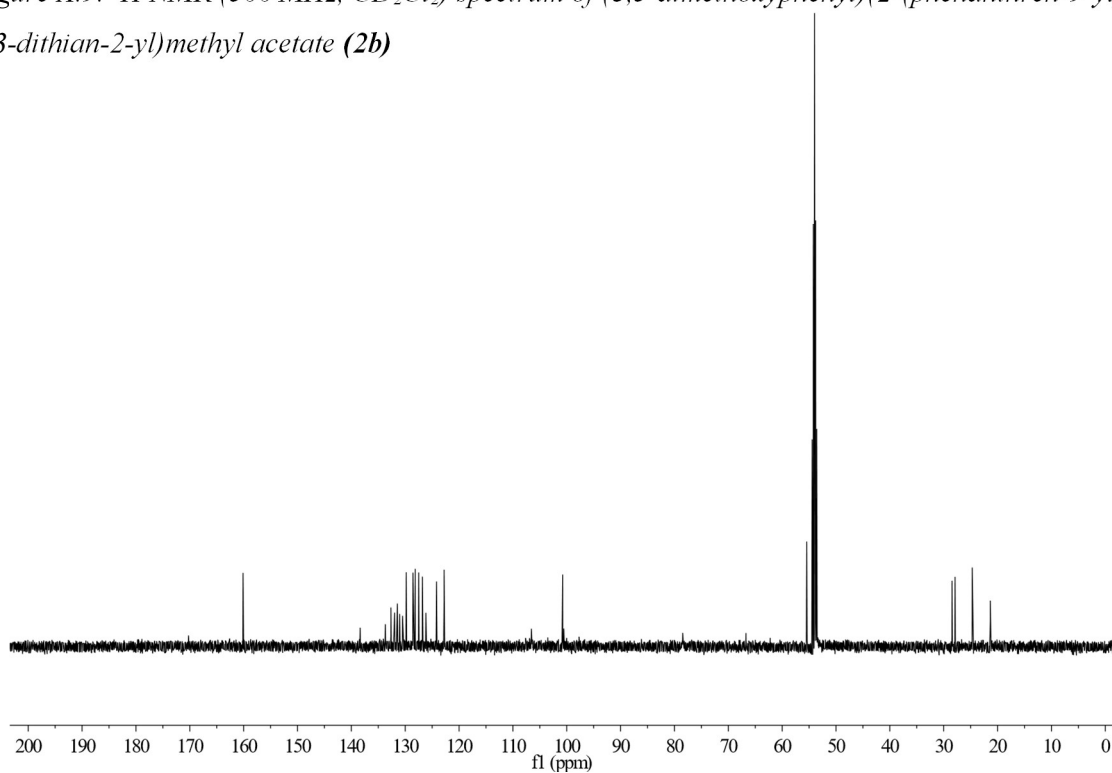


Figure A.10.  $^{13}\text{C}$  NMR (126 MHz,  $\text{CD}_2\text{Cl}_2$ ) spectrum of (3,5-dimethoxyphenyl)(2-(phenanthren-9-yl)-1,3-dithian-2-yl)methyl acetate (**2b**)

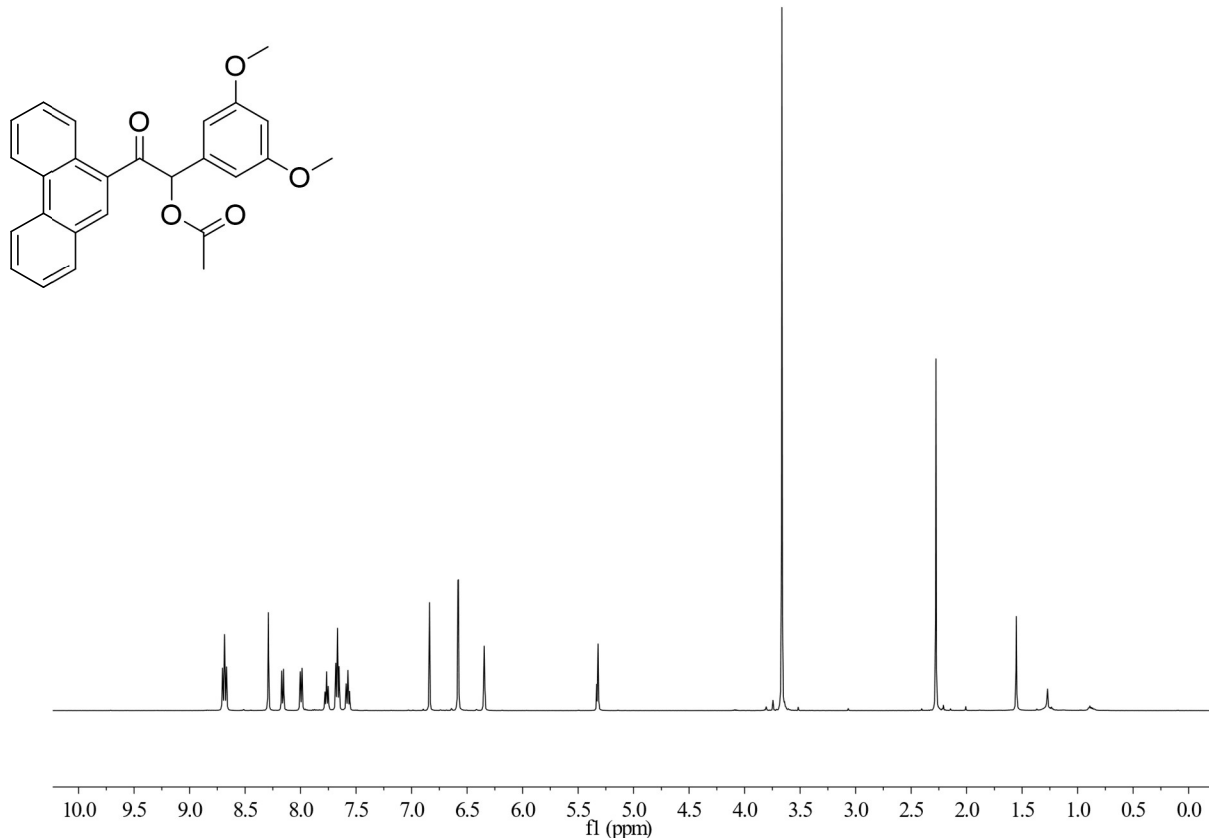


Figure A.11 <sup>1</sup>H NMR (500 MHz, CD<sub>2</sub>Cl<sub>2</sub>) spectrum of 1-(3,5-dimethoxyphenyl)-2-oxo-2-(phenanthrene-9-yl)ethyl acetate (**1b**)

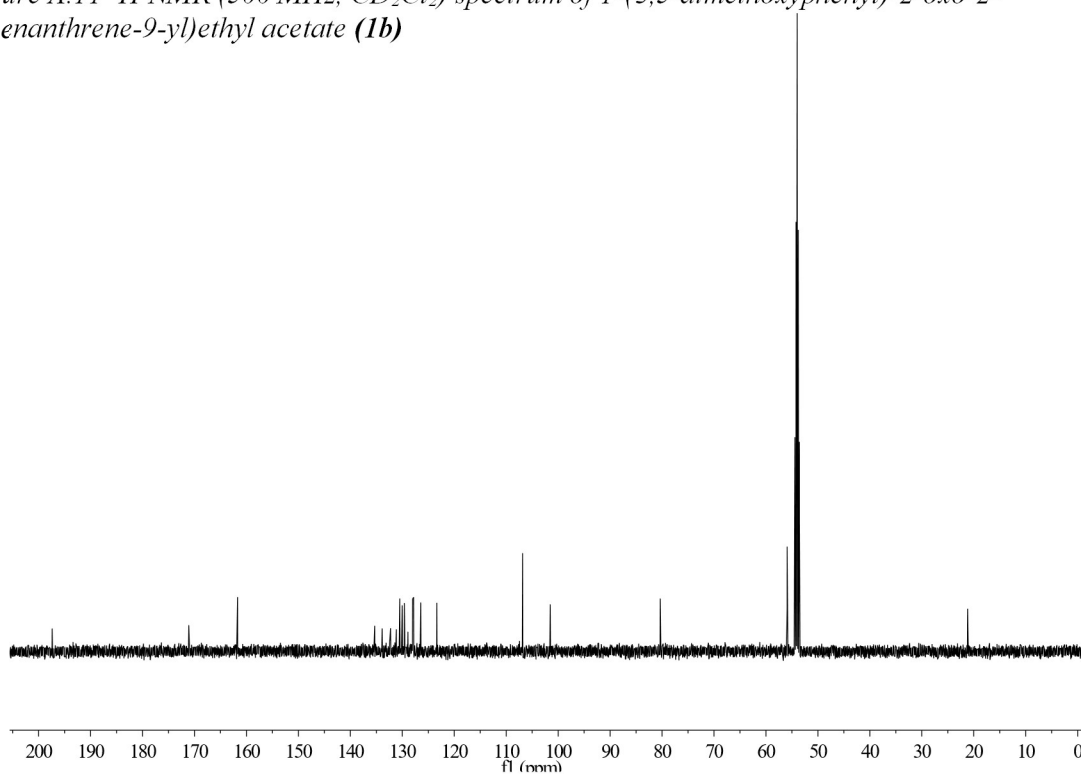


Figure A.12 <sup>13</sup>C NMR (126 MHz, CD<sub>2</sub>Cl<sub>2</sub>) spectrum of 1-(3,5-dimethoxyphenyl)-2-oxo-2-(phenanthrene-9-yl)ethyl acetate (**1b**)

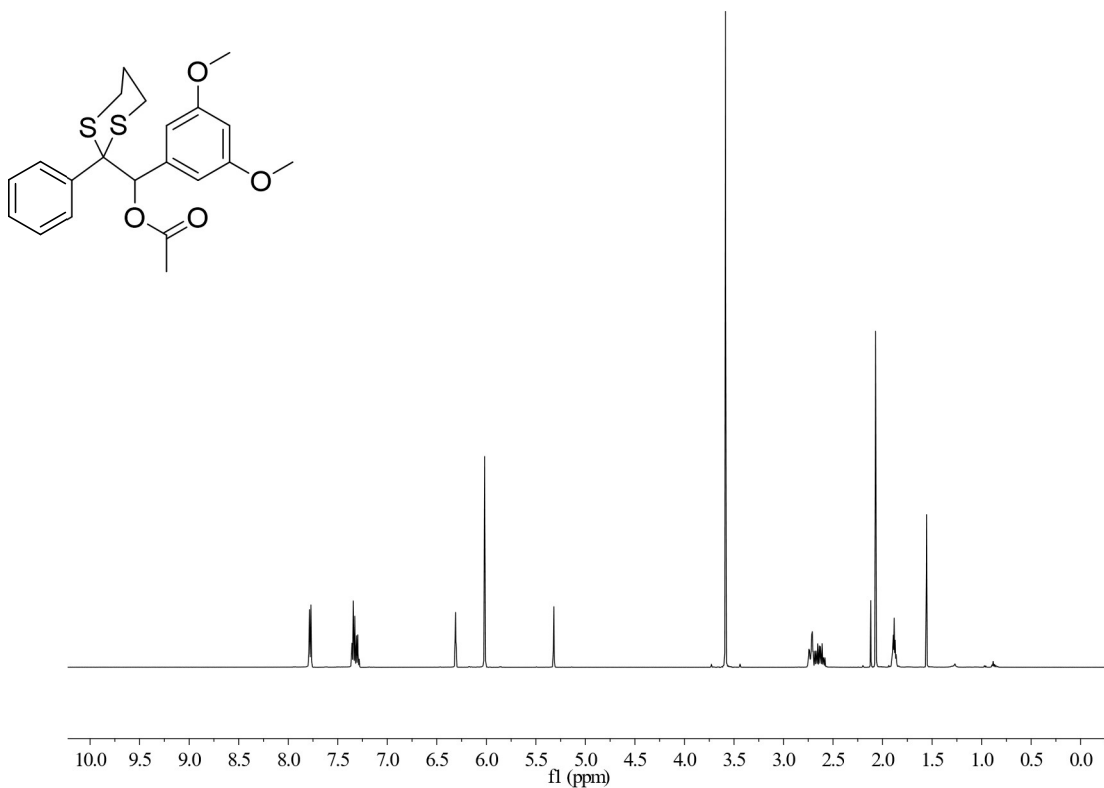


Figure A.13 <sup>1</sup>H NMR (500 MHz, CD<sub>2</sub>Cl<sub>2</sub>) spectrum of (3,5-dimethoxyphenyl)(2-phenyl-1,3-dithian-2-yl)methyl acetate (**2P**)

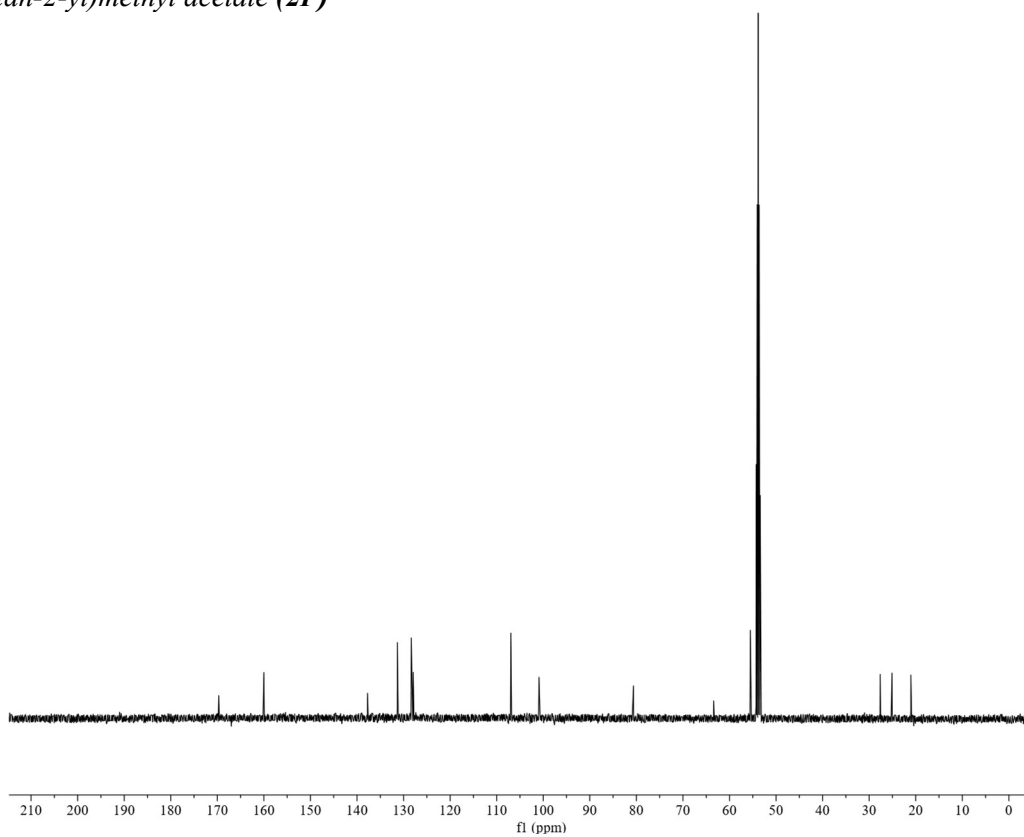


Figure A.14 <sup>13</sup>C NMR (126 MHz, CD<sub>2</sub>Cl<sub>2</sub>) spectrum of (3,5-dimethoxyphenyl)(2-phenyl-1,3-dithian-2-yl)methyl acetate (**2P**)

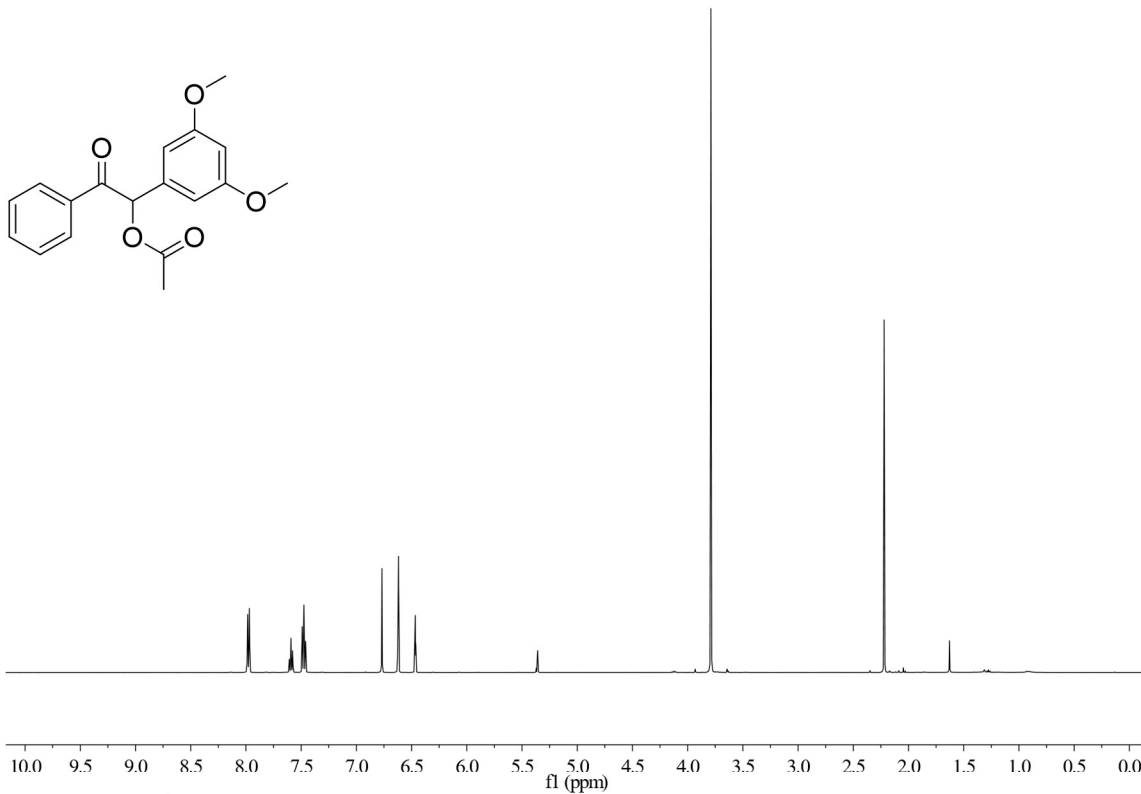


Figure A.15  $^1\text{H}$  NMR (500 MHz,  $\text{CD}_2\text{Cl}_2$ ) spectrum of 1-(3,5-dimethoxyphenyl)-2-oxo-2-phenylethyl acetate (**1P**)

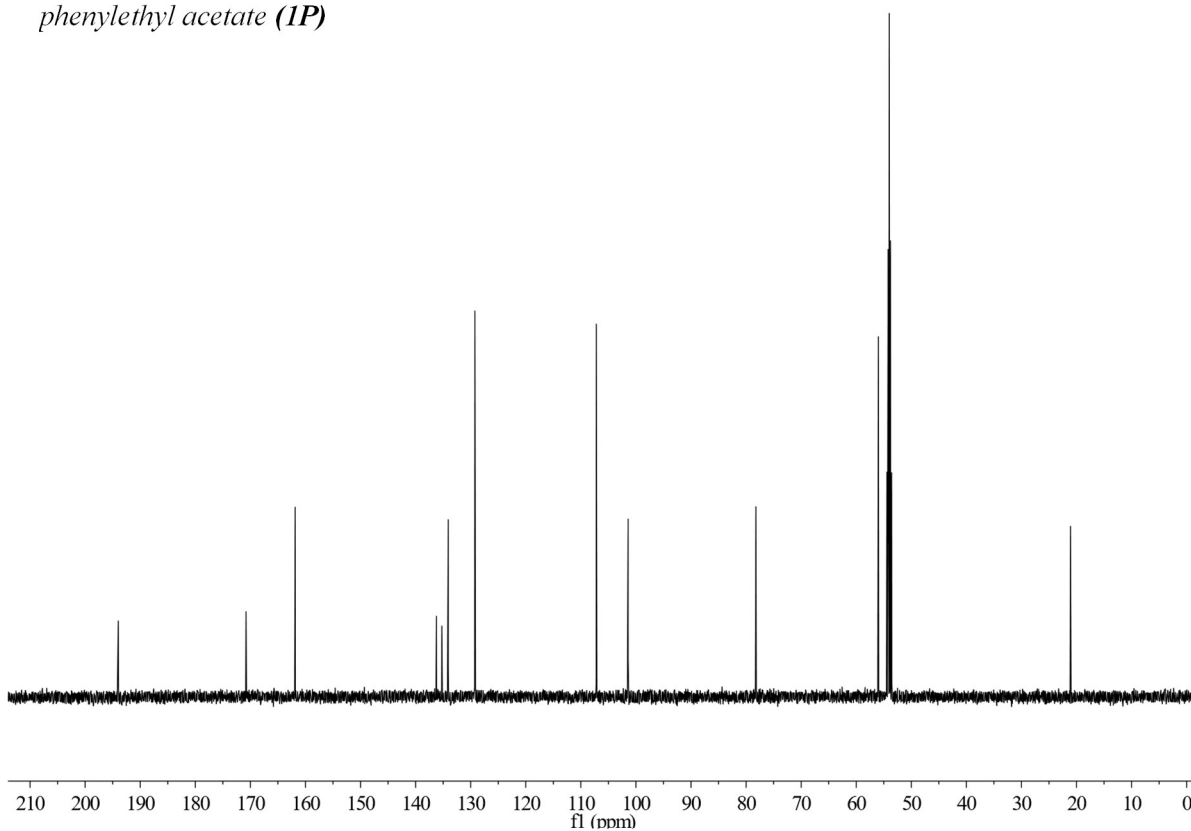


Figure A.16  $^{13}\text{C}$  NMR (126 MHz,  $\text{CD}_2\text{Cl}_2$ ) spectrum of 1-(3,5-dimethoxyphenyl)-2-oxo-2-phenylethyl acetate (**1P**)



## NMR Spectra- Compounds from Chapter 4

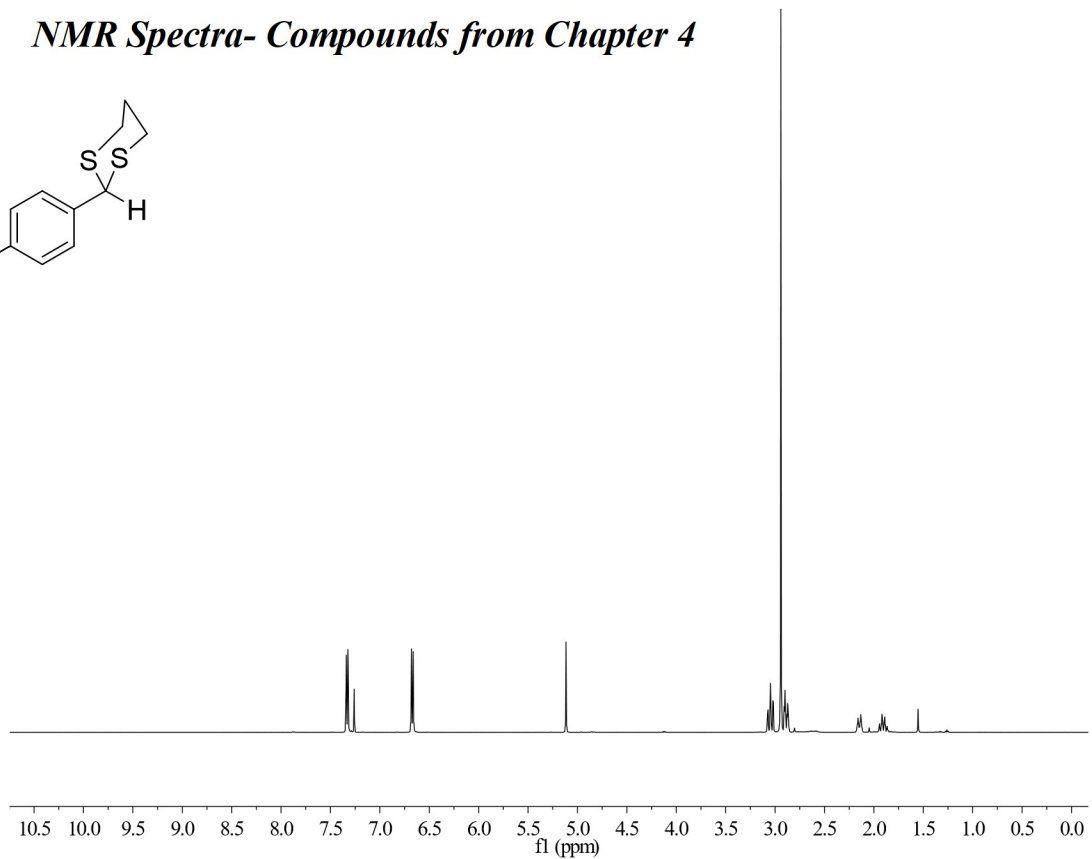
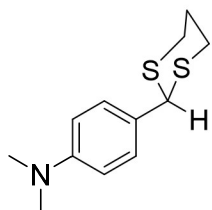


Figure A.17 <sup>1</sup>H NMR (500 MHz, CD<sub>2</sub>Cl<sub>2</sub>) spectrum of 4-(1,3-dithian-2-yl)-N,N-dimethylaniline (3-DMA)

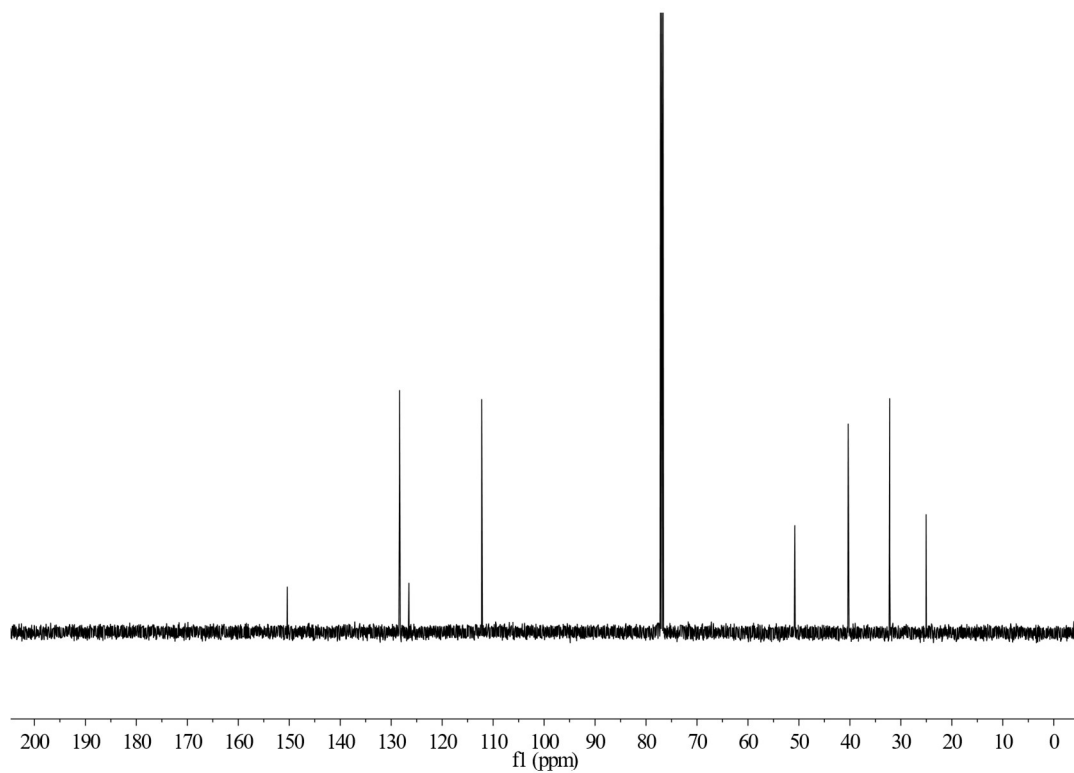


Figure A.18 <sup>13</sup>C NMR (151 MHz, CD<sub>2</sub>Cl<sub>2</sub>) spectrum of 4-(1,3-dithian-2-yl)-N,N-dimethylaniline (3-DMA)

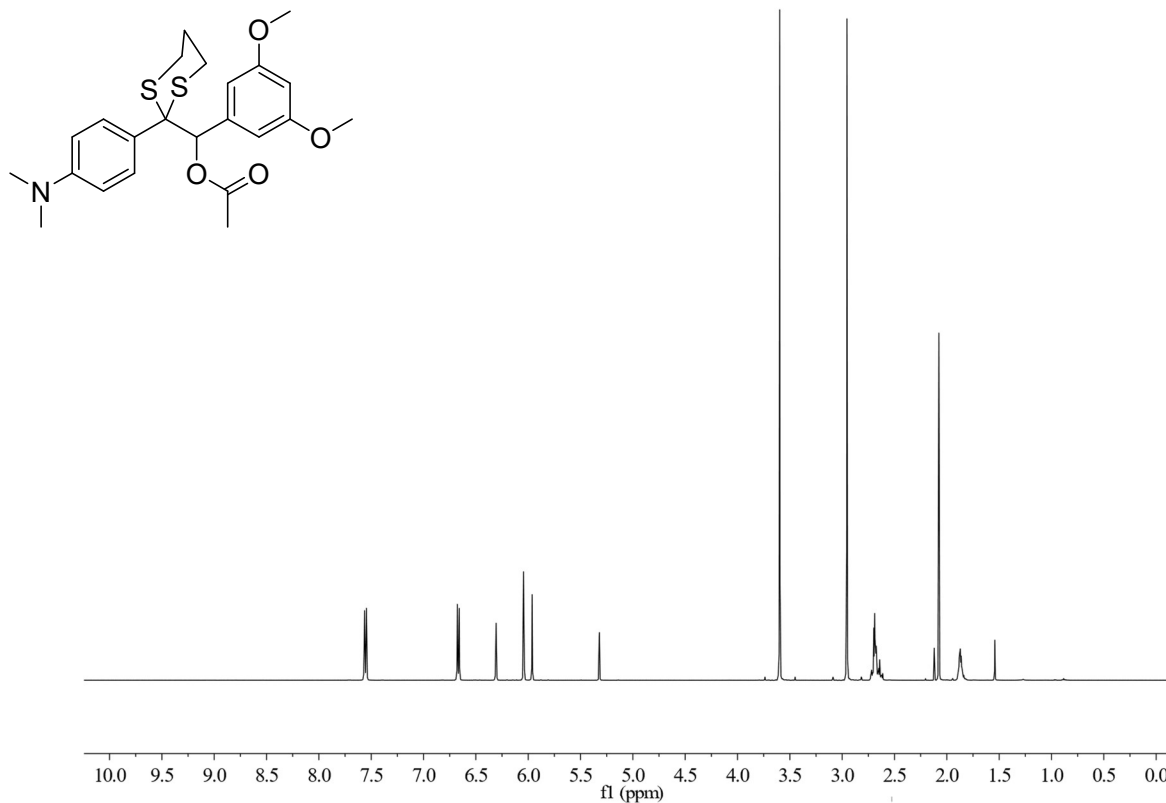


Figure A.19 <sup>1</sup>H NMR (500 MHz, CD<sub>2</sub>Cl<sub>2</sub>) spectrum of (3,5-dimethoxyphenyl)(2-(4-(dimethylamino)phenyl)-1,3-dithian-2-yl)methyl acetate (**2-DMA**)

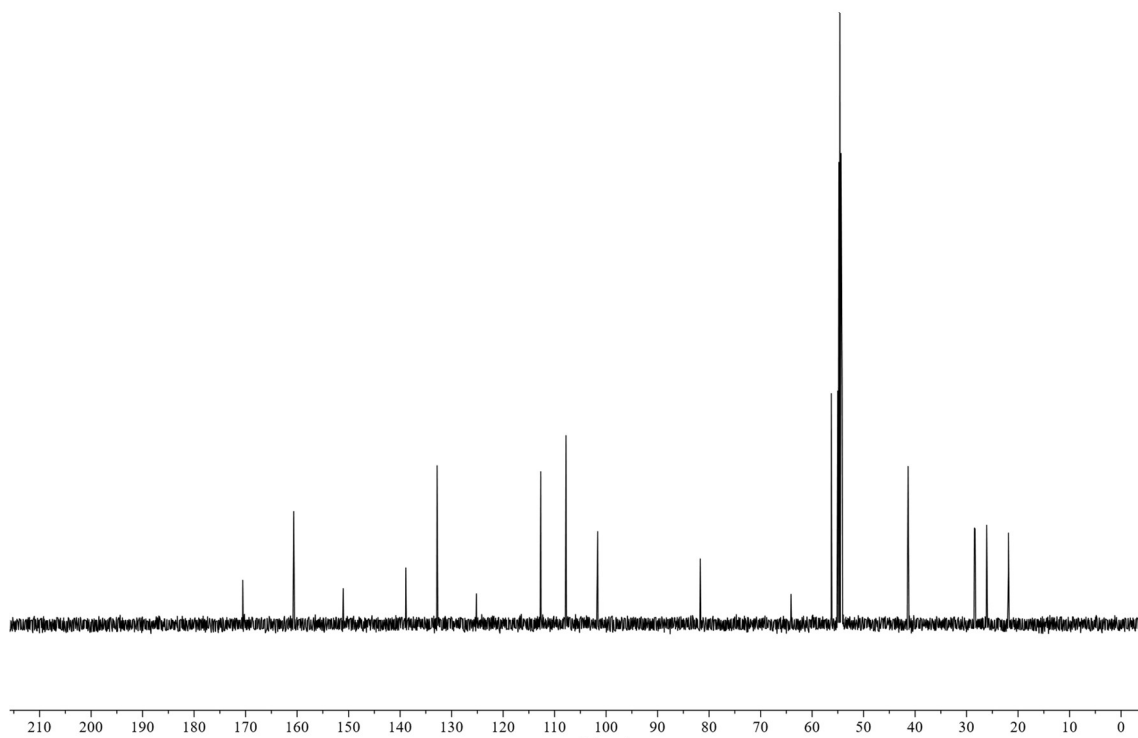


Figure A.20 <sup>13</sup>C NMR (126 MHz, CD<sub>2</sub>Cl<sub>2</sub>) spectrum of (3,5-dimethoxyphenyl)(2-(4-(dimethylamino)phenyl)-1,3-dithian-2-yl)methyl acetate (**2-DMA**)

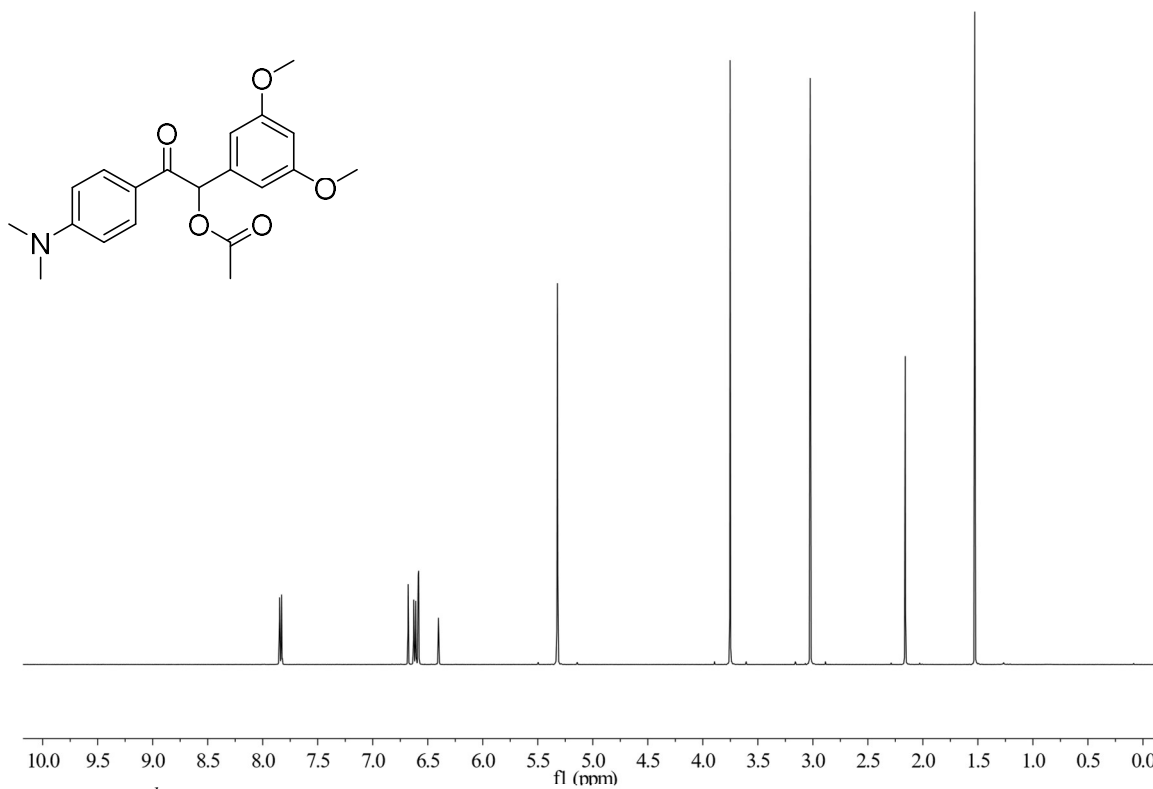


Figure A.21 <sup>1</sup>H NMR (500 MHz, CD<sub>2</sub>Cl<sub>2</sub>) spectrum of 1-(3,5-dimethoxyphenyl)-2-(4-(dimethylamino)phenyl)-2-oxoethyl acetate (**1-DMA**)

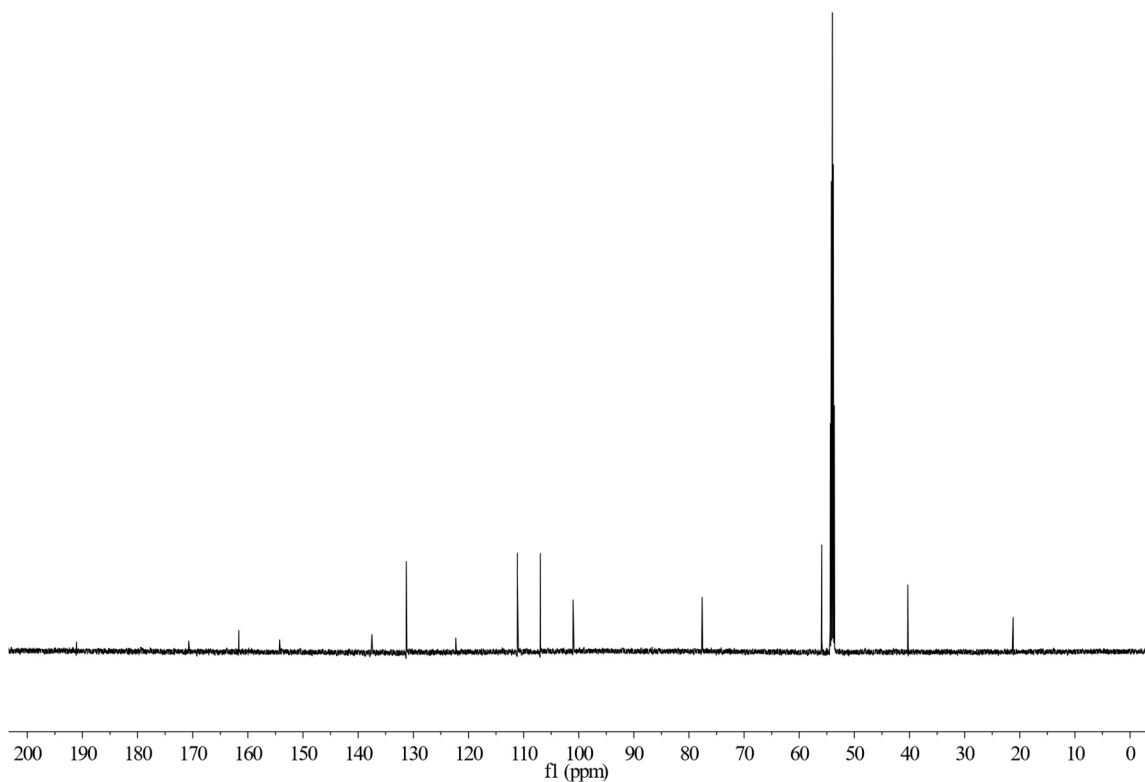


Figure A.22 <sup>13</sup>C NMR (151 MHz, CD<sub>2</sub>Cl<sub>2</sub>) spectrum of 1-(3,5-dimethoxyphenyl)-2-(4-(dimethylamino)phenyl)-2-oxoethyl acetate (**1-DMA**)

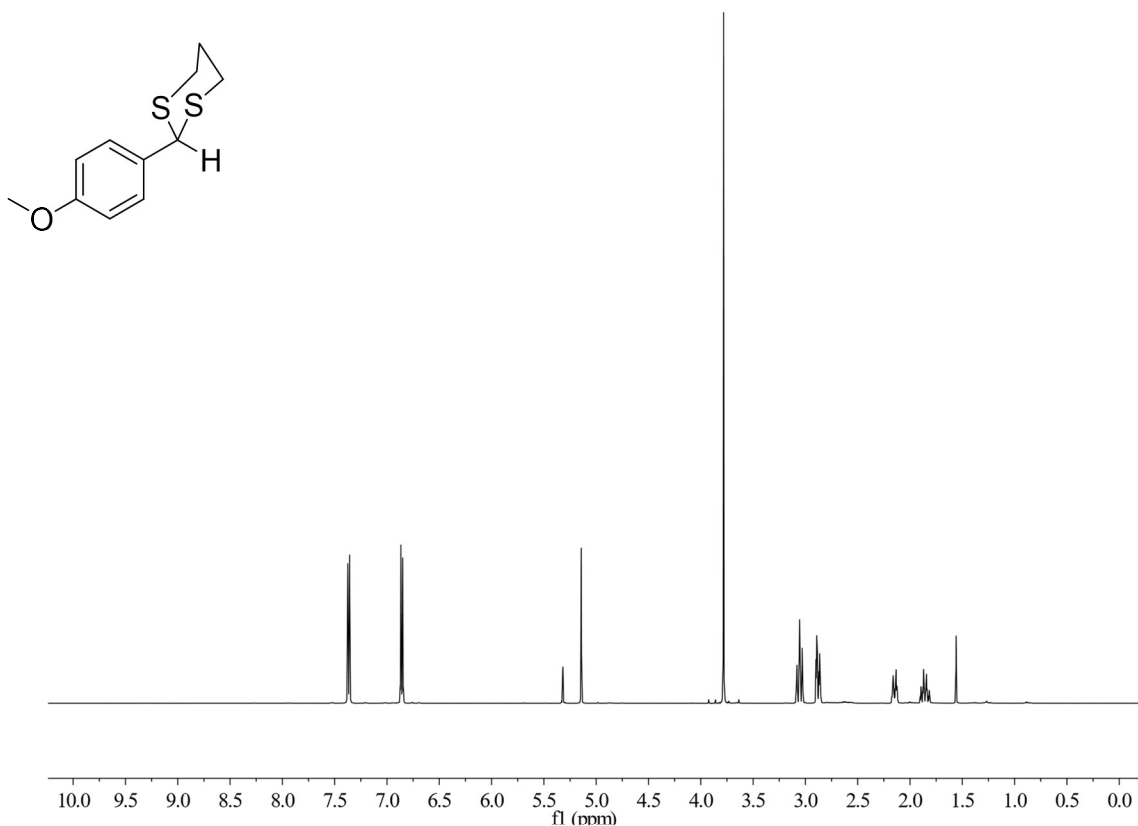


Figure A.23  $^1\text{H}$  NMR (500 MHz,  $\text{CD}_2\text{Cl}_2$ ) spectrum of 2-(4-methoxyphenyl)-1,3-dithiane (3-OMe)

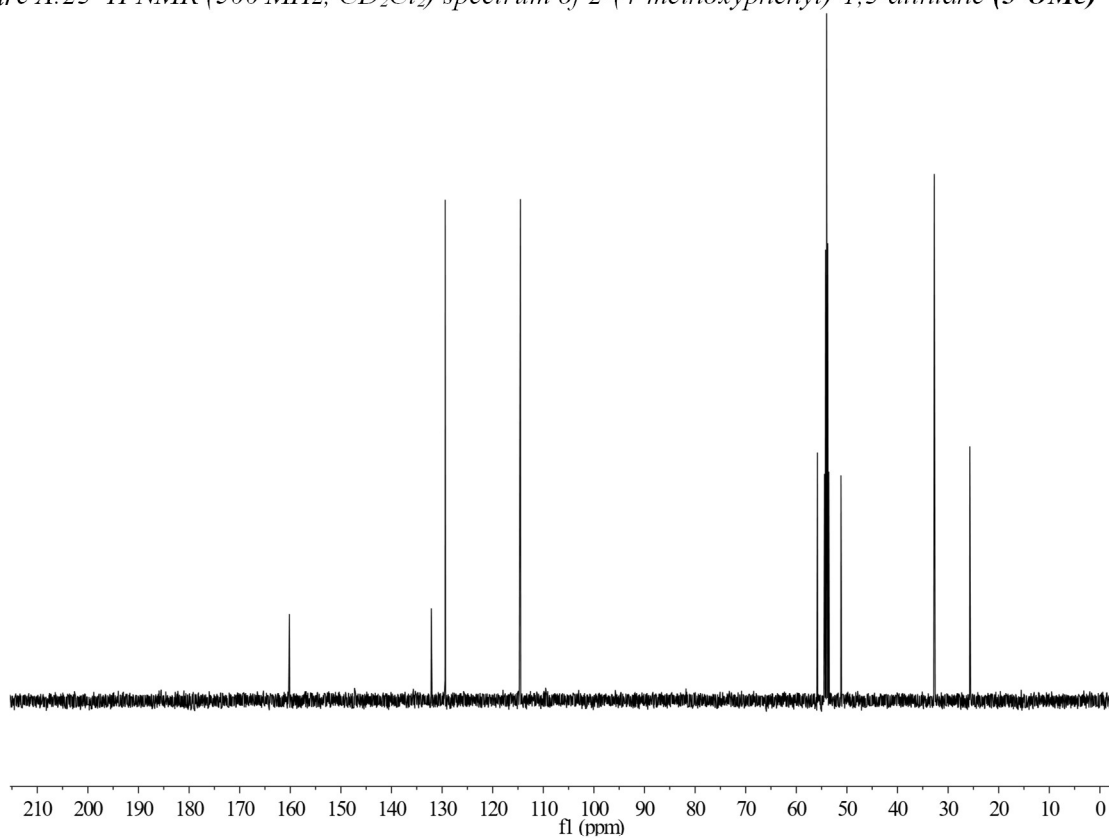


Figure A.24  $^{13}\text{C}$  NMR (126 MHz,  $\text{CD}_2\text{Cl}_2$ ) spectrum of 2-(4-methoxyphenyl)-1,3-dithiane (3-OMe)

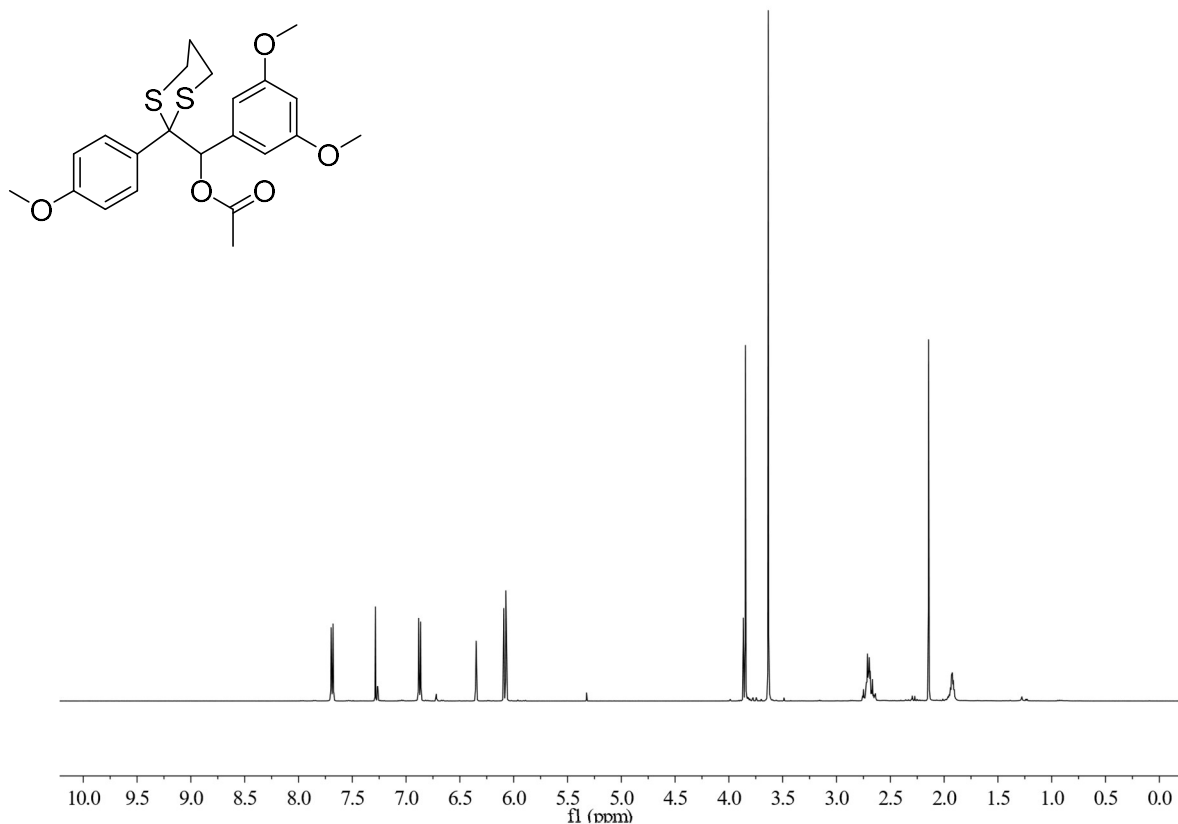


Figure A.25 <sup>1</sup>H NMR (500 MHz, CD<sub>2</sub>Cl<sub>2</sub>) spectrum of (3,5-dimethoxyphenyl)(2-(4-methoxyphenyl)-1,3-dithian-2-yl)methyl acetate (**2-OMe**)

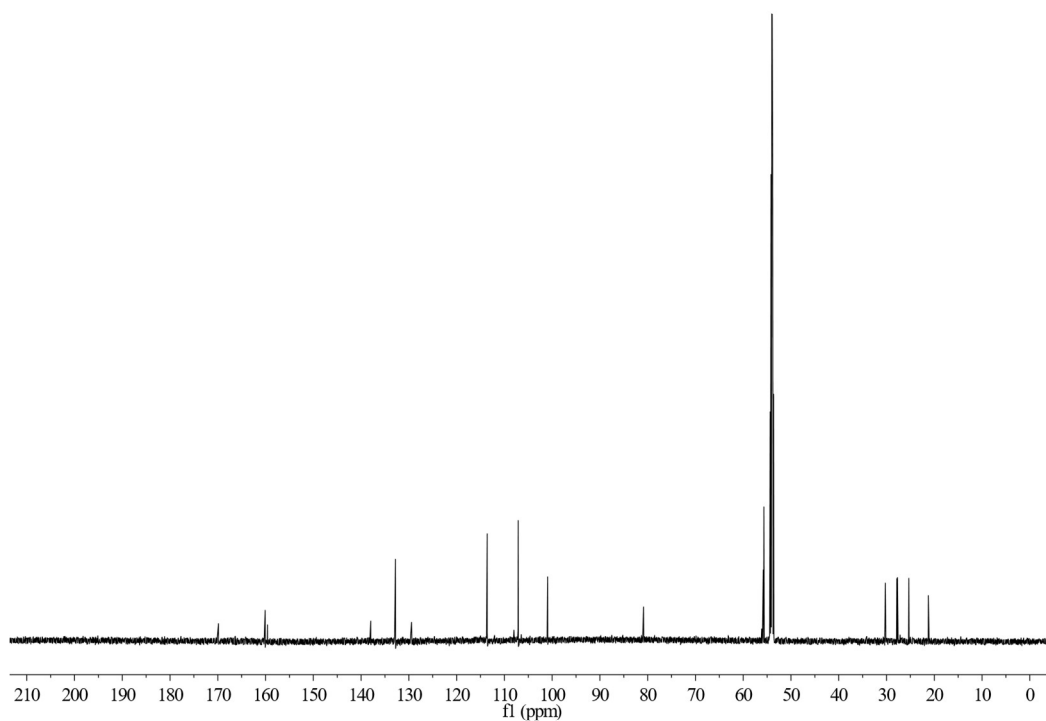


Figure A.26 <sup>13</sup>C NMR (151 MHz, CD<sub>2</sub>Cl<sub>2</sub>) spectrum of (3,5-dimethoxyphenyl)(2-(4-methoxyphenyl)-1,3-dithian-2-yl)methyl acetate (**2-OMe**)

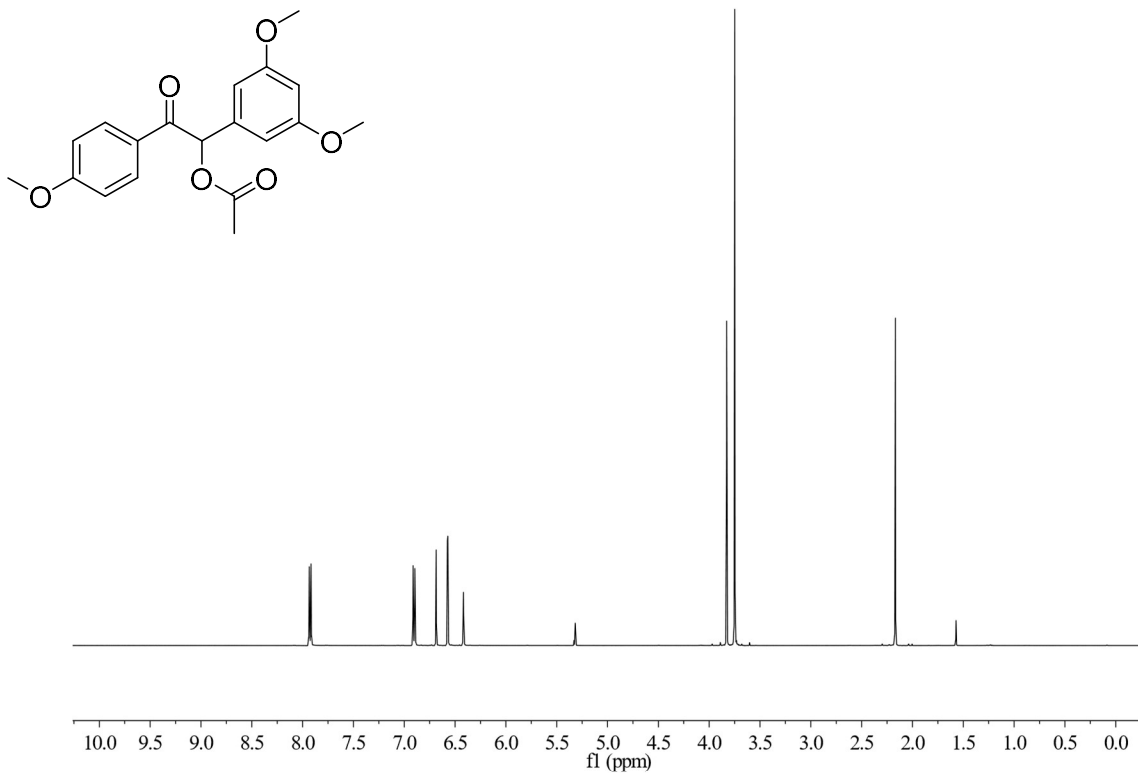


Figure A.27 <sup>1</sup>H NMR (500 MHz, CD<sub>2</sub>Cl<sub>2</sub>) spectrum of 1-(3,5-dimethoxyphenyl)-2-(4-methoxyphenyl)-2-oxoethyl acetate (**1-OMe**)

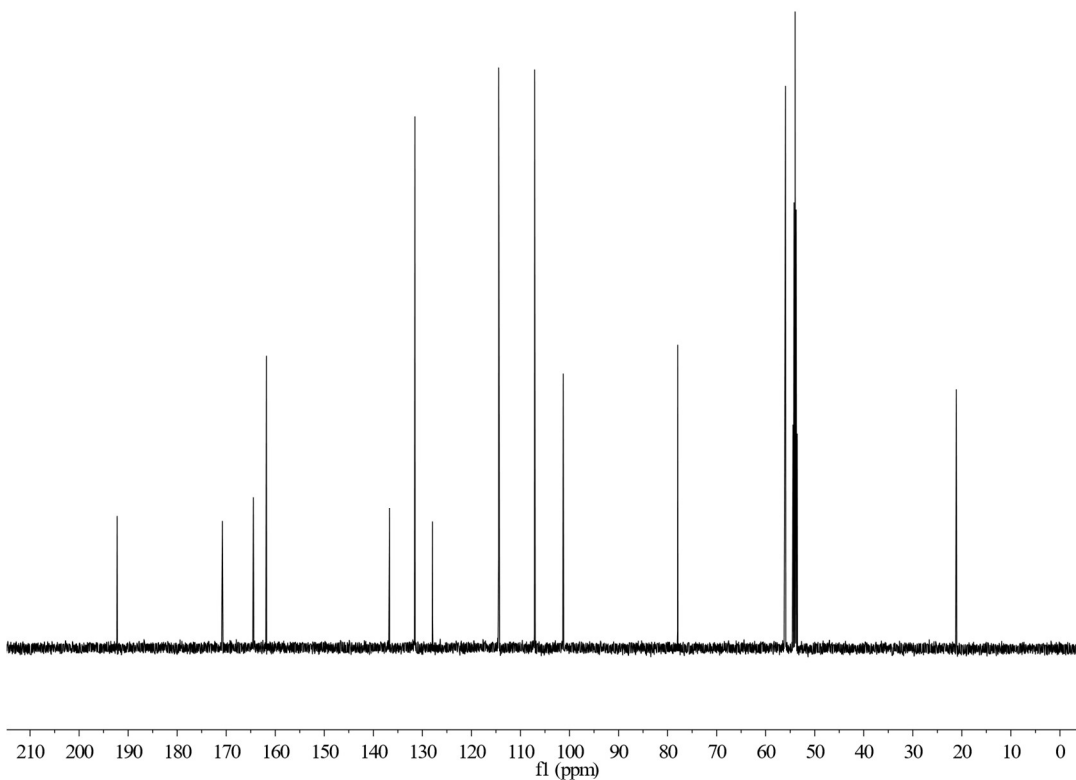
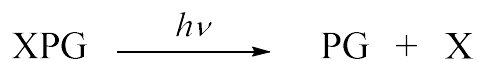


Figure A.28 <sup>13</sup>C NMR (126 MHz, CD<sub>2</sub>Cl<sub>2</sub>) spectrum of 1-(3,5-dimethoxyphenyl)-2-(4-methoxyphenyl)-2-oxoethyl acetate (**1-OMe**)

## Appendix B. Kinetics



XPG= Photoremovable protecting group

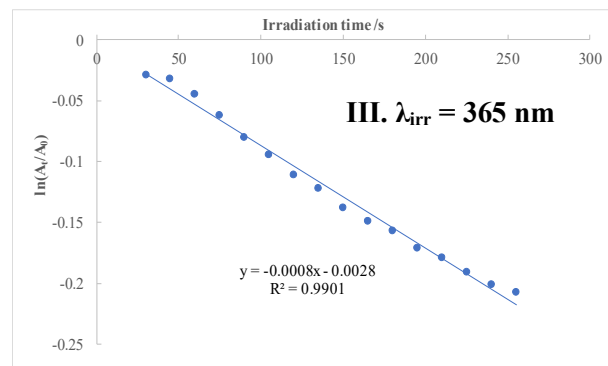
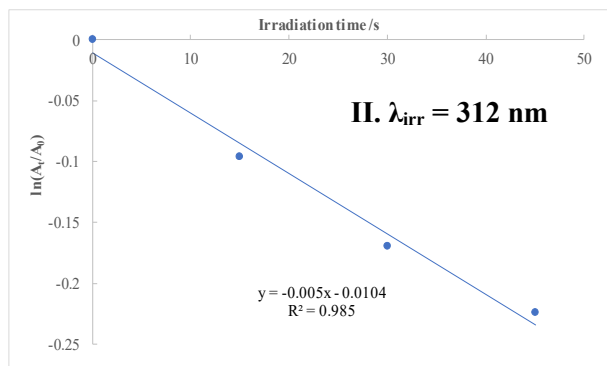
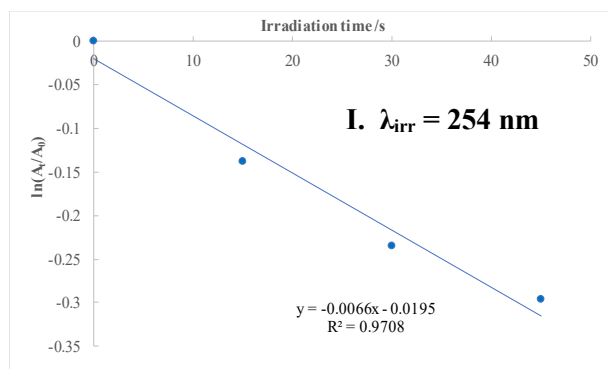
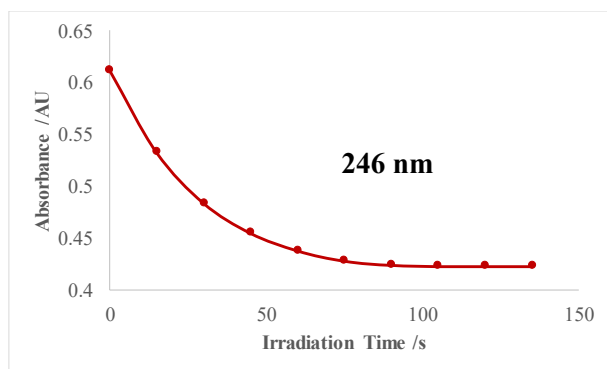
PG= Photoproduct

$$-d[\text{XPG}]/dt = k[\text{XPG}]$$

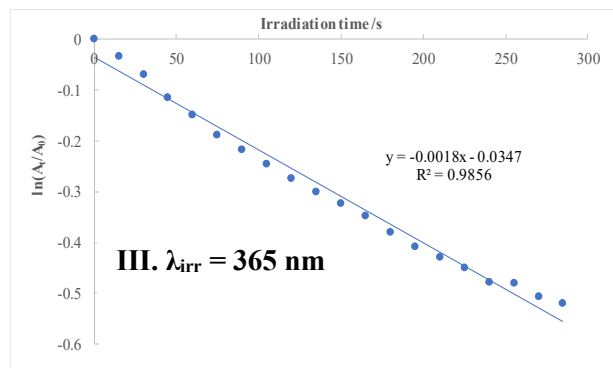
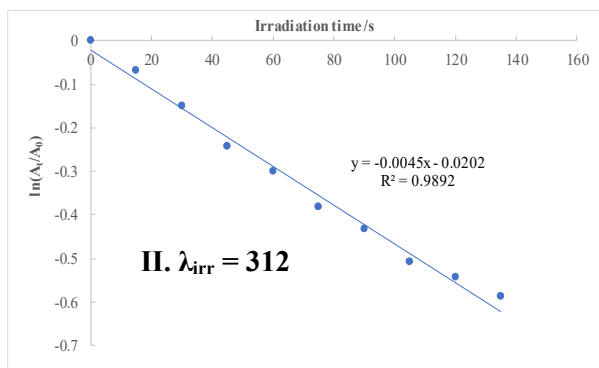
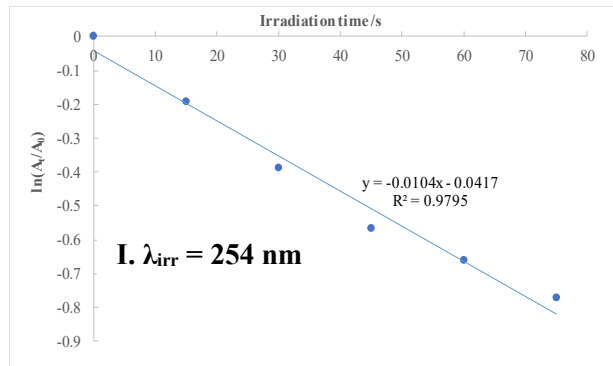
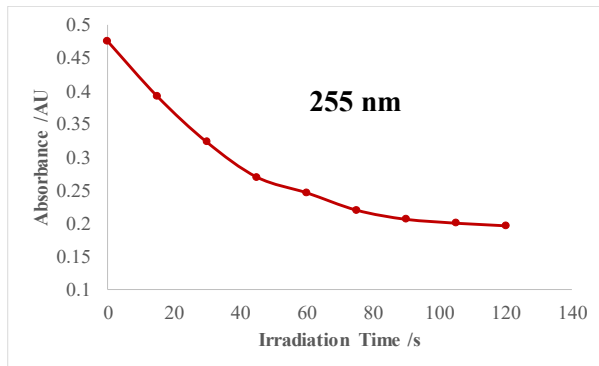
X= Uncaged species (Acetic acid)

Reaction rate is proportional to the intensity of incident light at the excitation wavelength and the uncaging cross section. At low concentrations these reactions are often considered to be pseudo-first order. When absorbance of PG exceeds that of XPG the inner filter effect becomes significant as the reaction progresses. This leads to a deviation from first order kinetics. In order to eliminate this, only data conforming to a first order fit is plotted. In cases where the inner filter effect is significant, this is the first several data points.

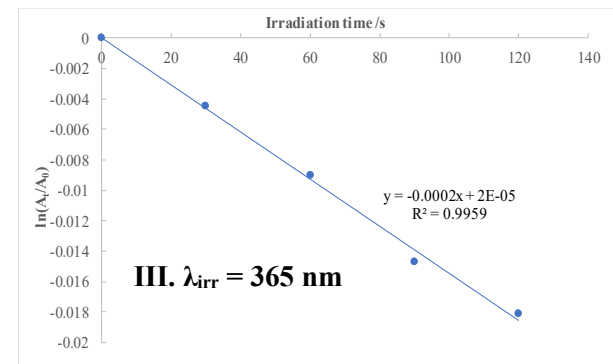
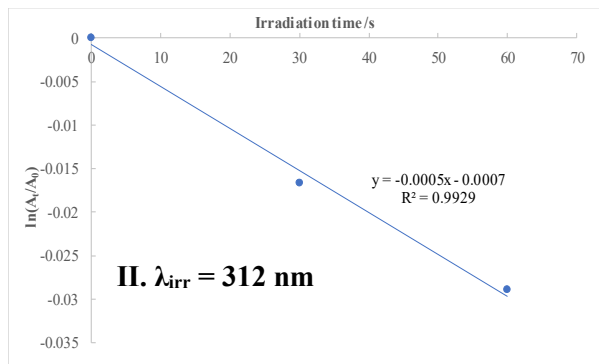
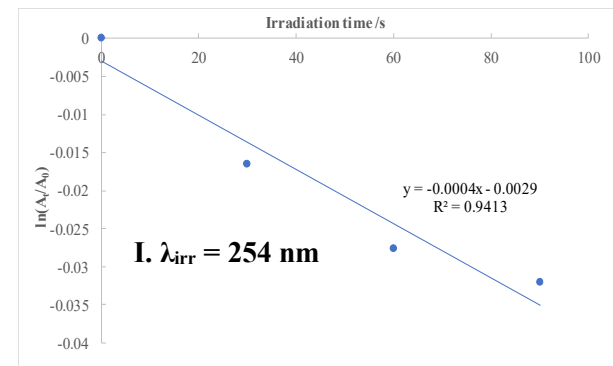
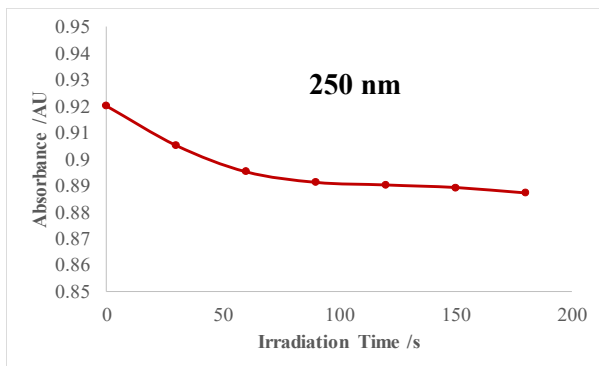
### 1P



# 1a



# 1b





# 1-DMA

